Leibniz Universität Hannover

Fakultät für Elektrotechnik und Informatik
Institut für Kommunikationstechnik

Relay Technology for Performance Improvement in WiMAX System

Von der Fakultät für Elektrotechnik und Informatik
der Gottfried Wilhelm Leibniz Universität Hannover
zur Erlangung des akademischen Grades
Doktor-Ingenieurin
genehmigte

Dissertation

von M.Sc. Anggia Nurul Kusuma Anggraini
geboren am 24. Dezember 1980 in Lembang, Indonesien

2012

Referent: Prof. Dr.-Ing. Thomas Kaiser
Korreferent: Prof. Dr. Jürgen Peissig
Vorsitzender: Prof. Dr.-Ing. Jörn Ostermann
Tag der Promotion: 24. Oktober 2012

ZUSAMMENFASSUNG

Die Anforderung nach hoher Datenübertragungsrate übersteigt die Leistungsgrenzen der bisherigen 3G-Systeme. ITU-R hat die fortschrittliche 4G Voraussetzungen definiert, die als IMT-Advanced bezeichnet werden, um die Erweiterung der Leistungsfähigkeit bestehender Wireless-Technologie zu verordnen. Diese berücksichtigen umfassende IP-basierte Lösung, effiziente Nutzung des Frequenzspektrums und hohe maximale Datenrate. WiMAX 2 wurde als eine der realen 4G Technologien außer der LTE-Advanced angesehen worden. Mit dem Ziel einer bessere Spektraleffizienz, breiteren Zellbereich und größere Reichweite zu erbringen, setzt WiMAX die Relais-Technologie als eine der wichtigsten Komponenten in ihrer Spezifikation ein. Der Schwerpunkt dieser Dissertation liegt auf der Leistungsanalyse von Relais-gestützten WiMAX-Systemen.

Die Leistungsfähigkeit der Relais-Technologie hängt nicht nur von der verwendeten Relais-Protokoll ab, sondern auch von der Ortung des Relaises. Daher wird einen Algorithmus zur Ermittlung einer optimalen Relais-Position vorgeschlagen. Danach werden die Leistungsanalysen von einem oder mehreren einzelnen Antennen-Relais in der Zwei-Hop-und Multihop-SISO-und MIMO-Systeme aufgezeigt. Weitere Untersuchungen bei die Nutzung der Mehrantennen-Relais in dem System werden ebenfalls durchgeführt. Die Nutzung von entweder Einzel-oder Mehrantennen-Relais in den Systemen führt zur Verbesserung der Bitfehlerrate, insbesondere wenn die Ortung des Relais optimal gewählt wurde. Zudem erhöht die Verwendung mehrerer Relaisknoten den räumlichen Diversität-Gewinn. Dies verbessert die Systemleistung trotz der hoheren Hardwarekosten und Implementierungskomplexität. Die Erhöhung der Relais-Hopanzahl im System ist jedoch nicht immer vorteilhaft, insbesondere wenn die Zustände der Relais-Kanäle schlecht sind. Es wurde festgestellt, dass der Einsatz von Decode-und-Forward (DF)-Strategie zur besseren Leistung als Amplify-und-Forward (AF)-Strategie in einem Multihop-System aufweist. Schließlich werden die Untersuchungen von Multi-Antennen-Relais für Multi-User-MIMO-System, bei dem das Relais sich wie der Multi-User-Sender verhält, durchgeführt. Zur Unterdrückung der Interferenz zwischen Nutzern werden zwei Verfahren nämlich die Block Diagonalisierung (BD)-und die Interferenz Ausrichtung (IA)-Methode vorgeschlagen. Es wurde festgestellt, dass die BD-Methode als die IA-Methode besser geeignet für dieses System ist. Jedoch nähert sich die Leistung des IA-Ansatz an die BD-Methode durch die Umsetzung der DF-Strategie.

Schlagwörter
Wireless Interoperability for Microwave Access (WiMAX), Relais, Diversität, Multiple-Input Multiple-Output (MIMO), Keyhole Kanal, Block Diagonalisierung, Interferenz Ausrichtung

ABSTRACT

The intensity of the demand for a high data rate transmission has exceeded the capability limit of the current 3G wireless broadband technologies. ITU-R has since defined the prospicient 4G requirements, referred to as IMT-Advanced, to boost the baseline capabilities of a wireless technology, which include all IP-based, better spectrum efficiency, and high peak data rate. WiMAX 2 specification has been accorded as one of the technologies, beside the LTE-Advanced, which qualifies as a true 4G technology. With the objective to offer better spectral efficiency, broader cell range, and larger coverage, WiMAX adopts the relay technology in its standard as one of the key components. This dissertation is focused on the performance investigation of the relay technology for a WiMAX system.

Beside on the relaying protocol, the performance of a relay technology depends mostly on the channel conditions, or rather, on the relay position. An algorithm is proposed based on the RSSI distribution of the cell/area to find an optimal position of the relay. Afterwards, the performance investigations of a SISO system equipped with single-antenna relay(s) are presented for the two-hop and the multihop cases. Further investigation on employing multi-antenna relay(s) on the MIMO system is also delivered. The results show that adding either a single-antenna or a multi-antenna relay to the system is proven to improve the performance in terms of BER, especially when the relay location is optimally chosen. In addition to that, employing more relay nodes increases the spatial diversity gain. This subsequently enhances the system performance, although at cost of more implementation complexity and hardware overhead. Nevertheless, adding more relay hops on the system is found not always beneficial, especially when the relay channel conditions are poor. It is found that, for our multihop system, applying the Decode-and-Forward (DF) strategy is more beneficial than the Amplify-and-Forward (AF) strategy. Finally, the investigation of a multi-antenna relay is also conducted for the multi-user MIMO system, where the relay behaves as the multi-user transmitter. The block diagonalization (BD) method and the Interference Alignment (IA) approach are implemented for interference cancellation. It is demonstrated that under the given system constraints, the BD method performs better than the IA approach. It is also shown that by implementing the DF strategy, the performance of the IA approach could level the performance of the BD method.

Keywords
Wireless Interoperability for Microwave Access (WiMAX), Relay, Diversity, Multiple-Input Multiple-Output (MIMO), Keyhole Channel, Block Diagonalization, Interference Alignment

CONTENTS

LIST OF TABLES

ACRONYMS

ACKCH   Acknowledgement Channel

AF   Amplify-and-Forward

BC   Broadcast Channel

BD   Block Diagonalization

BER   Bit Error Rate

BS   Base Station

BW   Bandwidth

CDF   Cumulative Distribution Function

CP   Cyclic Prefix

CQICH   Channel Quality Indicator Channel

CRN   Cognitive Radio Network

CSI   Channel State Information

DEM   Digital Elevation Model

DF   Decode-and-Forward

DL   Downlink

DMT   Diversity-Multiplexing Tradeoff

DoF   Degrees of Freedom

EIRP   Equivalent Isotropically Radiated Power

FDD   Frequency Division Multiplexing

FFT   Fast Fourier Transform

FSPL   Free Space Path Loss

FUSC   Full Usage of SubChannels

Gbps   Gigabit per Second

GI   Guard Interval

GPS   Global Positioning System

HARQ   Hybrid Automatic-Repeat-Request

IA	Interference Alignment
IEEE	Institute of Electrical and Electronics Engineers
IFFT	Inverse Fast Fourier Transform
IMT	International Mobile Telecommunications
ISI	Inter Symbol Interference
ITU	International Telecommunication Union
ITU-R	International Telecommunication Union Radiocommunication Sector
LoS	Line-of-sight
LS	Least Square
MAC	Multiple Access Channel
MAI	Multiple Access Interference
Mbps	Megabit per Second
MCS	Modulation and Coding Scheme
MED	Mean Excess Delay
MIMO	Multiple Input Multiple Output
MISO	Multiple Input Single Output
MRC	Maximum Ratio Combining
MU-MIMO	Multi-User Multiple Input Multiple Output
NLoS	Non-Line-of-Sight
OFDM	Orthogonal Frequency Division Multiplexing
OFDMA	Orthogonal Frequency Division Multiple Access
OSTBC	Orthogonal Space-Time Block Code
PDP	Power Delay Profile
PUSC	Partial Usage of SubChannels
RD	Relay-to-Destination
RMS	Root Mean Squared
RSSI	Receiver Signal Strength Indicator
SD	Source-to-Destination
SDMA	Spatial Division Multiple Access

SISO	Single Input Single Output
SIMO	Single Input Multiple Output
SINR	Signal-to-Interference-plus-Noise Ratio
SNR	Signal-to-Noise Ratio
SOFDMA	Scalable Orthogonal Frequency Division Multiple Access
SR	Source-to-Relay
SUI	Stanford University Interim
SU-MIMO	Single-User Multiple Input Multiple Output
SVD	Singular Value Decomposition
TDD	Time Division Multiplexing
UL	Uplink
WiMAX	Worldwide Interoperability for Microwave Access

INTRODUCTION

WiMAX has been considered as one of the wireless broadband access technologies to provide broadband services to isolated places in suburban/rural areas where a fiber connection is not an option. Although WiMAX offers high data rates and relatively large coverage, it still suffers from typical limitations like a low SNR over long distance and also at coverage holes, especially in the area with high terrain irregularities.

Furthermore, as to meet the rushing demands for high speed, high mobility, reliable, and ubiquitous communications, as well as comprehensive IP solutions, ITU-R issued an IMT-advanced specifications (also known as "systems beyond IMT 2000") in 2008. These requirements are specified for a standard that should be regarded as 4G system, which is expected to provide a peak data rates of 100 Mbps for high mobility users of up to 350 km/h, and 1 Gbps for low mobility users of up to 10 km/h (in both indoors and outdoors). It is also expected that the system could offer a greater security and quality services.

To overcome those challenges, a WiMAX task group 802.16j specified a multihop relay based standard (IEEE 802.16j–2009 [4]) as an optional deployment to give an additional coverage and a data rate improvement to the system. Featuring a simpler and less expensive device than a BS, relay technology is considered as a cost-efficient solution to overcome issues, such as spectrum limitation and poor signal reception at cell edge as well as at blank spot. In addition to that, the IEEE 802.16 working group has also standardized the IEEE 802.16m-2011 [5] (also called "WiMAX 2") to satisfy the IMT-advanced requirements. It also includes relay technology and MIMO solutions for single-user and multi-user as its key features to allow higher data rates and to reduce coverage holes.

1.1 MOTIVATION

Encouraged by the many already existing investigations of the relay technology, this thesis is mainly aimed to provide additional reference of the implementation and design of a relay model, specifically, in the WiMAX system. In particular, the motivation of this dissertation is to study the performance advantage of employing half-duplex relay(s) to the fixed WiMAX system, especially for downlink transmission.

There are already several existing strategies proposed for the relay network such as, Amplify-and-Forward (AF), Decode-and-Forward (DF), Compress-and-Forward, and their variants. Comparing one to the other,

each strategy has its own advantages and disadvantages. Furthermore, its performances vary according to the relay position or the link qualities. Therefore, the optimal position of the relay(s) in the system needs to be determined, particularly, by considering the terrain profiles of the area represented by the RSSI value distributions. In this thesis, we will only focus on two relaying strategies, namely the AF and the DF relaying strategies. Furthermore, in this work, the performance of the proposed relay models will be investigated limited to the BER performances.

The investigations are performed for varying cases of relay system. The simple implementation of relay system is the SISO two-hop model, where there exists only one relay node in-between the source node and the destination node. Cooperative scheme is considered when there exists a direct link between the source node and the destination node, and when more than one relay nodes are employed in the system. Moreover, a multihop system with L number of relay nodes are also studied.

Beside the performances of a single-antenna relay to the WiMAX SISO system, we also investigate a single-antenna relay in the WiMAX MIMO (2×2) system. This would be interesting for the case when, for example, having multi-antenna relay is not an option due to the implementation cost. In this case, the channel would experience the so-called keyhole-effect, that is when the rank of the channel degrades into one. It is to be proven whether a single-antenna relay could still provide a substantial performance improvement on the WiMAX MIMO system. Furthermore, we also study the effect of employing many single-antenna relays (multi-keyhole case) to the MIMO system performance. It is interested to see whether employing multi single-antenna relays on the MIMO system could exhibit significant improvement which can recompense the complexity (i.e., implementation and cost).

Moreover, harvesting the potential of relay technology combined with the multiplexing gain from the multiple antennas technology, our investigations are also encompassed the multi-antenna relay scenario. For this purpose, a multi-antenna relay system is proposed for the case of 2×2 single-user MIMO system, where the relay has also the same number of receive and transmit antennas. The BER performance analyses are covering the case of the single relay, the multi-relay and the multihop ((L+1)-hop) relay MIMO system with both aforesaid relaying strategies.

Additionally, as promoted in the IEEE 802.16m-2011 standard and as a key difference between the 3G and 4G systems, an implementation of relay technology on a multi-user MIMO scenario is also presented. In this thesis, the implementation is limited for the case of $K = 2$ users in a 2×2 MIMO relay system. In the system, single relay node with four antennas is employed to assist the multi-user communications. The linear precoding technique based on the ZF beamforming method, such as, the conventional

block diagonalization and the iterative interference alignment approach are applied and investigated for the proposed model.

1.2   DISSERTATION OUTLINE

This dissertation is outlined as follows. In Chapter 2, we describe a brief overview of the WiMAX technology, which includes its promising features and PHY layer aspects. Afterwards, we present our measurement campaign performed to the fixed WiMAX system deployed in rural areas of Hetzwege, Germany. The physical performances and the propagation analyses, including the large scale and small scale fading analyses, of the measured system are then carried out thereto based on the measurement results. A low resolution model of the area is generated based on the terrain profiles of the measured area for a ray tracing purpose. Afterwards, based on the ray tracing calculations, the propagation analyses of the generated model are compared with the real system. Furthermore, a MATLAB simulation model is therefrom defined to investigate the behaviour of the WiMAX relay system discussed in the succeeding chapters.

In Chapter 3, we present the relaying concept on the wireless technology. Specifically, two most-known strategies, namely the AF strategy and the DF strategy are discussed. Next, the performances of both strategies with and without the cooperative diversity scheme are briefly studied for a simple SISO two-hop cases. Lastly, an algorithm to define an optimal position of relay(s) based on the RSSI distributions is proposed. For the verification purpose, the algorithm is applied to the generated ray tracing model. The performance gain of the system with the proposed relay position is analysed in terms of the modulation and coding scheme improvement, as well as the blank spot reduction.

In Chapter 4, the BER performances of the WiMAX single-antenna relay system are studied for the SISO and the MIMO (2×2) models. For the SISO case, the spatial diversity gain offered by the relay nodes in the multi-relay scenario is investigated. Furthermore, the multihop ((L+1)-hop) relay scenario is also studied. The performances in terms of BER of the proposed models with the AF and the DF relaying strategies are investigated for the cases when the direct link is considered, and when it can be neglected. As for the MIMO case, two scenarios, i.e., the keyhole and the multi-keyhole cases are presented. A brief explanation regarding the keyhole and the multi-keyhole channels are first introduced. The impact of employing a single-antenna relay on a MIMO system, which forms a keyhole-like channel, is observed. In addition to that, the investigation is broaden to the case where multi single-antenna relays are inserted to the system (multi-keyhole case). It is evaluated whether the spatial diversity offered by the relay nodes is able to provide significant BER performance improvement.

In Chapter 5, we extend our investigations to a multi-antenna relay model for the WiMAX MIMO system. First, the investigations are focused on the single-user MIMO system. The observations are performed similar to the previous chapter, where the BER performances are studied for the single relay, the multi-relay, and the multihop ((L+1)-hop) relay scenarios for the case where the direct link is not considered. These observations provide useful insights of the potential gain offered by the relay technology combined with the multiple antenna technique. Lastly, our discussion is furthered to the multi-user MIMO system. The ZF-beamforming-based linear precoding techniques are presented, they are the conventional block diagonalization method and the iterative approach of interference alignment technique. Furthermore, a system is proposed where a four-antenna relay node assists the transmissions of the 2×2 multi-user MIMO system for K = 2 users. The performances of the proposed model with the aforementioned linear precoding techniques are investigated for both relaying strategies.

In Chapter 6, the contributions of the dissertation are summarized and the possible future research works are provided.

WIMAX MEASUREMENT

In this chapter, we will present an overview of the WiMAX system and its PHY layer parameters considered throughout this thesis. Furthermore, based on our deployed 3.5 GHz fixed WiMAX system, the measurement campaign procedure and the measurement results analyses will also be presented. Therefrom, the ray tracing model and the simulation chain model are proposed for use in the succeeding chapters.

This chapter is organized as follows. In Section 2.1 and Section 2.2, the WiMAX specification and its significant PHY layer parameters used in this thesis are described. Section 2.3 provides a description of the deployed WiMAX system, follows by the measurement campaign procedure and its analyses. Also thereinafter, the Wireless Insite ray tracing model and the MATLAB simulation model are developed. Finally, the summary of this chapter is given in Section 2.4.

2.1 WIMAX OVERVIEW

WiMAX is a broadband wireless technology based on the IEEE 802.16 standard. The purpose of WiMAX is to provide an affordable and omnipresent high speed IP-based wireless technology that can support fixed, portable, and mobile model profiles. As an 802.16 family, WiMAX is targeted for large metropolitan area networks with large numbers of users. It emphasizes on two key characteristics, namely optimal coverage and better spectral efficiency.

The first WiMAX solution is defined in the IEEE $802.16 - 2004$ standard [6], also known as IEEE 802.16d. It supports only fixed and nomadic applications, therefore referred to as 'Fixed WiMAX'. Its amendment, the IEEE 802.16e [7], also remarked as 'Mobile WiMAX' is published in 2005. It specifies the mobility functionality and amends the performance of fixed services. Both standards are incompatible to each other. The IEEE 802.16e has afterwards more often referred as the WiMAX standard, since it offers more benefits compared to the IEEE 802.16d. Table 1 describes the advantages of the IEEE 802.16e and also the differences with the IEEE 802.16d standard.

The version of WiMAX air interface considered in this thesis is the IEEE 802.16e which is also included in the IEEE $802.16 - 2009$. The latter is a rollup of the previous IEEE 802.16 standards ($802.16 - 2004$, $802.16 - 2004$/Cor 1, 802.16e, 802.16f, 802.16g and P802.16i). This version is further amended by IEEE 802.16j–2009 and IEEE 802.16h–2010, which specify

Parameter	802.16d	802.16e	Advantages of 802.16e
Multiple access scheme	OFDM	S-OFDMA	Offer flexibility to various spectrum allocations
Bandwidth (MHz)	Typically 3.5	5, 10, 8.75, 20	Accomodate high capacity applications
FFT	256	128, 512, 1024, 2048	Better NLoS
Frequency reuse	No	1 cell reuse	Better spectrum efficiency
MIMO	STC	STC and SMX	Improve capacity and coverage
Standard roadmap	Forward incompatible	Forward compatible	Upgrade capability

Table 1: Advantages and differences of the IEEE 802.16e compared to the IEEE 802.16d

multihop relay capability and cognitive radio capability, respectively. Another amendment which is the P802.16n, supports advanced air interface for higher data rates and higher reliability networks respectively. On May 2011, an advanced air interface standard IEEE 802.16m−2011 [5] or also called the Mobile WiMAX Release 2 or WirelessMAN-Advanced has been published as an amendment to IEEE 802.16 − 2009 standard. It features capabilities required by the ITU-R IMT-Advanced on 4G systems, such as data rates of 100 Mbit/s for mobile users and 1 Gbit/s for fixed users. The IEEE 802.16m−2011 standard integrates advanced communications technologies such as multi-user MIMO, multi-carrier (or carrier aggregation) operation, and cooperative communications. Furthermore, it also reenforces femto-cells, self-organizing networks, and relay technologies.

2.1.1 WiMAX Features

WiMAX technology has some significant features that give flexibility to its service offerings and its deployment alternatives. Some of those features are as follows: [8] [9] [10] [11] [12] [13]:

WiMAX PHY adopts the **OFDM-based technology** as its transmission strategy. OFDM allocates the data stream into a set of orthogonal narrowband adjacent subcarriers (FDM). Hence, instead of frequency selective fading, each of these narrowband subcarriers experiences almost flat fading, which simplifies the equalization process. A cyclic prefix is inserted in the guard interval of every OFDM symbol to preserve the orthogonality and to overcome the inter-symbol interference (ISI) problems. The cyclic prefix increases also the symbol duration, which in return can be used to compensate larger delay spread and multipath effect, and therefore able

to address NLoS challenges. More details about OFDM technology can be found in [9] [11] [13].

Subchannelization is an option for both, fixed WiMAX (uplink only) and mobile WiMAX (uplink and downlink) services. The use of subchannelization could improve the system gain significantly. Subchannelization means to group the active subcarriers into several subsets of subcarriers according to permutation rules. This subset is called subchannel (see Figure 1). This grouping allows a flexible bandwidth allocation and offers frequency diversity. The use of subchannelization in uplink (UL) expands the UL transmission range by permitting subscriber stations (SS) to allocate higher transmit power only on some selected subchannels. This could prolong the battery life of SS and offers better spectrum efficiency. In downlink (DL), subchannelization supports multiple access by allowing a subchannel to be allocated for different receivers based on their channel conditions. It is further extended into Scalable Orthogonal Frequency Division Multiple Access (SOFDMA) to allow a more flexible use of resources supporting mobile operation. Further explanations regarding subchannelization can be found in [9].
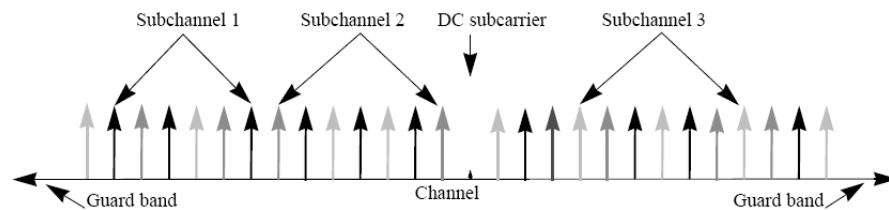
Figure 1: Subchannelization

WiMAX supports **very high peak data rates** which theoretically can reach up to 74 Mbps on 20 MHz bandwidth. Together with time duplexing division scheme on 3 : 1 (DL:UL) ratio on 10 MHz bandwidth, it can achieve data rate of 25 Mbps on downlink and 6.7 Mbps on uplink. These peak data rates are achievable when exploiting the 64 QAM 5/6, the highest modulation and coding scheme specified in the standard. Higher peak data rates may still be achieved favoring multiple antennas and spatial multiplexing technology.

Scalable PHY architecture in mobile WiMAX allows a flexible and low cost deployment by maintaining the basic physical layer parameters fix, i.e. the subcarrier spacing (frequency) and the symbol duration (time). Only the Fast Fourier Transform (FFT) size is made variable based on the need to scale the data rate according to available channel bandwidth. The scaling can be performed dynamically to permit roaming operation across different networks which may have different bandwidth requirements. Due to its flexibility to support various channel bandwidth from 1.25 MHz to 20 MHz with fixed subcarrier spacing, mobile WiMAX is able to anticipate ISI and

Doppler frequency shift problems [14].

WiMAX system applies an **adaptive modulation coding (AMC)** to maximize throughput and range in a time-varying channel for downlink as well as uplink transmission. The optimum modulation and coding scheme (MCS) is chosen based on the signal-to-noise ratio (SNR) conditions of the channel received by the BS and the SS. This ability to support different combined MCS technique on burst-per-burst basic, is a powerful feature to maintain link quality and stability of the system. WiMAX specifies tailbiting convolution encoding (CC) as its mandatory coding scheme. It also permits convolutional turbo codes (CTCs), block turbo codes (BTCs), and low density parity check (LDPC) code as an optional coding scheme. All of these coding schemes shall be modulated using either QPSK, 16QAM, or 64QAM.

2.1.2   *WiMAX In Comparison to other Broadband Wireless Technology*

WiMAX is not the only technology that could provide an ubiquitous high-speed wireless access. There are other technologies, such as 3G cellular, Wi-Fi, and LTE that offer similar services as WiMAX.

3G cellular technology is a long well-established technology in the market that offers mobile services. It benefits a wide network coverage and a better experience. Unlike WiMAX which is purposely designed for data transmission over IP, the 3G cellular technology is essentially designed for voice transmission. It defines different network architecture for data transmission. Furthermore, WiMAX accordingly offers a simpler and flatter architecture with wider bandwidth providing faster connection and better spectral efficiency.

The principal difference between Wi-Fi and WiMAX is the coverage or distance. Wi-Fi is intended for small area network (i.e., home, office, or public hotspot area) with maximum range of several hundred meters, meanwhile WiMAX is targeted for greater distance up to 50 km (i.e., small city). Both can be considered as a complement to each other. WiMAX can serve as backhaul service for Wi-Fi to connect to other WiMAX networks, and Wi-Fi provides connectivity to WiMAX subscribers within local area.

LTE, specifically LTE-Advanced, is considered as a competitor 4G technology to WiMAX 2 or IEEE 802.16m standard, since both are promising a very similar technology, performance, and capabilities. WiMAX might offer a low cost deployment, but on the other hand, LTE is designed to be backward compatible with cellular based networks, affording more natural upgrade. Hence, although WiMAX has made headway in deployments, LTE earns most support from the telecomm companies.

2.2 WIMAX PHYSICAL LAYER

The WiMAX system considered throughout this thesis is the mobile WiMAX adopting OFDMA PHY, which is defined in the IEEE 802.16e−2005 (also in IEEE 802.16 − 2009) standard as WirelessMAN-OFDMA PHY. It is designed for NLoS environment in the frequency bands below 11 GHz. WiMAX provides a standardized solution in both, licensed (i.e., 2.3 GHz, 2.5 GHz, and 3.5 GHz) and license-exempt bands (i.e., 5.x GHz or 3.65 GHz). While licensed band shall operate using either time division duplexing (TDD) or frequency division duplexing (FDD), licensed-exempt band supports only TDD mode. Nevertheless, the TDD mode has been specified in initial implementation profiles by the WiMAX Forum.

The PHY layer of the mobile WiMAX adopts the SOFDMA-based principles. OFDMA symbol is composed of orthogonal subcarriers, which hold data, pilot, DC, and guard band subcarriers. The number of subcarriers conforms to the FFT size and scales with bandwidth. By virtue of the effective subchannelization, active subcarriers (data and pilot) in one symbol can be allocated to multiple users gaining frequency diversity, see Figure 2.
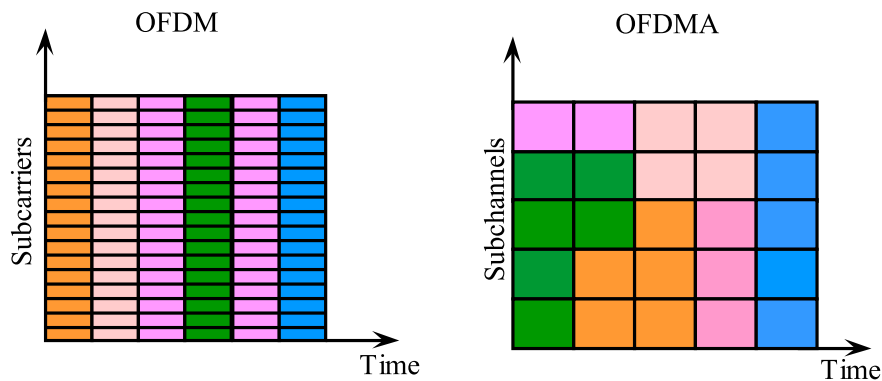
Figure 2: OFDM and OFDMA subchannelization

2.2.1 *Basic Parameters*

Mobile WiMAX standard defines two types of basic parameters characterizing the OFDMA symbol. These parameters are called the primitive parameters and the derived parameters. Derived parameters, as the name implies, can be derived from primitive parameters by a fix relation. Below are parameters defined as primitive specified in [1]:

- The nominal channel bandwidth, BW (Hz) is the bandwidth value allocated by the regulatory body. This value is not the actual bandwidth used, that is the range of frequencies physically occupied by the WiMAX signal. The used bandwidth should be smaller than the nomi-

nal bandwidth. Mobile WiMAX supports nominal channel bandwidth
of 1.25 MHz, 5 MHz, 10 MHz, and 20 MHz.

- N_{used} is the number of all used subcarriers including DC and pilot
  subcarriers. N_{used} value varies depending on the subchannel usage
  mode (PUSC or FUSC).

- n, the sampling factor is the ratio of the sampling frequency to the
  channel bandwidth, which determines the subcarrier spacing and the
  useful symbol time. See Table 2 for the supported sampling factor in
  the mobile WiMAX.

- G, the guard period ratio, is the ratio of the cyclic prefix (CP) time to
  the useful symbol time. The supported values are: $\frac{1}{32}$, $\frac{1}{16}$, $\frac{1}{8}$, and $\frac{1}{4}$.

Channel BW (MHz) - multiple of -	Sampling factor (n)
1.75	8/7
1.25, 1.5, 2, 2.75	28/25
Otherwise	8/7

Table 2: Sampling factor supported in mobile WiMAX

Derived parameters as defined in [1] are listed below:

- N_{FFT} is the FFT size which is the smallest power of 2 greater than
  N_{used}. The supported FFT sizes for mobile WiMAX OFDMA are 2048,
  1024, 512 and 128.

- F_s (Hz), the sampling frequency is the number of samples per second
  generated by the system. The value is given by:
  $F_s = floor(n \times BW/8000) \times 8000$.

- Δf (Hz), the subcarrier spacing which corresponds to the distance
  between two neighboring physical subcarriers. It is defined as the
  sampling frequency divided by the FFT size. For mobile WiMAX
  OFDMA, it is kept fixed at 10.94 kHz.

- T_b (sec), the useful symbol time is defined as $T_b = 1/\Delta f$. Please refer
  to Figure 3 for better illustration.

- T_g (sec), the guard interval duration or the CP duration, which is
  given by $T_g = G.T_b$.

- T_s (sec), the complete OFDMA symbol duration including the useful
  symbol time and the cyclic prefix, $T_s = T_b + T_g$.

- The sampling time (sec) is defined as T_b/N_{FFT}
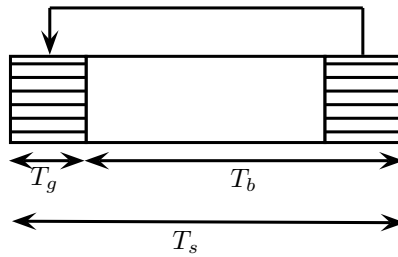
Figure 3: OFDMA symbol time structure

2.2.2 *OFDMA Frame Structure*

WiMAX frame structure has been designed to support a scalable bandwidth and data rate for both uplink and downlink directions. Several frame structures are specified in standard, depend on its duplexing method (FDD or TDD). In this section, only TDD frame structure is described, since our WiMAX system uses TDD mode as defined in initial certification profiles.

The IEEE $802.16 - 2005e$ standard permits a fixed frame size of 2.5 ms, 5 ms, 10 ms, and 20 ms. Hence, the number of symbols in one frame can be defined simply by dividing the frame duration with the symbol time. For initial implementation profiles, a frame size of 5 ms has been selected.
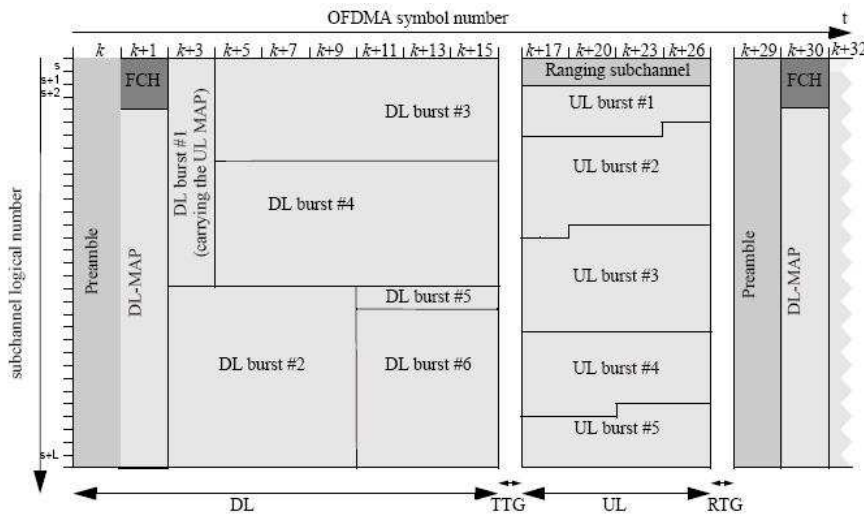
Figure 4: WiMAX frame structure [1]

As shown in Figure 4, a TDD frame structure consists of a DL subframe followed by an UL subframe. Transition gaps should be inserted at the end of each subframe to give time to the BS switching the transmission mode from transmit to receive and vice versa. These DL-UL and UL-DL gaps are called transmit/receive transition gap (TTG) and receive/transmit transition gap (RTG), respectively. TTG and RTG values are specified using Physical

Slot (PS) unit which are specified in the standard according to the BW of the system. A Physical slot is equivalent to 4/sampling frequency (F_s). The value differs also according to the channel bandwidth but should be at least 5 µs. In this thesis, we will consider only the downlink transmission, therefore further discussion will focus on the downlink part.

The downlink subframe is initiated with a BPSK modulated preamble symbol for synchronization and initial channel estimation purposes. It is followed by the frame control header (FCH) which carries information regarding the length of MAP messages, modulation and coding scheme, and subchannel allocations. FCH is followed by the DL map and UL map messages describing the time slot and subchannel assignment for each subscriber. The MAP messages are broadcasted over a reliable link using the most robust MCS, since all users must successfully receive and decode the MAP messages to be able to demodulate the received signal. The rest parts of the subframe are intended for DL traffic bursts.

2.3 WIMAX SYSTEM

To take a closer look at the WiMAX system transmission, a fixed 3.5 GHz WiMAX system based on the IEEE 802.16e OFDMA standard has been deployed in a suburban area of Hetzwege/Abbendorf in the county of Rotenburg (Wümme), Germany. This deployment is part of a research project "WiMAX field trial in Lower Saxony", which intents to provide a broadband wireless access to the houses in those areas.

The WiMAX BS is set up in a 25 meter high tower with three directional antennas of 120° from Andrew that pointing towards three sectors, of which, 49° azimuth (empty land), 115° azimuth (Hetzwege), 300° azimuth (Abbendorf). The operating frequencies are 3535.5 MHz, 3446.5 MHz, and 3436.5 MHz for Hetzwege, Abbendorf, and empty land, respectively. Each antenna transmits a 5 MHz bandwidth of WiMAX OFDMA signal with 35 dBm output power and an antenna gain of 23 dBi in TDD mode. Throughout this thesis, to limit the area of observation, only sector of Hetzwege is taken into consideration. Table 3 summarizes parameters used in the system. Figure 5 and Figure 6 depict the antenna and the WiMAX BS, respectively.

2.3.1 *Measurement Procedure*

We divided the measurement into two parts. The first part is the landscape measurement, which aims to obtain terrain and clutter (vegetation, street, buildings) characteristics of the area. These characteristic data were later used to generate deterministic channel through a ray tracing method. The second part is the signal quality measurement at every car-reachable locations in the region. The measured data were later used to calculate the power delay profiles (PDP) and to identify the performance of the system.

Base Station Parameters	
Frequency band (GHz)	3.5
Altitude (m)	25
Antenna	4-port planar array
	$APW435-12014-0N$
	from Andrew
Measured output power P_{Tx} (dBm)	35
Boresight antenna gain G_{Tx} (dBi)	23
Input power (W)	3.2
Horizontal beamwidth (°)	25
Vertical beamwidth (°)	50
Downtilt (°)	2
Polarization	Vertical
Geographical location	N: 53°11′46.27″
	E: 9°23′40.30″
WiMAX System Parameters	
Bandwidth, BW (MHz)	5
Number of used subcarriers, N_{used}	360
Lower frequency guard subcarrier	46
Higher frequency guard subcarrier	45
Sampling factor, n	28/25
Guard time ratio, G	1/8
FFT size, N_{FFT}	512
Sampling frequency, F_s (MHz)	5.6
Subcarrier frequency spacing (kHz)	10.94
Useful symbol time, T_b (μs)	91.4
Sampling time (μs)	0.1786
Guard time, T_g (μs)	11.4
OFDMA symbol duration, T_s (μs)	102.9
Frame duration (ms)	5
DL:UL	4 : 1
Duplexing mode	TDD
Permutation mode	PUSC

Table 3: Base station and WiMAX system parameters
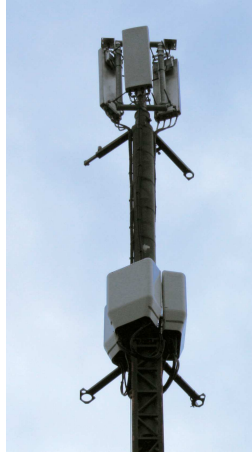
Figure 5: WiMAX base station antenna with three directional antennas of 120°

As the propagation characteristics may change in regard to the season, we need to note that our measurement was performed on April, 1st 2010. That was when the snow has completely melted and the canopy of the shed trees were starting to regrow back their leafage. The measurement was done between 18:08 PM and 19:21 PM (local time) in which the temperature was cool around 3.6°C to 4°C and the wind speed was considered light, thus introduces insignificant fading effect [15][16]. It can be reasoned out that the measurement was performed in a winter condition. Further investigation on the seasonal effect to the propagation characteristics of the designated area is reported in [17].

2.3.1.1 *Landscape Measurement*

Hetzwege consists of mixed characteristics of houses, roads, groups of tree, agriculture, animal farm, and forested area. It is a small area with population around 400 residents (data in 2009), which is concentrated on the middle part. Meanwhile, the rest of the areas are largely covered by open green fields represented by farming area or forested area. This area in general can be classified as a hilly with moderate-to-high density terrain. Therefore, it is also important to obtain the terrain profiles of the area to further study the propagation effects.

The terrain profiles were obtained by using the raw terrain data from Shutter Radar Topography Mission (SRTM) which is refined by using a realistic self-tailored 3D digital elevation model (DEM) of the area as depicted in Figure 7. Furthermore, the clutter distributions were identified from a high precision aerial picture from land surveying authority of Lower Saxony (*Landesvermessung und Geobasisinformation Niedersachsen, LGN*). On-site height measurements with laser scanning were also carried out to produce

Figure 6: WiMAX base station tower of height 25 m erected in Hetzwege

a 3D model of the clutter information. Further explanations regarding these works can be found in [18][19]. This part of measurement was mainly done by our project partner[1].

These terrain profiles and clutter information are used to model Hetzwege city as the study area, which later used in the Wireless Insite software from RemCom [20] to generate the deterministic channel characteristics of the area using a ray tracing method. The simplified model with reduced resolution has to be used instead since the available tool can only calculate a study area with limited resolution. Section 2.3.3 discusses this subject in more details.

2.3.1.2 *Signal Quality Measurement*

This measurement is performed to analyse the performance of the deployed system focusing on downlink transmission. To do this measurement, the test

---

[1] The measurement was done by Dr.-Ing. Kin Lien Chee from Institut für Nachrichtentechnik Technische Universität Braunschweig
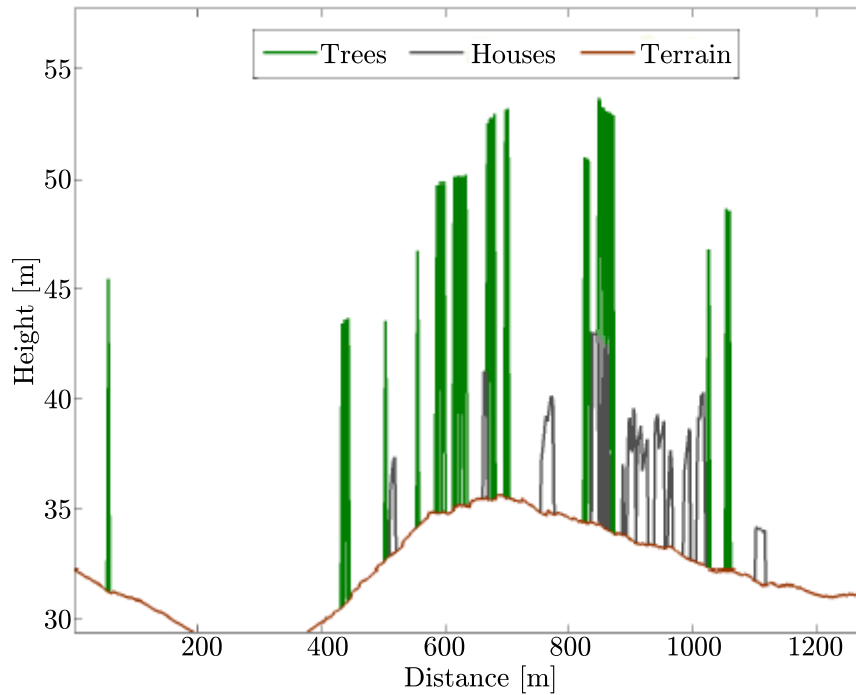
Figure 7: Terrain profile in Hetzwege derived from 3D DEM [2]. It implies that Hetzwege can be classified as SUI Type A terrain model: hilly terrain with moderate-to-heavy tree densities

vehicle was equipped with the WiMAX scanner from Rohde & Schwarz [21], an external GPS, and an omnidirectional receiving antenna mounted on the roof top ($\sim$ 2 m above ground). The parameter settings for the receiver are listed in Table 4. The received signals and its associated geographical locations were recorded while driving through every possible streets in the region with a constant speed of $\sim$ 40 km/h. The recorded data was transferred and stored into a laptop running a dedicated universal software ROMES v4.11 [22] to yield the needed parameters, i.e., the received signal strength indicators (RSSI in dBm) with its corresponding propagation delays of the wireless channel.

The measurement results show that the RSSI for the measured points are ranging from -121.41 dB to -42.53 dB with average of -82.29 dB. The farthest point from the BS which has high RSSI is at 1.26 km with -69 dB, and the nearest point from the BS which has low RSSI is at 0.52 km with -115.76 dB. Even though the system has somewhat wide coverage, but most points located at half-end part of the area, where many houses and/or group of trees exist, suffer from a low RSSI. The points with good reception mostly lie in the near midsection area or in the free land area where there is less obstructions. It can be observed that the terrain profile atypicalities of the area foreshorten the overall system performance. The measured downlink RSSI at each point is pointed in Figure 9. The two red

WiMAX Scanner Parameters	
Network analyser	R&S TSMW-K28
Software platform	R&S Romes v4.11
Receiver sensitivity	< -112 dBm (RSSI)
Measurement speed	5 Measurements/s
Resolution	1/(5 MHz) = 0.2 μs
Noise figure	typ. 7
VSWR	typ. 1.7
Receive Antenna Parameters	
Antenna	Omnidirectional
Gain	2 dBi
Altitude	2 m

Table 4: WiMAX receiver parameters
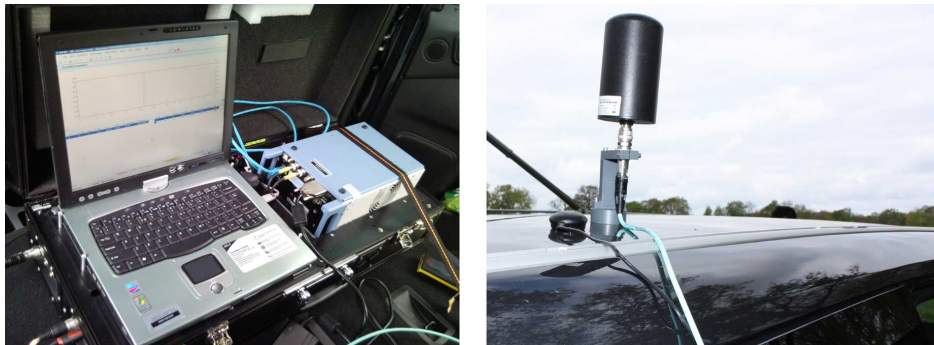
Figure 8: The R&S TSMW WiMAX scanner (left), the omnidirectional receiving antenna and the GPS tool on top of the test vehicle (right)

lines in the figure indicate the antenna beam direction. Points with redish color show the area with good RSSI, and points with blueish color show the area with low RSSI of approximately below -87 dB.

Figure 10 shows the CINR as a function of the RSSI of the measured points with its LS regression. The CINR values of the measured locations are ranging from -18.1 dB to 26.40 dB, giving average value of 8.67 dB. In the low RSSI range, the curve shows that the CINR and the RSSI values are closely correlated, where a 10 dB step-up in the RSSI yields a 10 dB increase
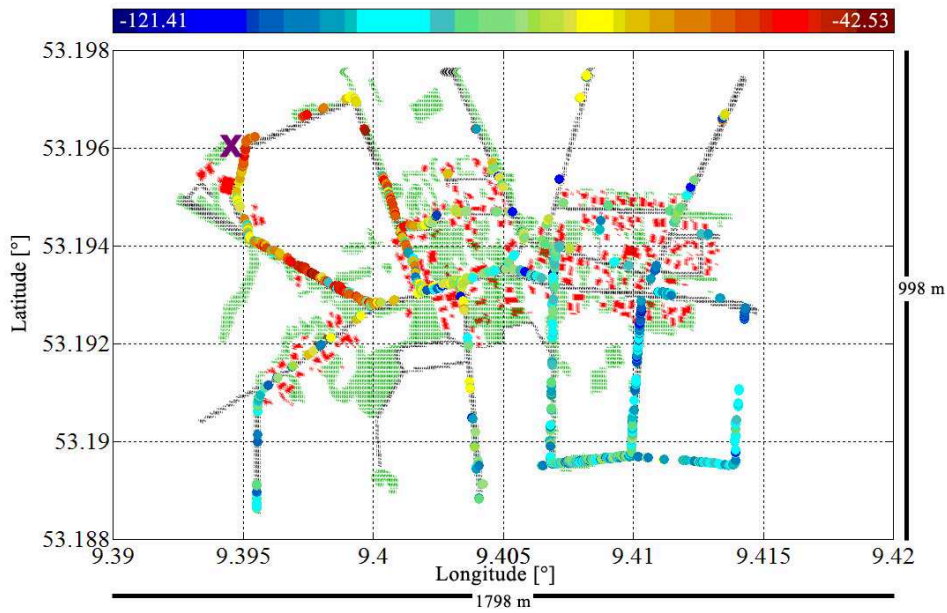
Figure 9: RSSI of the measured 3.5 GHz fixed WiMAX system in Hetzwege (purple X: Base station, green structure: the vegetation, red structure: the buildings). The points in the mid-first area still savour a high RSSI reception; the points in the mid-end area suffer a low RSSI reception

in the CINR. At higher RSSI values, the CINR values approach steadily the ~ 12 dB value due to the saturation effects introduce by the receiver [2] [23].

2.3.2 *Measurement Results Analysis*

In this section, we analyse the system performance based on the measurement results. Two aspects are evaluated, i.e., physical performance in terms of large scale fading, as well as in terms of small scale fading characteristics.

2.3.2.1 *Large Scale Fading*

For the large scale fading analysis, the path loss model of the indicated area is observed to study the contour irregularities effect to the propagation channel. For this purpose, the path loss values at each point are calculated based on the ratio of the EIRP of the BS to the measured RSSI. Afterwards, the calculated path loss values are compared to the standard empirical propagation path loss models. Regarding the frequency and terrain type of our system, some predictions models are evaluated for LoS and NLoS links, namely the COST-231 Hata model for suburban area [24] and the SUI type A model (hilly terrain with moderate-to-heavy tree density) [25][26]. Although

---

2 Receiver saturation is an indicative of the maximum received input power allowed before the receiver is saturated which occurs when the input signal has an amplitude higher than the receiver dynamic range.
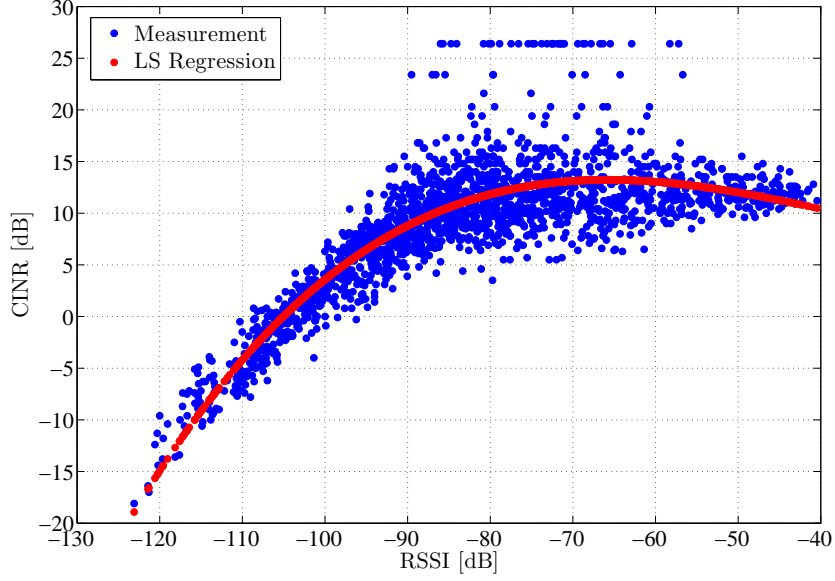
Figure 10: CINR vs RSSI curve of the measured 3.5 GHz fixed WiMAX system in Hetzwege. At lower RSSI range: CINR and RSSI values are closely correlated. At higher RSSI range: the CINRs move steadily around the $\sim$ 12 dB value due to the receiver saturation [23]

the COST-231 Hata model is meant for frequency of up to 2000 MHz, but its correction factors still accord to predict the path loss in the higher frequency range. Moreover, even though it is premissed for the BS antenna height of 30 m to 200 m, it can be applied for a lower BS antenna heights given that the building heights are substantially below the BS antenna [27]. The COST-231 Hata model for suburban area is formulated as

$$
\begin{aligned}
PL_{COST-231}[dB] \ = \ & 46.3 + 33.9 \log_{10}(f) - 13.82 \log_{10}(h_B) - a(h_R) \\
& + [44.9 - 6.55 \log_{10}(h_B)] \log_{10}(d),
\end{aligned}
\tag{2.1}
$$

where $a(h_R)$ is the receiver antenna height correction factor given by

$$
a(h_R) = (1.1 \log_{10}(f) - 0.7)h_R - (1.56 \log_{10}(f) - 0.8),
\tag{2.2}
$$

and f is the transmit frequency which is set to 3535.5 MHz. h_B and h_R are the BS antenna effective height and the receiver antenna effective height in meter, respectively. h_B and h_R values are adjusted according to the terrain profiles. d is the link distance in kilometer. Meanwhile, the SUI type A model for hilly terrain with moderate-to-heavy tree density is calculated according to the following formula,

$$
PL_{SUI-A}[dB] = A + 10\gamma \log_{10}(d/d_0) + X_f + X_{h_R} + s \quad \text{for} \ d > d_0,
\tag{2.3}
$$

where

$$
A = 20 \log_{10}(4\pi d_0/\lambda),
\tag{2.4}
$$

$$\gamma = (a - bh_B + c/h_B), \tag{2.5}$$

and λ is the wavelength in meter, γ is the path loss exponent for h_B in range of $10 - 80$ meters. d_0, a, b, and c are set to 100 meters, 4.6, 0.0075, and 12.6, respectively. s is the shadowing effect which follows the lognormal distribution and set to 10.6 [25]. X_f and X_{h_R} are the correction factors for the operating frequency and the receiver height, respectively. They are defined as follows,

$$X_f = 6.0 \log_{10}(f/2000), \tag{2.6}$$

$$X_h = -10.8 \log_{10}(h_R/2000). \tag{2.7}$$

In addition to that, for the LoS link, the measured path loss is also compared with the free space path loss model which is given by

$$FSPL[dB] = 20 \log_{10}(d) + 20 \log_{10}(f) + 32.45. \tag{2.8}$$

This model describes the path loss of a direct path (i.e., no diffraction and reflection) which is intuitively not the case in our object area. Nevertheless, it is still a good measure to be compared with the path loss of the measured area, since it can still provide a link quality figure of the system.

The previous mentioned models are calculated given the terrain profiles and parameters of the system in use. Afterwards, the error predictions are estimated by subtracting the measurement's path loss with the predictions. The path loss from the measured data is calculated as follows,

$$PL_{meas}[dB] = P_{Tx} + G_{Tx} - L_{Tx} + G_{Rx} - L_{Rx} - P_{Rx}, \tag{2.9}$$

where P_{Tx} and P_{Rx} are the transmit power and the receive power in dBm, respectively. G_{Tx} and G_{Rx} are the transmit antenna gain and the receive antenna gain in dBi, respectively. L_{Tx} and L_{Rx} are the loss at the transmitter and at the receiver in dB, respectively, which cover cable loss, connectors losses, fading margin, polarization mismatch, and other losses respective to the hardware imperfections. The resulted negative value signifies that the model underestimates the actual path loss, while positive value indicates that the model over-predicts the measured path loss.

A comparison for the LoS case shows that the COST-231 Hata model for suburban area induces a mean error of 4.75 dB and a standard deviation of 12.15 dB. Meanwhile, the SUI type A yields a mean error of -14.38 dB and a standard deviation of 19.20 dB. For the NLoS case, the COST-231 Hata model yields a mean error of 0.32 dB and a standard deviation of 12.62 dB. As for the SUI type A model, the mean error is -18.61 dB and the standard deviation is 17.74 dB. For both cases, the COST-231 Hata model

overestimates the path loss, nevertheless it gives the lowest mean error predictions and gives a better accordance with the LS results than the SUI type A model, especially in the case of NLoS. On the other hand, the SUI type A model ostentatiously under-predicts the actual path loss with a large mean error. Such discrepancies between measurement result and empirical model calculations are actually unsurprising since both empirical models do not take seasonal effect/foliage density into consideration. Figure 11 and Figure 12 consolidate the result for LoS and NLoS links, respectively. Another investigation of path loss analysis for this area compared to the COST-231 WI model with terrain correction can be found in [17].

2.3.2.2 *Small Scale Fading*

For the small scale fading analysis, the fading distribution due to the multi-path propagation is evaluated. The average power delay profiles (PDP) of the measurement points are sampled over a quarter of wavelength, with receiver movements of up to six meters. This is according to the suggestion in [28] for outdoor measurement at a frequency range from 450 MHz to 6 GHz, to guarantee enough spatial averaging. Therefrom, the cumulative distribution functions (CDF) are fitted using two-sample Kolmogorov-Smirnov test[3] [29][30] to the known channel fading distributions (i.e. Rayleigh, Ricean, Log-Normal, Weibull) to discover the amplitude distribution of the multi-path fading.

The result, as depicted in Figure 13, shows that the channel fading distributions in Hetzwege are mainly Ricean (NLoS). Subsequently, Ricean K-factors are also derived from each PDP to identify the spatial fading due to scattering introduces by the multipath components. They are defined by calculating the power ratio of the strongest path which represents the fixed component, to the remaining multipaths which represent the scatter components. It is obtained that the mean value of the K-factors is 10.32 dB with minimum value of 3.07 dB and maximum value of 25.41 dB. A high K-factor indicates that the channel is prevailed by one component while the rest of the components are relatively weak. In oppose to that, a low K-Factor implies inadequate dominant component due to the equally distributed energy or because more than one strong component exist. The K-factor of the measured area can be considered as modest or average, presuming that a high K-factor is when $\geqslant$ 20 dB and a lower K-factor is when $\leqslant$ 5 dB [31].

To learn the multipath spread and the time dispersion or the frequency selectivity within the channel of the area, the delay spread characteristics

---

3 Kolmogorov-Smirnov test is a general non-parametric and distribution-free method to determine the difference of two samples based on the maximum distance between the empirical distribution function of the given samples and the CDF of the reference distribution.
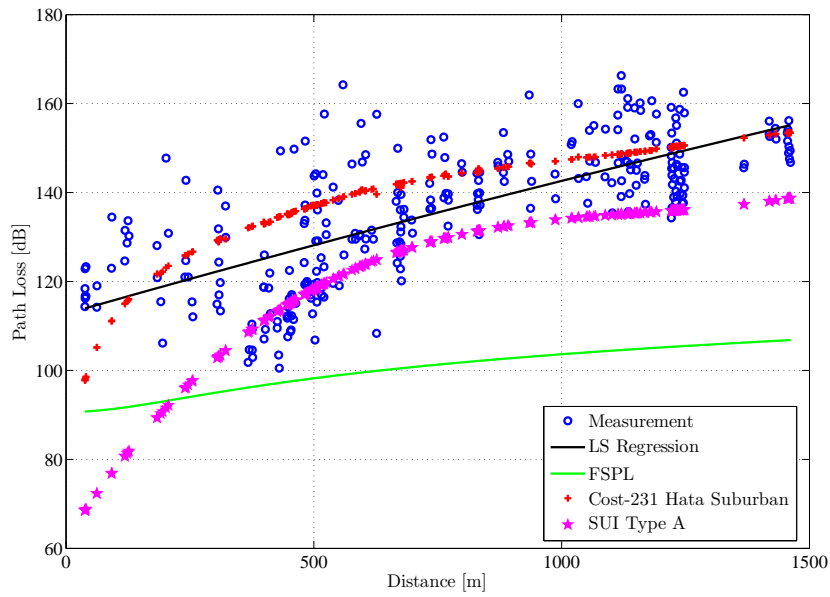
Figure 11: Path loss of the measured 3.5 GHz fixed WiMAX system in Hetzwege (LoS, winter). The COST-231 Hata model shows a closer estimation to the LS of the measurement results with a mean error of 4.75 dB and a standard deviation of 12.15 dB. The SUI type A model gives a mean error of −13.38 dB and a standard deviation of 19.20 dB
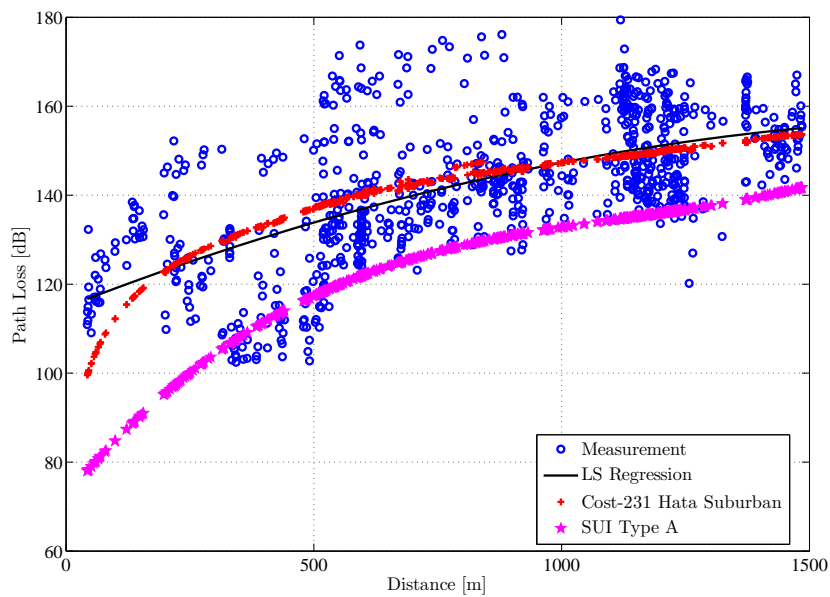
Figure 12: Path loss of the measured 3.5 GHz fixed WiMAX system in Hetzwege (NLoS, winter). The COST-231 Hata model shows a closer estimation to the LS of the measurement results with a mean error of 0.32 dB and a standard deviation of 12.62 dB. The SUI type A model gives a mean error of −18.61 dB and a standard deviation of 17.74 dB
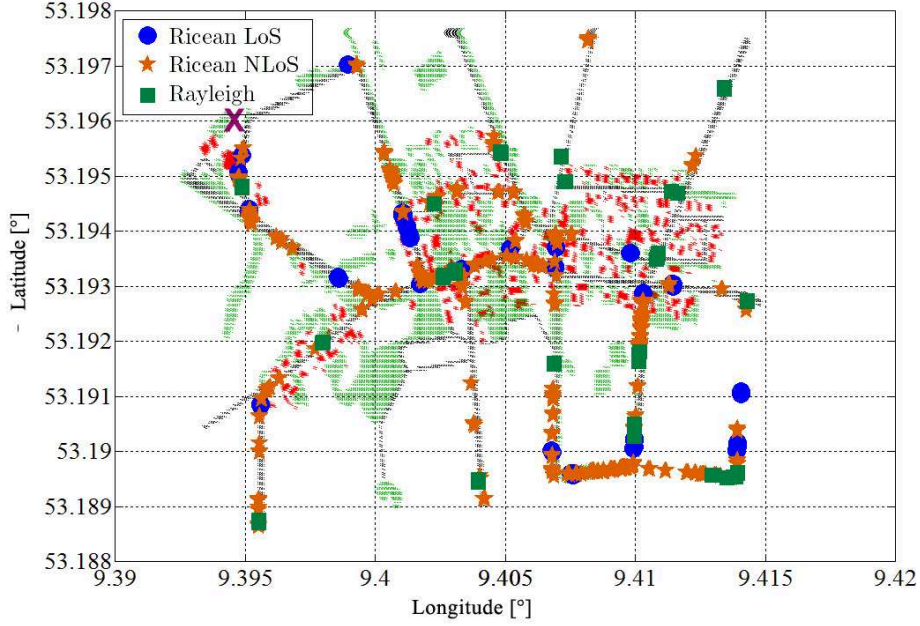
Figure 13: Fading distributions of the measured 3.5 GHz fixed WiMAX system in Hetzwege (purple X: Base station, green structure: the vegetation, red structure: the buildings). The channel fading distributions in Hetzwege are dominated by the Ricean (NLoS)

are also derived following the RMS delay spread (σ_{RMS}), which is the square root of the second central moment of the PDP, given by

$$\sigma_{RMS} = \sqrt{\frac{\sum_{i=1}^{N} P_i (\tau_i - \mu_m)^2}{\sum_{i=1}^{N} P_i}}, \tag{2.10}$$

where μ_m is the mean excess delay (MED) or the first moment of the PDP which is defined as

$$\mu_m = \frac{\sum_{i=1}^{N} \tau_i P_i}{\sum_{i=1}^{N} P_i}, \tag{2.11}$$

N is the number of taps, P_i is the PDP at the i-th tap, and τ_i is the delay of the i-th tap. Based on the calculation, the investigated area has an RMS delay spread of 0.25 µs which corresponds to a maximum excess delay of 0.70 µs using 10 dB threshold, or a maximum excess delay of 1.01 µs using 20 dB threshold. The maximum excess delay value which is far below the specified guard interval duration of 11.4 µs [1] indicates that the WiMAX system in the measured area does not suffer from frequency selective fading. More details about this work can be found in [17].

Furthermore, comparing the propagation characteristics of Hetzwege with those of the SUI models described in [32] shows that, even though the terrain profile of Hetzwege is classified as the SUI type A model, the

RMS delays estimation shows a proximity with the SUI-3 model which has terrain type B with the RMS delay of 0.264 μs for omnidirectional receiver antenna. Also, the K-Factor value, when considering only its mean value, indicates closeness to that of SUI-1,2,3 channel models of 75% coverage, which are ~ 13 dB, ~ 10.41 dB, and ~ 8.45 dB, respectively.

2.3.3 *Ray Tracing Model*

The Hetzwege city is modeled using the Wireless Insite tool for acquiring the deterministic channel characteristics. At first, a precise model was generated using the data acquired from the landscape measurement. However, the simplification of the model is necessary since the tool can only process the data with limited number of faces (2^{15}). The precise model and the simplified model of the study area are shown in Figure 14 and Figure 15, respectively, for comparison.

There are three features generated for our model. First, the terrain feature which describes the height of the ground from the sea level or the contour characteristic of the area. We assume the surface is a wet earth with dieletric half-space type. Second, the city feature which features the buildings/ houses arrangement in the designated area. We consider the building has concrete material with one-layer dielectric type. Last, the vegetation feature which identifies tree's height variation and density which covers the area. It is assumed that the vegetation has a dense foliage, hence introducing 1 dB/m attenuation. The BS position is marked with X in the figure, whereas the receivers are distributed along the area with 30 m spacing. The antenna beam direction is indicated by the two red lines. The BS and the receiver parameters used for the ray tracing purposes are summarized in Table 5. After the propagation is calculated by the Wireless Insite, the PDP and accordingly the RSSI value of each receiver node are obtained, which further be used to analyse the propagation characteristics of the area.

As performed in Section 2.3.2, the path loss analysis is also carried out for the generated area by comparing with the well-known empirical model, such as the COST-231 Hata for suburban area and the SUI type A. The results show that for LoS and NLoS links, the COST-231 Hata model overestimates, withal it shows the closest prediction with 10.29 dB mean error and 17.01 dB standard deviation of for LoS links; and also a mean error of 6.29 dB and a standard deviation of 13.38 dB for NLoS links. On the contrary, the SUI type A model underestimates the prediction by −13.12 dB mean error and 22.16 dB standard deviation for LoS links; likewise −15.28 dB mean error and 20.16 dB standard deviation for NLoS links. The path loss comparison for LoS and NLoS cases are depicted in Figure 16 and Figure 17, respectively.

Moreover, the study area introduces a channel characteristic with an RMS delay spread of 0.236 μs and an maximum excess delay of 0.54 μs using

998 m

1730 m

25.946 m   46.971 m
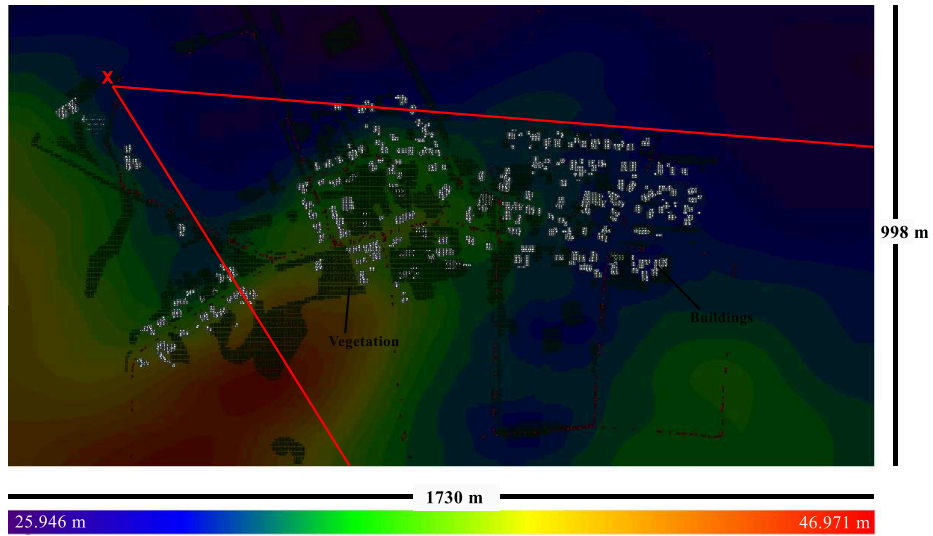
Figure 14: Generated Wireless Insite study area with high resolution (The red X is the BS location and the two red lines illustrate antenna beam direction)

598 m

1730 m

25.000 m   47.000 m
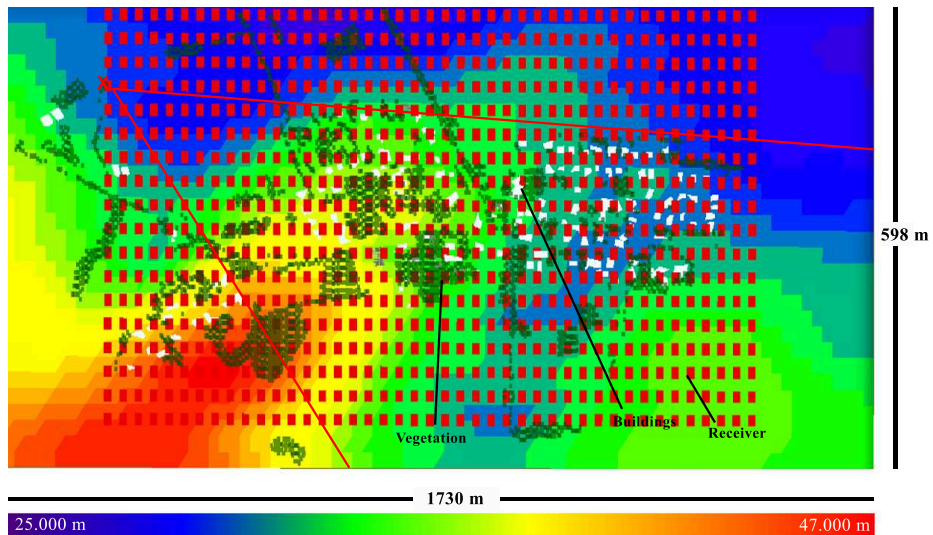
Figure 15: Generated Wireless Insite study area with low resolution (The red X is the BS location, the two red lines illustrate antenna beam direction, the red-square: the receiver node with 30 m spacing)
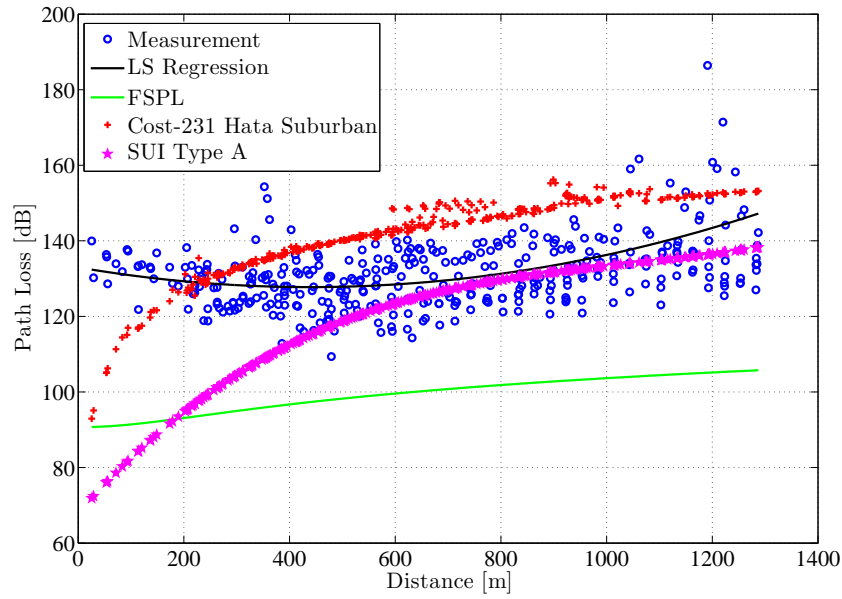
Figure 16: Path loss comparison for LoS links based on the ray tracing model. The COST-231 Hata model gives closer prediction with a mean error of 10.29 dB and a standard deviation of 17.01 dB. The SUI type A model gives a mean error of −13.12 dB and a standard deviation of 22.16 dB
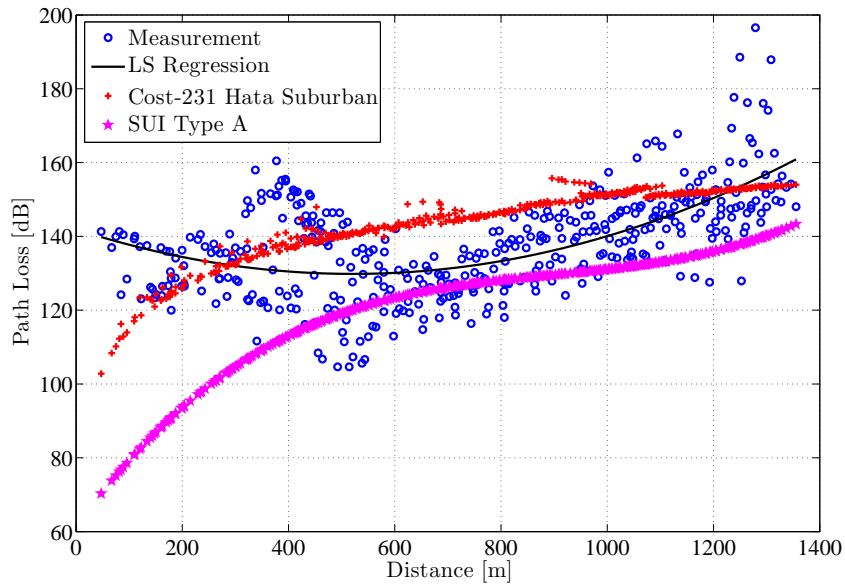
Figure 17: Path loss comparison for NLoS links based on the ray tracing model. The COST-231 Hata model gives closer prediction with a mean error of 6.29 dB and a standard deviation of 13.38 dB. The SUI type A model gives a mean error of −15.28 dB and a standard deviation of 20.16 dB

10 dB threshold, or 0.85 μs using 20 dB threshold. Furthermore, with the same method to determine the fading distribution used in Section 2.3.2, the amplitude distribution of multipath fading for this study area almost evenly follows Ricean (LoS) and Ricean (NLoS) distribution, with percentage of 47% and 43%, respectively (see Figure 18). The mean K-factor value is 11.04 dB with the minimum and the maximum value of 3.55 dB and 22.06 dB, respectively. Although these results cannot really characterize the generated area, since the PDP value are recorded every 30 m (> 6 m as suggested in [28]). We could assume that the recorded PDP value at each point represents the average PDP value of the surrounding area.
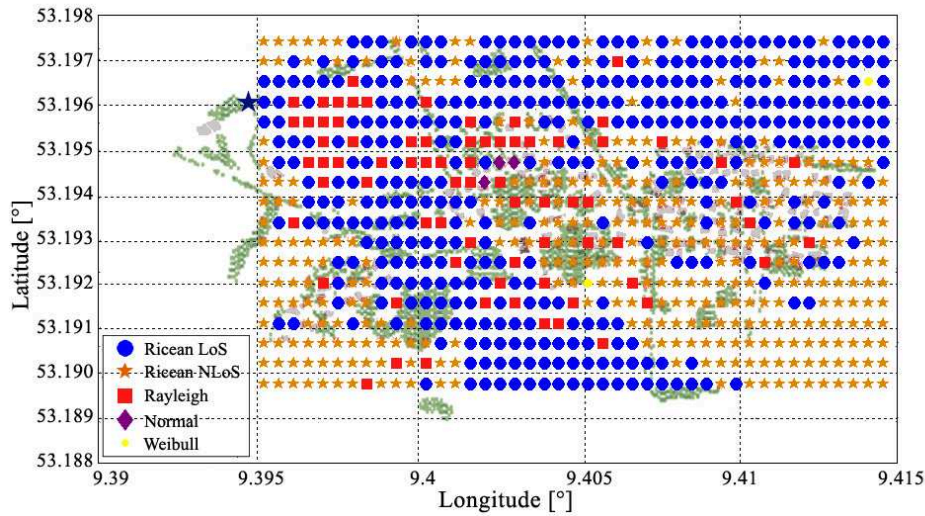
Figure 18: Fading distribution of the generated area based on the ray tracing model (purple X: Base station, green structure: the vegetation, grey structure: the buildings). It evenly follows Ricean (LoS) and Ricean (NLoS) distribution

Note that the antennas used in the model are different from what we used on the actual measurement, which adding more discrepancies to the results. As analysed above, the generated model does not represent the actual condition of the area and cannot be used to further analyse the channel characteristics of the real system. However, this simplified model will later be used to investigate the performance of the proposed algorithm for predicting the optimal relay position described in Section 3.4.

2.3.4 *Simulation Model*

In this thesis, the effects of employing relay technology to the performance of WiMAX systems are investigated through MATLAB simulation. The simulation used is taken from the WiMAX simulator studied in [33] which is based on the OFDM PHY in IEEE 802.16 − 2004 standard [6]. Some modifications are introduced to make it complies with the OFDMA PHY in

Parameter	Value
Number of reflections	max. 6
Number of diffractions	1
Buildings height [m]	$4-6$, max. 11
Trees height [m]	15, max. 22
Ray tracing method	SBR
Base Station Parameters	
Antenna type	Horn
Antenna height [m]	25
Transmit power [dBm]	35
Antenna gain [dBi]	17
Relay Parameters	
Antenna type	Omnidirectional
Relay antenna height [m]	2
Transmit power [dBm]	30
Antenna gain [dBi]	0
Receiver Parameters	
Antenna type	Omnidirectional
Receiver antenna height [m]	2
Antenna gain [dBi]	0

Table 5: Wireless Insite parameters

IEEE $802.16 - 2009$ [1] standard. The parameters used in the simulation are listed in Table 6.

Parameter	Value
Bandwidth, BW (MHz)	5
Frequency carrier (GHz)	3.5
Sampling factor, n	28/25
Guard time ratio, G	1/8
FFT size, N_{FFT}	512
Sampling frequency, F_s (MHz)	5.6
Frame duration (ms)	5
DL:UL	$4 : 1$
Modulation and coding scheme	16 QAM 1/2
Number of used subcarriers, N_{used}	360
Number of pilot subcarriers, N_{pilot}	60
Number of training symbols, $N_{training}$	2
Number of frames, N_{frame}	1
Total number of symbols/frame	40
Total number of bits/frame	28800
BS transmit power (dBm)	58

Table 6: MATLAB simulation parameters

Figure 19 illustrates the WiMAX OFDMA simulation chain implemented for our investigations. For simplicity reasons, the subchannelization part is omitted and only downlink transmission is considered. The STC (Alamouti coding [34]) blocks are applied for multi-antenna cases. Furthermore, a perfect synchronization and channel estimation in each receiving node are considered.

Our system, unless otherwise stated, is considered for single user communications. Hence, the MAI caused by other signals from other concurrent users is also disregarded. The MAI case will be considered only for multi-user scenario which will be discussed in Section 5.3. Moreover, throughout this thesis we assume that the relay node transmits and receives in an orthogonal channel (in time/frequency/space) to avoid self-interference or feedback from the relay transmit antenna(s) to the relay receive antenna(s).

2.4 CHAPTER SUMMARY

In this chapter, we presented a field measurement and analyses of our WiMAX system deployed in suburban area of Hetzwege, Germany. From
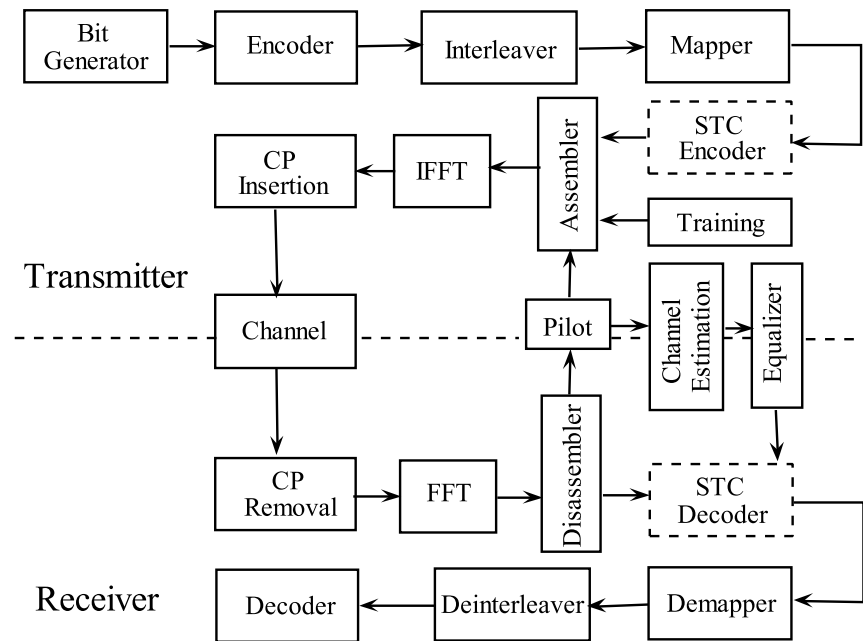
Figure 19: WiMAX OFDMA simulation chain

the measurement results, it can be deduced that Hetzwege area can be classed as a SUI type A terrain model (hilly terrain with moderate-to-heavy Tree Density). Nevertheless, its small scale fading characteristics are closer to the SUI-3 channel model which has the type B terrain characteristics. Also from our large scale fading investigation, after comparing with the measurement results for LoS and NLoS cases, the COST-231 Hata model yields less mean error than the SUI type A model. In fact, for the NLoS case, the former nearly agrees with the LS results. Furthermore, our small scale fading analysis shows that Hetzwege area has predominately Ricean fading characteristic with K-factor's mean value of 10.32 dB. Moreover, the RMS delay and the maximum excess delay value are also derived resulting 0.38 μs and 1.20 μs, respectively, which lead into conclusion that the WiMAX system on the measured area does not experience a frequency selective fading.

RELAY BASED WIRELESS TECHNOLOGY

As mentioned in the first chapter, ITU-R specified the IMT-Advanced requirements for the 4G next-generation mobile wireless broadband communication systems [35]. In the 4G broadband wireless system, a very high performance in terms of data rate or throughput of internet access has become a compulsory demand. The IMT-Advanced system specifies a peak data rates of up to 100 Mbps and 1 Gbps for high mobility environments (up to 350 km/h) and low mobility environments (up to 10 km/h), respectively.

Beside the ever increasing demand of high data rate system, other issues such as larger coverage, low deployment cost, and longer network lifetime have also become major challenges. For many years, relay technology has been actively studied and considered as one foreboding option to cope with these demands. It has also been proven in many researches that relay technology could exploit diversity and extend the coverage [36][37][38][39][40]. Because of its promising performance, relay has been included in the standardization e.g., the Third Generation Partnership Project (3GPP) LTE-Advanced [41] and the IEEE 802.16m [5].

The rest of this chapter is organized as follows. Section 3.1 provides a short overview of a relay channel capacity reported in several papers. In Section 3.2, cooperative diversity scheme is discussed. Section 3.3 presents the relaying strategies and their performance comparison. An algorithm to find an optimal position of the relay is proposed in Section 3.4, and the summary of this chapter is given in Section 3.5.

3.1 OVERVIEW OF RELAY CHANNEL CAPACITY

The capacity of the wireless relay channel has been widely studied. Nevertheless, the capacity of the general relay channel has not yet been established. Relay capacity depends on the processing capability of the relay node, i.e., full-duplex or half-duplex. A full-duplex relay means that the relay can transmit and receive in the same frequency band and at the same time. This model is often used to study the fundamental features of a relay channel. However, a full-duplex relay is difficult and expensive to put into practice due to the need of a robust receiver front-end and an efficient cross interference cancellation between the transmitted and the received signal caused by the high orders of power difference between both signals ($\sim$ 100dB). Nevertheless, counting on the advanced analog processing devices together with an efficient interference suppression technique, a full-duplex relay implementation could potentially be realised. For example, as investigated in [42] with pre-nulling technique, in [43] [44] with zero forcing technique,

and in [45] with weight filter technique. On the contrary, a half-duplex relay is easier to be implemented since it receives and transmits not simultaneously by using orthogonal signals or through orthogonal channels (time/frequency). Hence, it introduces delays and less spectral efficiency compared to the full-duplex system.

For a classical relay channel as firstly suggested by Van der Meulen (1971) in [46], the lower and upper bounds of the relay channel capacity are obtained for the discrete, memoryless single-relay channels. The capacity of Gaussian channels are studied in [37] [47], and [48] for single-relay and multi-relay channels, respectively. The asymptotic capacity of relay systems has been studied in [49] which shows that in a dense relay network as the number of relay nodes increases, the capacity per node sinks to zero. Also in [50] which proves that under a proposed relay traffic pattern, the capacity of a size n relay network abides by $\log n$ bits per second, hence improving the capacity per node as n increases. In fading environment, the ergodic capacity of relay systems is studied in [51], [52], and [53]. In [54], the authors present the outage capacity analysis for cooperative relay systems based on high SNR assumptions.

Relay transmission with multiple-antenna nodes (MIMO relay) are also gaining much interest. In [55], tradeoffs between the diversity and multiplexing are analysed for various MIMO relay channels. The capacity bounds of MIMO relay channels have been found in [56] and the references therein. Furthermore, in [57], the SER is analysed for beamforming in two-hop AF relay networks with the source and the destination deploying multiple antennas. In [58] and [59], performance analysis of orthogonal space-time codes (OSTBC) transmission in cooperative relay networks is presented for the DF strategy and and the AF strategy, respectively. Moreover, the capacity of the MIMO relay with the presence of keyhole effects is firstly introduced by Chizhik et al in [60] and by Levin et al in [61] for single keyhole case and multi-keyhole case, respectively.

3.2 COOPERATIVE DIVERSITY SCHEME

Cooperative diversity is also defined as user cooperation [38][39] which corresponds to the relay concept. The idea of cooperative diversity is to improve the system performance by exploiting the inherent characteristic of wireless medium which propagates the signal not only to the destination node but also to neighbouring nodes [62]. With the fact that each link has an independent channel fading statistic (spatial diversity), the neighbouring nodes can contribute by relaying the copy of the received signal to the destination node. The destination node will combine and decode the received signals using a specified combining method. Therefore, it offers a means of so-called virtual MIMO, that is to profit the gain of using multiple antennas by equipping each node with only a single antenna or less antennas. Subsequently, a power gain can be profited due to the fact that

each of the relays adds additional transmit power. Macrodiversity gain which allows to combat shadowing can also be achieved through spatial diversity. Nevertheless, there are trade-offs related with the coordination costs, i.e., twice more bandwidth is required for half-duplex system; the cost of additional hardware to relay between one another; the power allocation and the network management need to be considered.

As depicted in Figure 20, cooperative diversity scheme is distinguished in two stages process. At the first stage, the source node (S) broadcasts the signal which is received by the relay node (R) and the destination (D) node. At the second stage, the relay may or may not forward the received signal orthogonally with the source node (in time/frequency/space) to the destination node, depends on the employed cooperation strategies. For example, the relay node will only forward the signal if it correctly decodes the received signal, or if only it is requested by the destination node. More about cooperation strategies can be found in [38] [51] and the references therein. However, if the distance between the source node and the destination node is too large or when the link quality in-between is very low, then the signal from the source node is negligible. So the destination node will only process the signal received from the relay node. Accordingly, a relay node in this circumstance is aimed to extend the coverage performance rather than to offer diversity to improve the throughput performance. However, by increasing the number of relay nodes to assist the transmission, a spatial diversity gain is expected, provided that each relay undergoes independent fading paths. By establishing multiple independent paths, the reliability of the system increases with the fact that it is less probable that all links are severely degraded.
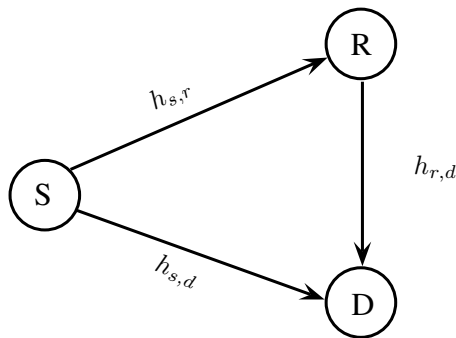
Figure 20: Cooperative diversity

In this thesis, we consider that the relay node always forwards the received signal and operates in half-duplex manner. As previously discussed, half-duplex means the relay node transmits and receives at different instant, which can reduce the complexity in the interference cancellation between the relay's receive and transmit antennas. Furthermore, in this work, the

maximum ratio combining (MRC) is chosen as the combining method at the destination node.

3.3 RELAY STRATEGIES

Beside on the cooperation protocol, the performance of the relay channel depends as well on the relaying strategy. Many different strategies have been proposed in literatures, nevertheless they are all basically rooted from the two well-known strategies, which are the Amplify-and-Forward (AF) and the Decode-and-Forward (DF). In the following sections, more details about each strategy will be discussed and a brief BER performance comparison of both strategies in a SISO relay system under Rayleigh channel will also be presented.

3.3.1 *Amplify-and-Forward*

As the name implies, the relay with AF strategy simply forwards the signal by amplifying the received signal, likewise the noise at the relay node irrespective of the SR link quality. Thus, this method does not introduce significant processing delay and has low complexity, yet its performance degrades at low SNR. Moreover, since the forwarded signal might undergo a heavy amplitude fluctuation caused by the channel, it is very sensitive to a non-linear amplifier distortion. Such issue can actually be solved by using a highly linear amplifier which is very costly in terms of power and price.

In the basic AF scheme, at the first stage the source transmits the signal to both the relay and the destination, where the received signals at each node are expressed as follows

$$y_{s,r} = h_{s,r} \sqrt{P_s}\, x_s + w_{s,r}, \qquad (3.1)$$

$$y_{s,d} = h_{s,d} \sqrt{P_s}\, x_s + w_{s,d}, \qquad (3.2)$$

where $y_{s,r}$ is the signal received at the relay and $y_{s,d}$ is the signal received at the destination. x_s and $\sqrt{P_s}$ are each the transmitted signal from the source and the transmit power at the source, respectively. $h_{s,r}$ is the channel impulse response between the source and the relay, and $h_{s,d}$ is the channel impulse response between the source and the destination. $w_{s,r} \sim \mathcal{CN}(0, \sigma_{s,r}^2)$, $w_{s,d} \sim \mathcal{CN}(0, \sigma_{s,d}^2)$ are the additive white Gaussian noise at the relay and at the destination, respectively.

In the second stage, the relay normalizes the signal by scaling the received signal y_r, then transmits it to the destination with a transmit power of P_r. The relayed signal received at the destination is expressed as follows

$$y_{r,d} = h_{r,d} \sqrt{P_r}\, x_r + w_{r,d}, \qquad (3.3)$$

where x_r and $\sqrt{P_r}$ are each the transmitted signal from the relay and the transmit power at the relay, respectively. $h_{r,d}$ is the channel impulse response between the relay and the destination, and $w_{r,d} \sim \mathcal{CN}(0, \sigma_{r,d}^2)$ is the additive Gaussian noise at the destination. We can define the transmitted relay signal as

$$x_r = \beta\, y_{s,r}, \tag{3.4}$$

where β is the scaling factor given by Equation 3.5 if the relays knows the CSI to calculate the channel gain $|h_{s,r}|^2$ [63] [64]; or by Equation 3.6 if the CSI is unavailable at the relay [65] [66],

$$\beta^{(1)} = \frac{1}{\sqrt{E[\,|y_{s,r}|^2 \mid |h_{s,r}|^2\,]}} = \frac{1}{\sqrt{P_s\,|h_{s,r}|^2 + \sigma_{s,r}^2}}, \tag{3.5}$$

$$\beta^{(2)} = \frac{1}{\sqrt{\sigma_{s,r}^2 + \sigma_{s,r}^2}}, \tag{3.6}$$

where $\sigma_{s,r}^2$ is the variance of the relay's received signal. Hence, the received signal $y_{r,d}$ at the destination node can be expressed as

$$y_{r,d} = \sqrt{\frac{P_s\,P_r}{P_s\,|h_{s,r}|^2 + \sigma_{s,r}^2}}\; h_{s,r}\, h_{r,d}\, x_s$$

$$+ \sqrt{\frac{P_r}{P_s\,|h_{s,r}|^2 + \sigma_{s,r}^2}}\; h_{r,d}\, w_{s,r} + w_{r,d}. \tag{3.7}$$

Let us define $\gamma_{s,r} = P_s|h_{s,r}|^2/\sigma_{s,r}^2$, $\gamma_{r,d} = P_r|h_{r,d}|^2/\sigma_{r,d}^2$, and $\gamma_{s,d} = P_s|h_{s,d}|^2/\sigma_{s,d}^2$ be the received SNR of the SR signals, the RD signals, and the SD signals, respectively. If non-cooperative mode is assumed, that is when the destination node can only receive signals from the relay node, only $y_{r,d}$ is considered. From Equation 3.7, the received SNR at the destination node can be computed as

$$\gamma_{AF,NC} = \frac{\frac{P_s P_r}{P_s|h_{s,r}|^2 + \sigma_{s,r}^2}|h_{s,r}|^2|h_{r,d}|^2}{\frac{P_r \sigma_{s,r}^2}{P_s|h_{s,r}|^2 + \sigma_{s,r}^2}|h_{r,d}|^2 + \sigma_{r,d}^2} = \frac{\gamma_{s,r}\gamma_{r,d}}{\gamma_{s,r} + \gamma_{r,d} + 1}, \tag{3.8}$$

then the capacity is given by [67]

$$C_{AF,NC}(\gamma_{s,r}, \gamma_{r,d}) = \frac{1}{2}\log\left(1 + \frac{\gamma_{s,r}\gamma_{r,d}}{\gamma_{s,r}\gamma_{r,d} + 1}\right). \tag{3.9}$$

Meanwhile, if cooperative mode is considered, $y_{s,d}$ (3.2) and $y_{r,d}$ (3.7) are merged using the MRC method. Thus, the combined signal $\hat{y}_d$ can be expressed as

$$\hat{y}_d = \frac{\sqrt{P_s}h_{s,d}^*}{\sigma_{s,d}^2}\, y_{s,d} + \frac{\sqrt{\frac{P_s P_r}{P_s|h_{s,r}|^2 + \sigma_{s,r}^2}}\, h_{s,r}^* h_{r,d}^*}{\frac{P_r}{P_s|h_{s,r}|^2 + \sigma_{s,r}^2}|h_{r,d}|^2\, \sigma_{r,d}^2 + \sigma_{s,d}^2}\, y_{r,d}. \tag{3.10}$$

$$\gamma_{AF,C} = \frac{P_s |h_{s,d}|^2}{\sigma_{s,d}^2} + \frac{P_s |h_{s,r}|^2 / \sigma_{s,r}^2 \quad P_r |h_{r,d}|^2 / \sigma_{r,d}^2}{P_s |h_{s,r}|^2 / \sigma_{s,r}^2 + P_r |h_{r,d}|^2 / \sigma_{r,d}^2 + 1}$$

(3.11)

$$= \gamma_{s,d} + \frac{\gamma_{s,r} \gamma_{r,d}}{\gamma_{s,r} + \gamma_{r,d} + 1}.$$

$$C_{AF,C}(\gamma_{s,r}, \gamma_{r,d}, \gamma_{s,d}) = \frac{1}{2} \log \left(1 + \gamma_{s,d} + \frac{\gamma_{s,r} \gamma_{r,d}}{\gamma_{s,r} \gamma_{r,d} + 1} \right). \quad (3.12)$$

Afterwards, the SNR after the MRC process can be described as in Equation 3.11. Furthermore, the capacity of AF strategy with diversity combining is given in Equation 3.12 [67].

The optimal diversity gain achieved by using the AF relaying strategy, given the multiplexing gain $r \leqslant K$ [68], is upper bounded by [69]

$$d(r) \leqslant (1 - r) + (K - 1)(1 - \frac{r}{1 - a})^+, \quad (3.13)$$

where $(.)^+$ means $\max\{x, 0\}$ and K is the number of relay nodes. a is the waiting interval of the relay node before starting the transmission, which is set to 0.5 to obtain the upper bound. The first term represents the source-destination transmission and the second term corresponds to the source-relay(s)-destination transmission.

3.3.2 *Decode-and-Forward*

A relay in a basic DF mode decodes and re-encodes the received signal before forwarding it to the destination. The performance relies upon the reliability of the relay to correctly decode the received signal. Hence, it introduces processing delay and has higher computational complexity. Even so, it is often reported that it has better performance than AF. However, it is reported in [62], that the AF strategy could in fact perform better than the DF strategy in multihop channel under a total power constraint, if the relay nodes close to the destination. This is owing to the fact that the DF strategy may propagate decoding errors along the channel. Therefore, the DF strategy will most likely perform better than the AF strategy, if the relay is near to the source.

As in the AF strategy, by the basic DF strategy [67], the received signals at the relay and the destination at the first stage are expressed in Equation 3.1 and 3.2, respectively. Then at the second stage, the relay transmits the re-encoded signal x_r to the destination. If the relay encodes using the same codebook as in the source, hence $x_r = x_s$. Or else x_r is the re-encoded version of x_s which may contain error if the error correction code is not

implemented. The received signal at the destination node can be expressed as

$$y_{r,d} = h_{r,d} \sqrt{P_r} \, x_r + w_{r,d}, \tag{3.14}$$

where $y_{r,d}$ is the relayed signal received at the destination. x_r and $\sqrt{P_r}$ are the transmitted signal from the relay and the transmit power at the relay, respectively. $h_{r,d}$ is the channel impulse response between relay and destination. $w_{r,d} \sim \mathcal{CN}(0, \sigma_{r,d}^2)$ are the additive white Gaussian noise at the destination.

For a non cooperative mode, where only $y_{r,d}$ is taking into account, the capacity of the DF strategy is given by [67]

$$C_{DF,NC}(\gamma_{s,r}, \gamma_{r,d}) = \frac{1}{2} \min \left\{ \log_2 (1 + \gamma_{s,r}), \log_2 (1 + \gamma_{r,d}) \right\}, \tag{3.15}$$

where $\gamma_{s,r} = P_s |h_{s,r}|^2 / \sigma_{s,r}^2$ and $\gamma_{r,d} = P_r |h_{r,d}|^2 / \sigma_{r,d}^2$ are the receive SNR from the source node to the relay node, and from the relay node to the destination node, respectively. In the cooperative mode, the MRC-combined signals y_d at the receiver node can be written as

$$y_d = \begin{bmatrix} y_{s,d} \\ y_{r,d} \end{bmatrix} = \begin{bmatrix} \sqrt{P_s} h_{s,d} \\ \sqrt{P_r} h_{r,d} \end{bmatrix} x_s + \begin{bmatrix} w_{s,d} \\ w_{r,d} \end{bmatrix}, \tag{3.16}$$

where $y_{s,d}$ and $y_{r,d}$ are weighted with $\sqrt{P_s} h_{s,d}^*$ and $\sqrt{P_r} h_{r,d}^*$ [67], respectively, inducing

$$\begin{aligned} \widehat{y}_d &= [\sqrt{P_s} h_{s,d}^* \ \sqrt{P_r} h_{r,d}^*] \, y_d \\ &= (P_s |h_{s,d}|^2 + P_r |h_{r,d}|^2) \, x_s + \widehat{w}_d, \end{aligned} \tag{3.17}$$

where $\widehat{w}_d = \sqrt{P_s} h_{s,d}^* w_{s,d} + \sqrt{P_r} h_{r,d}^* w_{r,d}$. And $\widehat{w}_d \sim \mathcal{CN}(0, \sigma_{s,d}^2 (P_s |h_{s,d}|^2 + P_r |h_{r,d}|^2)$ is the effective noise after the MRC. The SNR after the MRC process is thus given by

$$\gamma_{DF,C} = \frac{P_s |h_{s,d}|^2}{\sigma_{s,d}^2} + \frac{P_r |h_{r,d}|^2}{\sigma_{r,d}^2} = \gamma_{s,d} + \gamma_{r,d}. \tag{3.18}$$

Hence, the capacity is given by [67]

$$C_{DF,C}(\gamma_{s,r}, \gamma_{r,d}) = \frac{1}{2} \min \left\{ \log_2 (1 + \gamma_{s,r}), \log_2 (1 + \gamma_{s,d} + \gamma_{r,d}) \right\}, \tag{3.19}$$

under assumption that the codeword is sufficiently long and the channel is constant along a codeword transmission but may vary independently and identically for each block.

The upper bound of the optimal diversity gain for a relay system with the DF relaying strategy given the multiplexing gain r is characterized by [69] [70]

$$d(r) \leqslant K(1 - r), \tag{3.20}$$

for $K - 1$ relay nodes and $\frac{1}{K} \geqslant r \geqslant 0$.

3.3.3 *Performance Comparison*

The system considered for this investigation is a SISO system assisted with single-antenna relay node(s). To investigate the BER performance of the AF and DF relaying strategies on the system, MATLAB simulations are performed under a Rayleigh distribution flat fading channel for a single relay using the simulation model described in Section 2.3.4. The path loss scenario applied is the FSPL model. We evaluate the performance of each strategy considering the SD link (direct link) availability with parameters specified in Table 7. We study also therein the effect of the relay position or the SR and RD link qualities, represented by the distance and the SNR value, to the system performance, which indirectly also deals with the power allocation of each node.

Modulation	16QAM 1/2
Channel estimation	Perfect
Channel	Rayleigh
Path loss model	FSPL

Table 7: Simulation parameters

3.3.3.1 *Single-Relay Scenario*

The proposed system model is shown in Figure 21. There are five cases to be evaluated as summarized in Table 8. The source node and the destination node are located two kilometers apart and the relay position is in-between and located varyingly for each case. We assume that the SNR values of the SR and RD links depend on the distance, such that the larger the distance the smaller the SNR value and vice versa. The $' + X'$ sign indicates that the SNR value is X dB higher than that without relay. We can see thence, that case 5 represents the best case, while case 4 represents the worst case. For case 4, the distance between the relay node and the destination node is assumed to be very near but still ensures that the channels are uncorrelated. In our simulation, we use a distance of fifty meters, hence only an AWGN channel is implemented for this link.
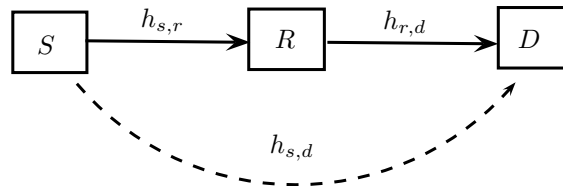
Figure 21: SISO two-hop single-antenna relay

Condition	Case 1	Case 2	Case 3	Case 4	Case 5
S-D Distance [km]	2	2	2	2	2
S-R Distance [km]	0.5	1	1.5	2	1
SNR S-R [dB]	+10	+5	+5	+0	+10
SNR R-D [dB]	+5	+5	+10	+10	+10

Table 8: Simulated single-antenna relay cases

In absence of the direct link, the results after 100 channel realisations are presented in Figure 22. The analysis is performed for the BER of 10^{-3}. It can be observed that for cases 1-3 and 5, the DF strategy always outperforms the AF strategy in all SNR regions, which is reasonable on account of the decoding gain offered by the structure of the DF strategy. Furthermore, of all the five cases, this strategy yields best performance in case 5 with ~ 9 dB enhancement, where the relay node is in the middle between the source node, and the destination node with the SNR of the SR and RD links are 10 dB higher than that of the SD link. Then, it is followed by case 1 and case 3 with ~ 5 dB improvement, that is when the link quality of the SR link is considered finer. Similarly, the AF strategy also performs equally well in the same consecutive order. As for case 2, where the relay is in the middle or when the link quality of the SR and RD links are not much favorable than the SD link, both strategies present less gain. In this case, even the AF performances of case 1 and 3 could exceed the DF performance of case 2. Furthermore, when the link qualities of the SR and SD links are identical but with a better RD link as given in case 4, the result shows in the least improvement. In this case, when the relay links are equally poor, the usage of a relay is therefore not suggested.

Also, comparing the results of case 1 (the relay node is near to the source node) and case 3 (the relay node is near to the destination node), we can resolve that without the direct link the DF strategy gives slight better gain when the relay node is nearer to the source node (a good SR link quality), which is in conformity with investigation performed by Kramer et al. in [48] [71]. Likewise, the AF strategy exhibits also almost similar performance for case 1 and 3. These results are also evidenced in [63], which stating that the AF strategy is considered for the system with the relay node located halfway between the source node and the destination node and when the transmit power is high (case 5), or when the relay node located near to the source/destination node and when the transmit power is low (case 1 and case 3).

The BER performances of the AF and DF relaying strategies for single relay where the SD link is taking into account are shown in Figure 23. It is interesting to see that for the first four cases in this instance, the AF strategy provides more performance improvement than in the previous

Figure 22: SISO two-hop AF-DF single relay performance comparison without direct link (16 QAM 1/2, Rayleigh channel, 100 channel realisations). The DF strategy yields better performance for all cases
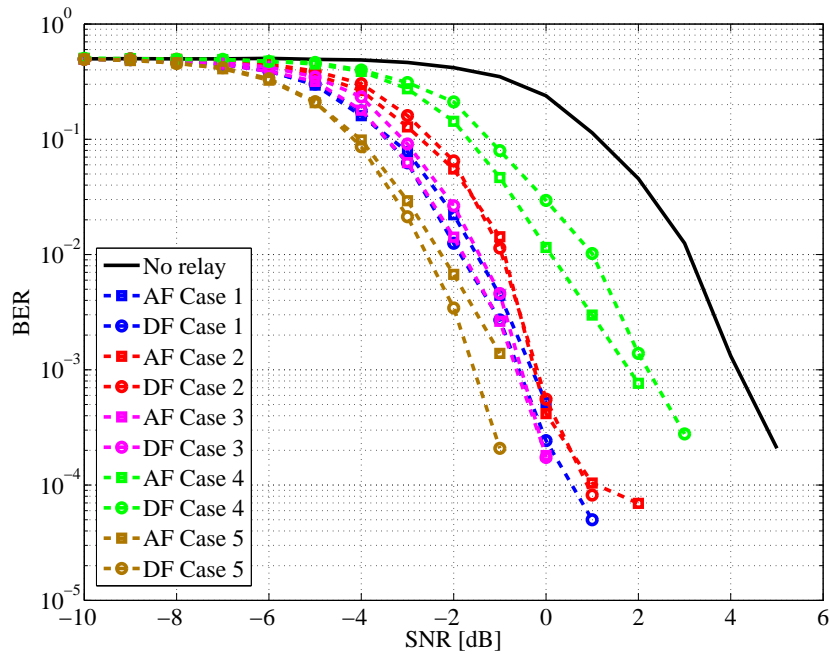
Figure 23: SISO two-hop AF-DF single relay performance comparison with direct link (16 QAM 1/2, Rayleigh channel, 100 channel realisations). The diversity offered by the SD link gives benefit for the case 4 (poor SR link), but degrades the performance of case 5 (good SR and RD links)
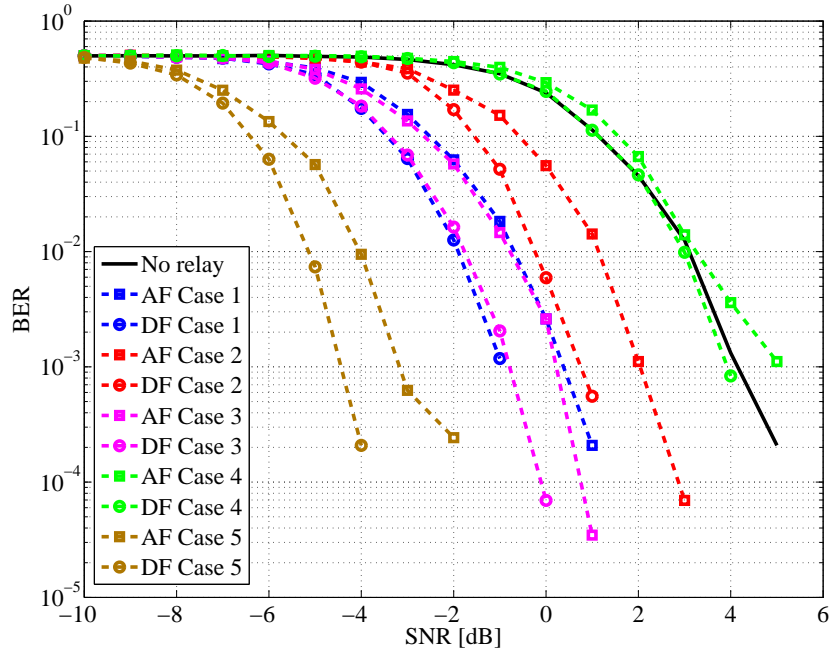
results where the SD link is discounted. In fact, it could even up those of the DF strategy. It implies that even when the SD and SR links are worse than the RD link, combining the received signal with the AF-relayed signal in the destination may result in a better outcome of around 1-2 dB, owing to the diversity gain. On the contrary, the DF strategy does not offer significant refinement compare to the former results, except for case 4 whereof it increases the result by 3 dB. Furthermore, the results for case 5 outperform other cases, therein the DF strategy has almost similar performance than the AF strategy, which is expected since the signal has a better quality hence can be forwarded with less noise or alternatively less coding errors.

In this scenario, both strategies exhibit almost similar performance in all cases. However, in contrast with the former scenario, it can be observed that when the relay node is located near to the destination node (case 3), the DF strategy demonstrates a better result. On the contrary, when the relay node is positioned near to the source node (case 1), the AF strategy shows better result. Eventually, it is demonstrated from our investigation that the performance of each relaying strategy very much depends on the relay position or link qualities as also stated in [64].

From the BER performance of the investigated scenario, it is evidenced that although the DF strategy could outperform the AF strategy at high SNR region, but both have equally low performance at low SNR region. This is in accordance to the results reported in [72] which is stating that both strategies have comparable average performance. It is therein also stated that the DF strategy only slightly better than the AF strategy, and that both strategies perform equally bad at low SNR. This is because they are equivalent to repetition coding, which relatively inefficient at low SNR [73].

3.4 RELAY POSITIONING

Relay is considered as a low-cost alternative to enhance the coverage performance of the system rather than setting up an additional BS. Nevertheless, as it has been discussed in the previous section, employing more relays does not render linear effect. Hence, it should be emphasized that for an efficient network deployment, the number of relays employed should be kept to a minimum while still ensuring a good coverage of the service area [74].

As also mentioned in [51] [63] [64] [66] [72] and likewise observed in the previous section, the SR and RD link qualities or more precisely the relay position have a significant impact to the system performance. The aforementioned references investigate the position optimization jointly with the energy allocation as part of the resource allocation optimization. However, all of them do not consider the effect of terrain irregularities to the channel conditions, which makes the distance alone not representative

enough to describe the performance of a relay system. In this thesis, we will focus on the location optimization with constant energy allocation taking terrain irregularities (i.e., represented by the RSSI value distribution in the area) into account.

3.4.1 *Algorithm Proposal*

On the following, we propose a simple algorithm to allocate the optimal relay position based on the RSSI value distribution. The aim is to improve the coverage performance of the system, although it can also be used to increase the system throughput by adjusting some additional parameters (i.e., antenna direction). The proposed algorithm is divided into two subalgorithms. The first subalgorithm divides the cell equally into slot(s) then finds for each slot the optimal relay position. The second subalgorithm groups the low-reception nodes then locates the optimal relay position for each group. The first algorithm is intended for the area that has sparse low-reception nodes. On the contrary, the second algorithm is for the area that has clustered/grouping low-reception nodes.

The proposed algorithm is defined as follows,

1. Define a threshold value to classify whether a node has a good or a bad reception. It can be set according to any metric, for example in our work, we adopt the receiver minimum sensitivity [1] (R_{sens}) level equation below [1]:

$$R_{sens} = -114 + SNR_{Rx} - 10\log_{10}(R)$$

$$+ 10\log_{10}\left(\frac{F_S \, N_{Used} \, 10^{-6}}{N_{FFT}}\right) + ImpLoss + NF, \tag{3.21}$$

where SNR_{Rx} is the receiver SNR based on the MCS used for the AWGN channel with BER $< 10^{-6}$ as per Table 545 in WiMAX 802.16 − 2009 standard [1]. R is the repetition factor which is defined as 2. F_S is the sampling frequency and equals to $5.6 \, 10^6$ Hz (see Table 3). $ImpLoss$ indicates the implementation loss which is specified as 5 dB. NF is the receiver noise figure which is set to 8 dB. In addition, an averaged fade margin[2] value (fm) is also considered in our metric, which is defined as,

$$fm = mean(RSSI - R_{sens}). \tag{3.22}$$

Subsequently, a node is considered to have a good reception when its RSSI value at least equal to the threshold value obtained by adding 3.21 and 3.22, otherwise it is considered to have a bad reception.

---

1 Receiver sensitivity is the minimum acceptable value of the received power required to allow an acceptable BER performance.

2 Fade margin (in dB) is the difference between the received signal strength with the minimum signal strength required by the system. Therefore, a system with a high fade margin has also high reliability.

2. Divide the area into slots. There are two subalgorithms defined which can be chosen according to the needs. The first subalgorithm divides the area into slots with equal size and assigns a relay node for each slot. Meanwhile the second subalgorithm groups the low-reception nodes and assigns a relay node for each group. The difference is mainly on the form and the size of slot/group. The subalgorithms are defined as follows

   First subalgorithm:

   - Divide the area into N slots, which can be set manually or by calculating the percentage of the local low-reception points in the designated slot, `level_err_local(n)`. If the latter is the case, then we consider initially the whole area as one slot (N = 1), then divide the area equally into smaller slots until exists a slot with `level_err_local(n) > th_err`. `th_err` specifies the percentage of nodes with an RSSI value below the threshold. Therewith, for each slot we seek the area that has most nodes with low RSSI values, which presumptively needs a relay. Afterwards, the slot radius (`slot_dist_diff`) is calculated by defining the distance between two midpoints. This value can also be specified according to the relay transmit antenna properties, such as the antenna height and the EIRP which define the transmit range and therefore can also be used to specify the slot radius. Afterwards, we decide whether the slot with `level_err_local(n) < th_err` should or should not be assigned a relay. Since it can also be considered that the slot has a good enough performance therefore no relay is necessary.

   - Next step is to find nodes in every slot with the RSSI value above or equal to the defined threshold, and with the most number of neighbours with low RSSI values. Neighbour node is a node within radius of `slot_dist_diff/2` (if antenna parameter is unknown) or within antenna range (if antenna parameter is known). This is intended to avoid choosing a relay location among high P_{Rx} nodes. Keep in mind that we should focus mainly on the low reception nodes.

   Second subalgorithm:

   - Group the low-reception nodes located near to each other into slot(s). It is assumed that a slot should at least contain ten nodes. If it is less, then it will not be considered as a slot.

   - In every slot, find node(s) with the RSSI value above the threshold and with the most number of low-reception neighbours.

3. For each slot, there could be several candidate nodes yielded from the previous step. One node is chosen of all which provides mostly larger LoS angle-of-arrival to its neighbour nodes, compared to the LoS angle-of-arrival from the BS to the candidate's neighbour nodes. This is intended to consider the case as depicted in Figure 24. That

is, when there exists a neighbour node with a low-reception caused by the presence of obstruction in the direction of the BS. Thus, we are avoiding of taking a candidate node which has similar angle-of-arrival as the BS, since the candidate node (when relaying a signal) is presumably cannot reach the intended node as well. In the example on Figure 24, by considering the angle-of-arrival, Candidate 1 is more preferably chosen as a relay than Candidate 2.
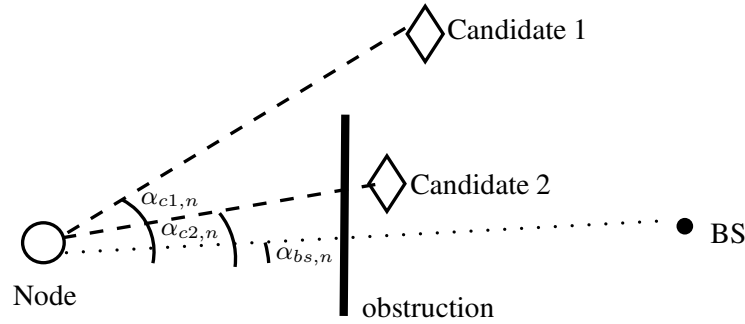
Figure 24: LoS angle-of-arrival (α)

4. If the antenna parameters are not defined yet, then they can be now specified according to the relay position and the needed transmit range.

3.4.2 *Applicability*

For our investigation, we consider the simplified generated model of Hetzwege city as the object model. Here, the receiver nodes are distributed along the area with 30 m spacing. Afterwards, a ray tracing calculation is performed by the Wireless Insite to produce the RSSI and the PDP values as already described in Section 2.3.3. By following steps from the proposed algorithm on the previous section, one or several nodes are subsequently chosen as candidate(s) for relay position(s). It is assumed that the slot is automatically assigned and the antenna parameters are unknown.

Initially, the threshold value is defined based on the receiver sensitivity for QPSK(1/2) modulation scheme referring to the Equation 3.21, thus $R_{sens} = -93.06$ dB. The fade margin is calculated from the RSSI values retrieved from the ray tracing process of nodes that undergo NLoS links only, which yields $fm = 13.65$ dB. Therefore, the threshold value is set to -79.41 dB. Subsequently, it can be calculated that there are 63.9% of the nodes with the RSSI values higher than the threshold value.

3.4.2.1 *First Subalgorithm*

Following the second step, by adjusting th_err = 55%, we get the area divided into four slots with the slot radius (slot_dist_diff) of 630 meters, where each slot has level_err_local of 33.33%, 77.25%, 3.41%, and 27.38%, respectively.

Using the parameters calculated in the first and second steps and following the first subalgorithm, the third step yields the selected relay locations for the defined slots marked in red-filled circle, as shown in Figure 25. The blue-star marks the location of the BS. The nodes with blue-cross marking denote the low-reception nodes. The magenta-diamond nodes mark the first ten candidates having a high RSSI value and the most number of low-reception neighbours. The third slot is not assigned with a relay because the slot is considered to have a good performance hence it is believed that adding a relay to the slot will only induce more cost than performance gain.

For comparison, another trial is performed by defining the slot manually. For this case, we assume that we want only one slot, thus only one relay is expected for the whole cell. As shown in Figure 26, the relay position is marked with the red-filled circle.

Finally, based on the relay node position and the location of low-reception nodes, the relay antenna parameters can be adjusted subsequently. For example, for the first result a directional antenna with less power can be used in slot 1 and slot 4, and an omnidirectional antenna for slot 2. Meanwhile, for the second result, an omnidirectional antenna can be used to cover the area. Intuitively, this subalgorithm is well suited if the relay is intended not only to overcome coverage gaps but also to improve the throughput performance within a slot.

3.4.2.2 *Second Subalgorithm*

On the other hand, based on the second subalgorithm, the second step divides the area into three slots/groups. As depicted in Figure 27, the nodes belong to each group are marked by red cross, red square and red circle, for the first, second and third groups, respectively. Other low-reception nodes marked with blue cross that do not belong to any slot, are simply ignored. Next, assuming the neighbour radius of $60\sqrt{2}$ m, the third step generates the selected relay position for each slot which is plotted as the red-filled circle.

In this subalgorithm, the relay is concentrated to a group of low-reception nodes. Therefore, it is proposed for the case where the relay is mainly aimed to overcome the coverage gaps. In this case, a power allocation and an antenna direction adjustment are the major concerns to the system performance.
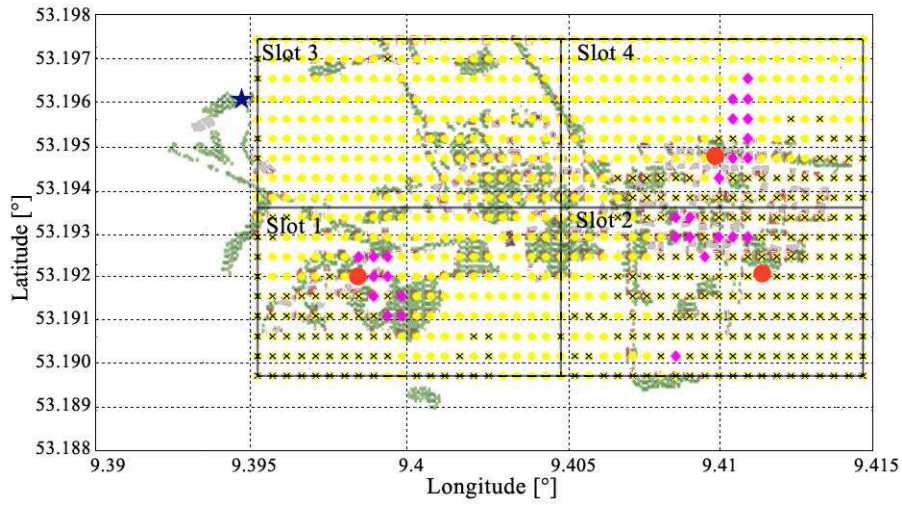
Figure 25: Relay positioning, first subalgorithm: selected relay position, automatic slotted (blue-star: the BS, red-circle: the proposed relay location, magenta-diamond: the first 10 candidates for relay position, blue-cross: the low-reception node)
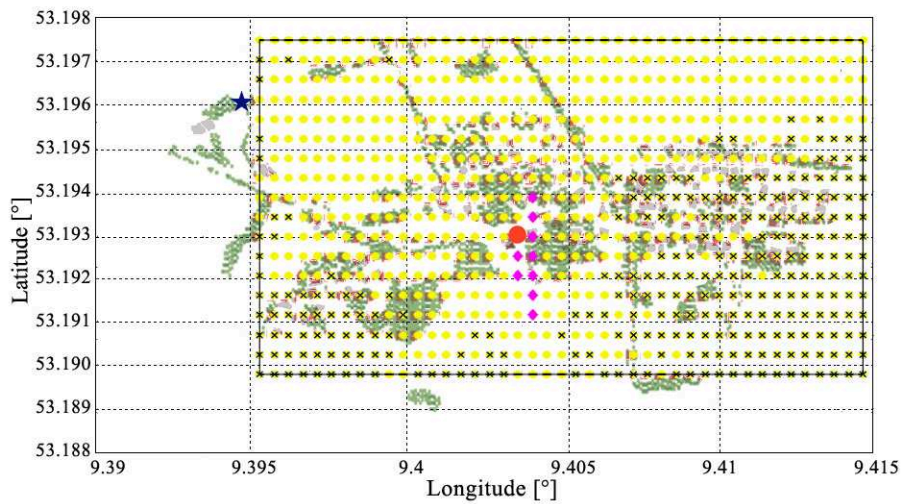
Figure 26: Relay positioning, first subalgorithm: selected relay position, manual slotted (blue-star: the BS, red-circle: the proposed relay location, magenta-diamond: the first 10 candidates for relay position, blue-cross: the low-reception node)
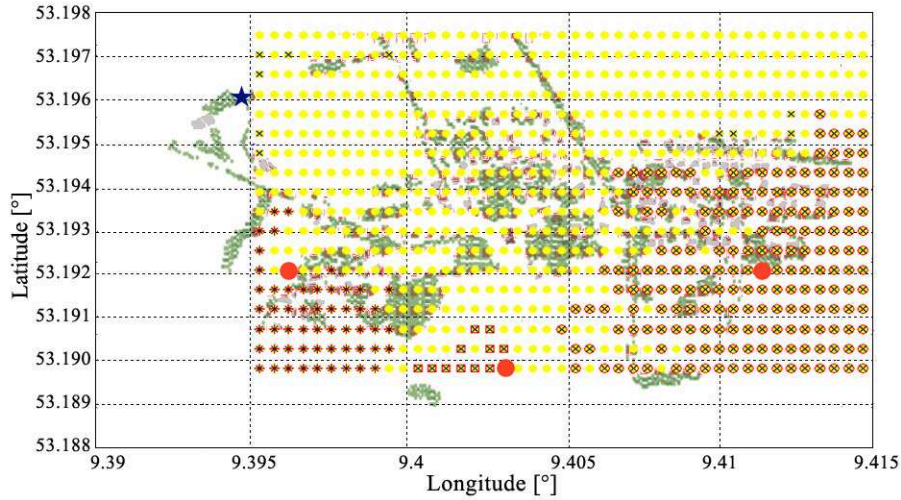
Figure 27: Relay positioning, second subalgorithm: selected relay position (blue-star: the BS, red-filled-circle: the proposed relay location, red-cross: the first group node, red-square: the second group node, red-empty-circle: the third group node, blue-cross: the low-reception node)

3.4.3 *Performance Evaluation*

For each relay scenario generated from the proposed algorithm in the previous section, a ray tracing process is performed by using the Wireless Insite tool to get the RSSI value of each node. The RSSI value taken is the strongest RSSI value from either the BS or the relay. Afterwards, the performance of the proposed algorithm is evaluated by simply identifying the appropriate MCS according to the RSSI value for each node. It is done by comparing the RSSI value to the minimum allowed RSSI value for each MCS. That is, in this work, the sum of the receiver sensitivity and the fade margin. The receiver sensitivity value of each MCS is obtained from Equation 3.21 with the same parameters as used in Section 3.4.1. The fade margin is also set to 13.65 dB. The mapping of the MCS to the RSSI values is listed in Table 9.

Therefrom, the throughput improvement of the system can be estimated from the MCS used in the system. The more percentage of higher MCS used, the better the throughput of the system. As shown in Figure 28, the system with relay(s) allows for a higher percentage in 64QAM (5/6). This indicates that the throughput of the system is improved compared to the system without the relay. Moreover, the MCS improvement, as presented in Figure 29, shows that the systems with the proposed relay position(s) provide an MCS betterment of 50.13%, 33.89%, and 39.81% for the first subalgorithm with four slots, the first subalgorithm with one slot, and the second subalgorithm with three groupings, respectively. It can also be noticed from both figures that the system which has more relays understandably yields higher

MCS	Minimum RSSI
QPSK (1/2)	−79.41 dB
QPSK (3/4)	−76.41 dB
16QAM (1/2)	−73.91 dB
16QAM (3/4)	−70.41 dB
64QAM (2/3)	−68.41 dB
64QAM (3/4)	−66.41 dB
64QAM (5/6)	−64.41 dB

Table 9: Mapping of the MCS to the RSSI value

throughput performance.

Meanwhile, the system coverage improvement can be observed from the reduced percentage of the blank spots or the coverage holes in the system, as depicted in Figure 30. It can be seen that the system with relay(s) offers $70\% - 98\%$ betterment in eliminating the coverage holes compared to the system without the relay. Similarly for both metrics, the throughput and the coverage performances, the system of the first subalgorithm with four slots yields more improvement, succeeded by the system of the second algorithm with three groupings, and the system of the first algorithm with one slot, respectively.

It can be reasoned out by taking example of the system with the least performance, i.e., the system of the first subalgorithm with one relay. The system does offer a substantial gain of more than 30% throughput improvement and 71% blank spot reduction. The performance evaluation discussed in this section is obviously not valid enough to state that the proposed algorithm offers the most optimal solution, since it is not compared to another algorithm. Therefore, this performance evaluation issue would be considered as the limitation of this thesis. Nevertheless, the evaluation results can be used as a measure to estimate whether the improvement offered by the relay(s) is quite significant and can compensate for the complexity.

3.5 CHAPTER SUMMARY

In this chapter, we have discussed a brief overview of a relay concept in the wireless technology. We have described as well the two most-known relaying strategies, namely, the AF and the DF. The BER performances of both strategies are analysed and compared for several cases under a flat fading Rayleigh distributed channel. It has been simulatively proven that the performance varies accordingly to the relay location, and the SR and RD link qualities or the power allocation. Yet for each case, the DF strategy always outperforms the AF strategy although only slightly. It is also
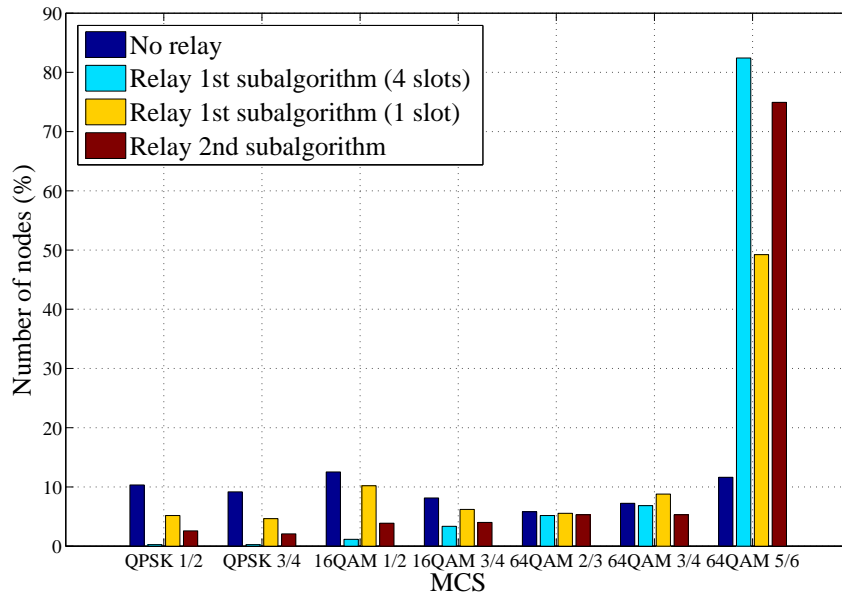
Figure 28: The increasing number of nodes with the highest MCS (64 QAM 5/4). The proposed relay schemes improve the RSSI which accordingly increase the MCS that can be used by the node. (see Table 9)
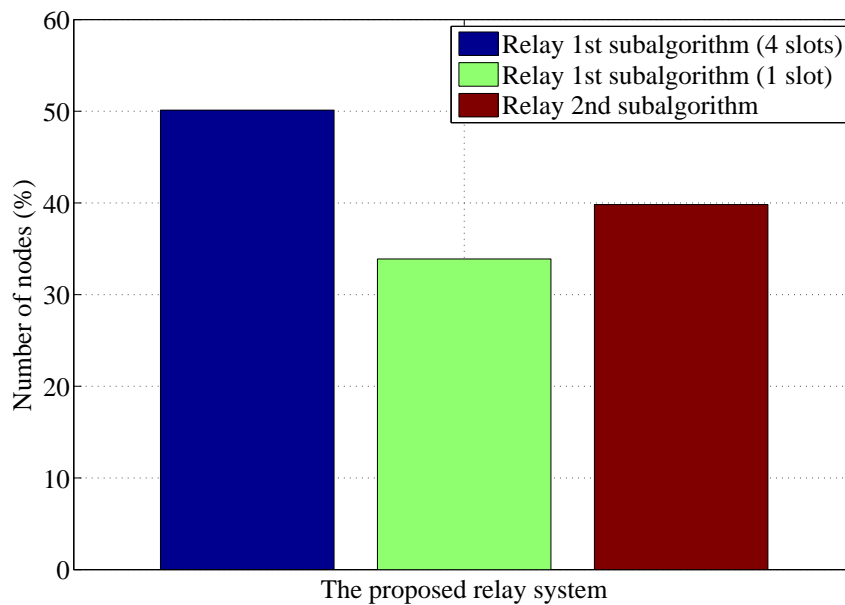
Figure 29: The percentage of nodes which experience the MCS improvement. The 1st subalgorithm (4 slots), the 1st subalgorithm (1 slot) and the 2nd subalgorithm, each induces 50.13%, 33.89%, 39.81% of the nodes experience the MCS betterment
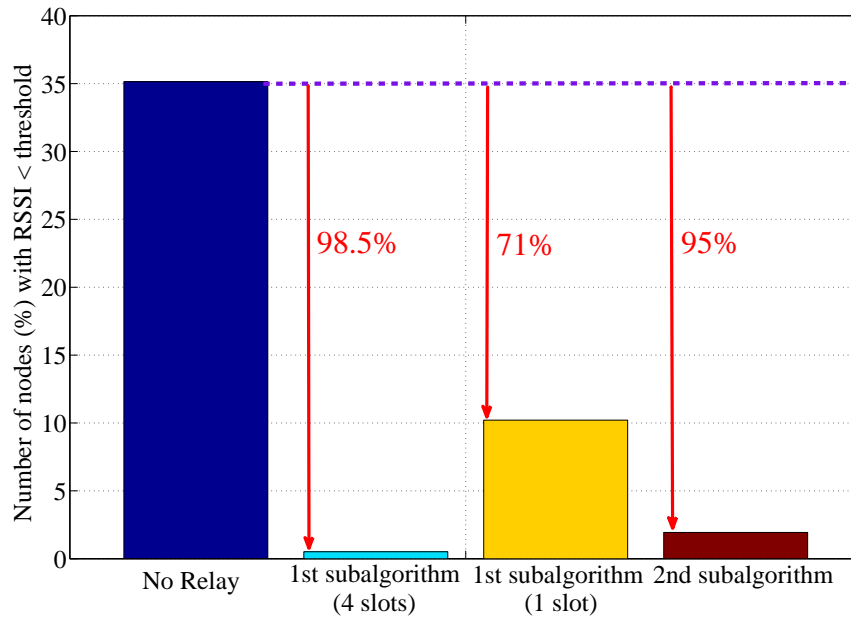
Figure 30: Blank spot reduction. The proposed schemes reduce the number of nodes with the RSSI lower than the threshold, which, in our case, equals to the minimum RSSI for QPSK $1/2 = -79.41$ dB

demonstrated that both strategies do not offer performance improvement at low SNR due to the noise propagation caused by the AF strategy or the decoding error propagation induced by the DF strategy. Lastly, we have also proposed an algorithm to define the optimal position of the relay based on the RSSI distributions in the area. It has also been demonstrated that the proposed algorithm could enhance the throughput and the coverage performance of the system.

SINGLE-ANTENNA RELAY IN WIMAX SYSTEM

In this chapter, we present the performance evaluation of employing single-antenna relay(s) to the WiMAX system through MATLAB simulations. There are two scenarios considered in this chapter, namely for the SISO system and for the MIMO system. For the MIMO scenario, following our small scale fading analysis on the deployed fixed WiMAX system in Section 2.3.2, we are choosing the SUI channel type 3 as described in [32] for our channel model to simulate a suburban area with light-to-moderate tree densities and moderate terrain characteristic. Similar to the previous section, if it is not otherwise stated, the simulation model and parameters are set as described in Section 2.3.4.

The remainder of this chapter is organized as follows. Section 4.1 presents the performance evaluation for a multi-relay and a multihop single-antenna relay on the SISO system scenario. As for the case of single-antenna relay on the MIMO system is discussed in Section 4.2 which covers keyhole and multi-keyhole scenarios. Lastly, the results of this chapter are summarized in Section 4.3.

4.1 SINGLE-ANTENNA RELAY ON SISO SYSTEM

Single-antenna relay(s) usage for a SISO system has also been discussed in the previous section (see Section 3.3.3), where a two-hop single-antenna relay system under a flat fading Rayleigh distributed channel is studied. It has also been shown that a relay could improve the BER performance of the system. In this section, we will investigate the performance of the system when employing more relay nodes to constitute a multi-relay and a multihop scenario. Furthermore, for each scenario the case when the direct link between the source node and the destination node is considered will also be investigated.

4.1.1 *SISO Two-hop Multi-relay*

As briefly discussed in Section 3.3, the diversity gain for a SISO relay system depends majorly on the number of relay nodes employed (see Equation 3.13 and 3.20). As the number of relay nodes increases, the spatial diversity gain would also increase. Therefore, employing more relay nodes contributes to the enhancement of the system performance. On the following section, the BER performance improvement of a SISO relay system on account of spatial diversity gain will be presented.

4.1.1.1 *System Model*

In this scenario, we consider a half-duplex relay system with a pair of single-antenna transmitter and receiver with K number of single-antenna relay nodes as shown in Figure 31. The system works similarly as discussed on Section 3.3. On the first stage, the source node broadcasts the signals to the relay nodes and to the destination node. Thus, the signal received at the first stage by the relay node k and at the destination node (if the direct link is considered) can be expressed as
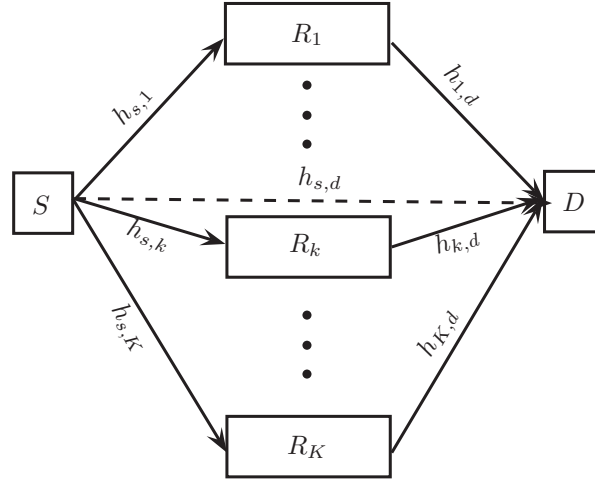
Figure 31: SISO two-hop multi-relay scenario

$$y_{s,k} = h_{s,k} \sqrt{P_s}\, x_s + w_k, \tag{4.1}$$

$$y_{s,d} = h_{s,d} \sqrt{P_s}\, x_s + w_{s,d}, \tag{4.2}$$

where $h_{s,k}$ is the channel coefficient between the source node and the k-th relay node. $h_{s,d}$ is the channel coefficient between the source node and the destination node. P_s is the source transmit power. $w_k \sim \mathcal{CN}(0, \sigma_k^2)$ and $w_{s,d} \sim \mathcal{CN}(0, \sigma_{s,d}^2)$ are the AWGN noise at the k-th relay node and at the destination node, respectively. x_s is the signal transmitted by the source node. On the second stage, all relay nodes forward the signals according to the relaying strategies used to the destination node, where they will be combined using the MRC method. The signal received by the destination node from the k-th relay on the second stage is given by

$$y_{k,d} = h_{k,d} \sqrt{P_k}\, x_k + w_{k,d}, \tag{4.3}$$

where $h_{k,d}$ is the channel coefficient between the k-th relay node and the destination node. P_k is the transmit power at the relay node k. x_k is the amplified signal from the k-th relay node which is given by Equation 3.4 if the AF strategy is used; or the re-encoded version of x_s if the DF strategy is applied.

4.1.1.2 *Simulation Results*

We focus our inquiry for the case where the link qualities of the SR and RD links are 5 dB better than that of the SD link. Aside from that, we also investigate the effect of employing up to $K = 30$ relays to the BER performance. The system will be investigated for both scenarios where the direct link is considered and when it can be neglected (i.e., due to a poor SD channel condition). In this context, all relays are located halfway between the source node and the destination node, and are assumed to be separated one another with a distance that still ensures the received signals to have statistically independent fading. We assume that the source node and the relay nodes, each transmits the signals over an orthogonal channel (time/frequency/space), hence causing no interference to other nodes. Furthermore, for easiness purpose, all relays are perfectly synchronized. Hence, the signals from the relay nodes arrive at the same time or perfectly separated in time at the destination node. The simulations are conducted for ten channel realizations with number of relays, $K = \{1, 2, 3, 4, 5, 10, 15, 20, 25, 30\}$.

In this scenario, it is demonstrated that the AF strategy interestingly features slightly better than the DF strategy starting at $K = 3$. This is because of the imperfect decoding process introduces by the DF strategy which results the relay nodes to re-encode and to forward the already erroneous signal, especially at low SNR regions. Furthermore, equivalent to the results of the earlier scenario, taking the direct link into consideration does not exhibit further improvement for both strategies as the number of relays K increases. This can be understood since as number of relays K increases, the direct link, which has a low quality, invests small effect in the MRC process and consequently gives no significant impact to the overall BER performance. The simulation results for the multi-relay scenario without considering the direct link are plotted in Figure 32 and Figure 33 for the AF strategy and the DF strategy, respectively. Figure 34 and Figure 35 present the simulation results for the multi-relay scenario of the AF strategy and the DF strategy, respectively, when the direct link is taken into consideration.

From the simulation results, it is evidenced that irrespective of the applied relaying strategy, increasing the number of relay nodes in a two-hop system does enhance the performance of the system, although not linearly. Similar with the observation in [75], that the simultaneous use of multi-relay nodes exhibits a logarithmic increase of the achievable capacity between the source node and the destination node. This is owing to the spatial diversity gain obtained through different relay nodes. However, the performance gain must also be compensated with the hardware complexity, since the more number of antennas used implies on the increasing of radio front end complexity and price [76] [77].

The usage of more relays yields a better average SNR which subsequently allows the possibility to perform higher MCS. Thus, it leads to a better throughput performance of the system. Although until certain level, it

Figure 32: SISO two-hop AF multi-relay performance without direct link (16 QAM 1/2, Rayleigh channel, 10 channel realisations). The BER performance improves as the number of relays K increases owing to the spatial diversity gain. At higher K number, the AF strategy shows more significant improvement than the DF strategy

Figure 33: SISO two-hop DF multi-relay performance without direct link (16 QAM 1/2, Rayleigh channel, 10 channel realisations). The BER performance improves as the number of relays K increases owing to the spatial diversity gain. Due to its imperfect decoding process, starting at $K = 3$, the DF strategy is outperformed by the AF strategy, especially at lower SNR

Figure 34: SISO two-hop AF multi-relay performance with direct link (16 QAM 1/2, Rayleigh channel, 10 channel realisations). The direct link with low link quality invests small effect in the MRC process, hence it gives no significant impact
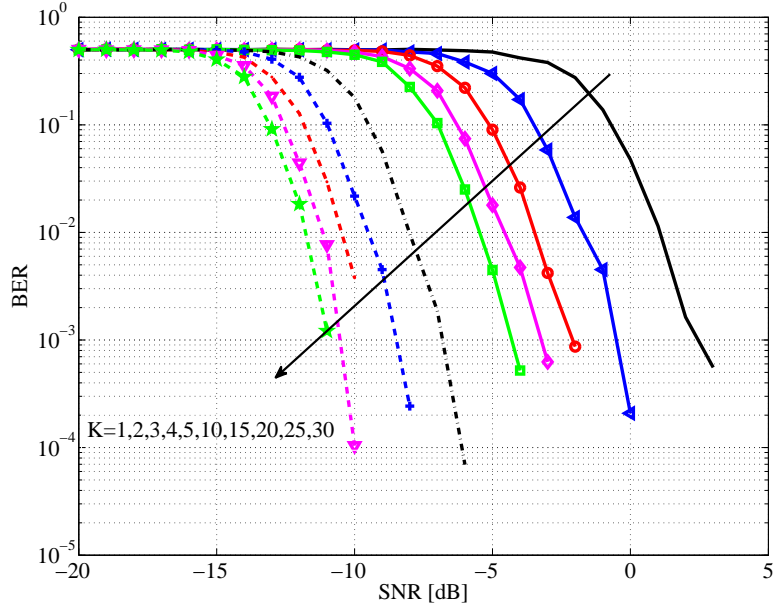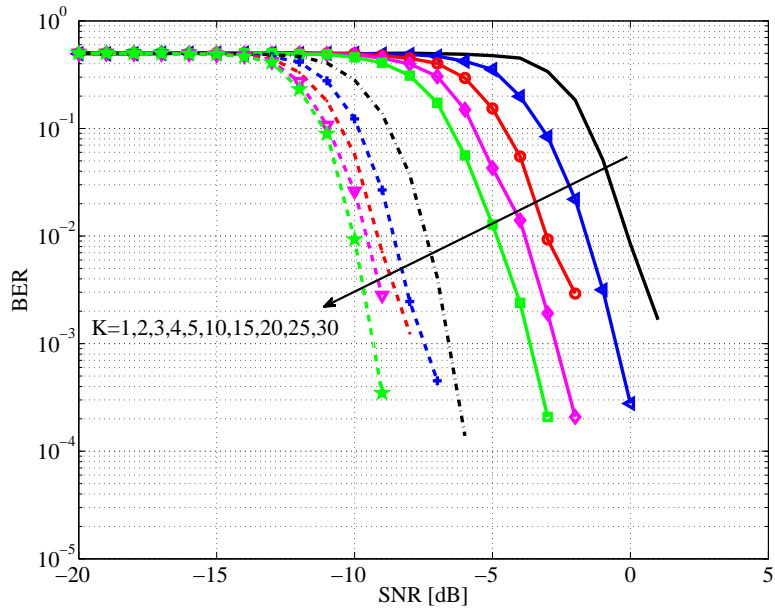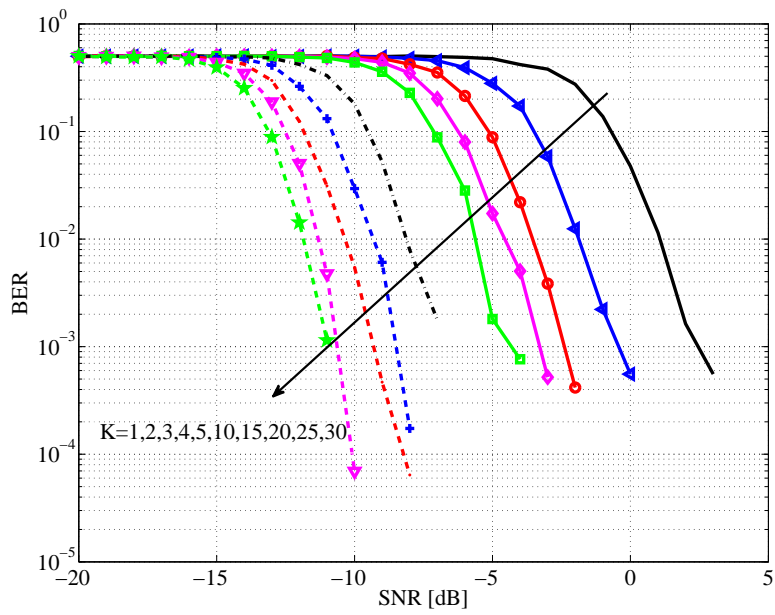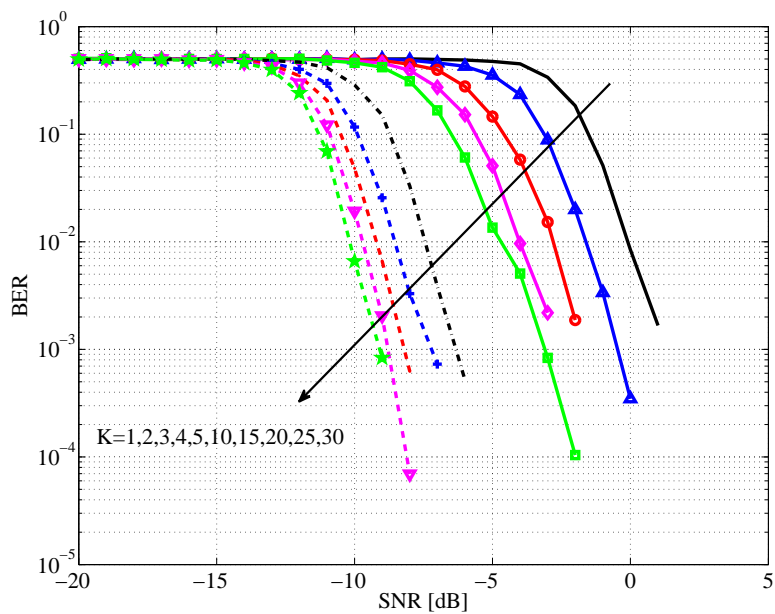

Figure 35: SISO two-hop DF multi-relay performance with direct link (16 QAM 1/2, Rayleigh channel, 10 channel realisations). The direct link with low link quality invests small effect in the MRC process, hence it gives no significant impact

shows no significant improvement. In this instance, starting from $K = 5$, the improvement rate is declining, making it worthless to add more relay nodes. Similar results are also reported in [74] where employing more relays contributes to minimization or even elimination of coverage gaps which at some level becomes inefficient since the performance improvement could not counterbalance the costs (i.e., bandwidth, hardware, coordination).

4.1.2 *SISO Multihop Relay (L>2)*

Multihop system is a cost-efficient approach to broaden the coverage and to improve the throughput of the system [78]. In a multihop scenario, the signal is transmitted from the source node to the destination node via several relay nodes serially or in a single route. This scheme is beneficial, for example, in the network where the distance between the source node and the destination node is large. Hence, the signal from the source node experiences a deep fade and cannot reach the destination node. Nevertheless, a multihop system has also some drawbacks, such as, signaling overhead, relaying interference, latency, radio resource management and scheduling cost [79].

Some investigations on the performance of a multihop system have also been performed by Boyer et al. in [62] [80] [81] for the system with diversity and without diversity. Furthermore, the outage probability analyses of a multihop system under several fading channels have been reported in [82] [83] [84] [85] [86] [87]. Based on those investigations, it is reported that a multihop system could outperform a system without relay (single-hop) system. Moreover by increasing the number of hops, the performance of the system will also increase, given the conditions that the relay nodes are intelligently positioned to provide good link qualities.

4.1.2.1 *System Model*

The considered SISO system is a multihop system which consists of a source and a destination pair as well as L relay nodes ($(L + 1)$-hop relay system), as shown in Figure 36. All nodes are equipped with a single-antenna. There are two scenarios considered, i.e., when the direct link between the source node and the destination node is taking into account; and when it can be neglected, for example, because the signal is severely faded due to a large distance or a poor channel condition. The relay nodes are located between the source node and the destination node, in other words, the SD distance is always larger than the SR distance. For simplicity, we assume that the relay nodes can only receive signals from the immediate preceding node, therefore there is no diversity in the relay nodes. Hence, the signal received at the relay node l can be expressed as

$$y_l = h_{l-1,l} \sqrt{P_{l-1}} \, x_{l-1} + w_l, \, l \in \{0, \dots L\} \tag{4.4}$$

where $h_{l-1,l}$ is the channel coefficient between the relay node $l-1$ and the relay node l, P_{l-1} is the transmit power of the relay node $l-1$. $w_l \sim$

$\mathcal{CN}(0, \sigma_l^2)$ is the AWGN noise at the relay node l and x_{l-1} is the forwarded signal from the relay node $l-1$. Moreover, the node l is the source node if $l == 0$; and is the destination node if $l == L+1$. If the AF strategy is applied, x_{l-1} is given by

$$x_{l-1} = \frac{y_{l-1}}{\sqrt{P_{l-2}|h_{l-2,l-1}|^2 + \sigma_l^2}}. \tag{4.5}$$

If the DF strategy is applied, x_{l-1} will be the re-encoded version of x_{l-2} which can contain error since the error correction code is not implemented in our model, consequently a propagation error is induced. The received signals at the destination node are derived in the same ways as in Equation 3.7 and 3.10 in case the AF strategy is applied; or Equation 3.14 and 3.17 if the DF strategy is used.
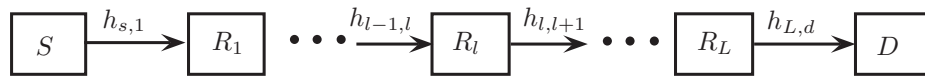
Figure 36: SISO (L + 1)-hop system

In our model, it is assumed that the channels are orthogonal, therefore the relays do not cause interference to one another. Furthermore, the relays are assumed to be equidistant and they are assigned with equal power allocation.

4.1.2.2 *Simulation Results*

Our goal is to study the BER performance of the (L + 1)-hop system for $L = \{1, 2, ..., 10\}$ under two cases, i.e., with and without the direct link (SD link) being considered. The impact of adding more hops to the system is here to be investigated. For the simulation purposes, we assume that the source node and the destination node are five kilometers distant and the relay nodes are located equidistantly in-between with 5 dB more SNR than that of the SD link. For this investigation, the simulation is performed under Rayleigh channel for ten channel realisations.

From the simulation results as shown in Appendix A.1, it can be observed that given the aforementioned assumptions, adding more hops in the system does not necessarily offer a better BER performance compared to the case without relay (single-hop), regardless of the relaying strategy used. The system with a single relay (two-hop) still yields better performance than those with more hops (L $\geqslant$ 2). As the number of hops (L) increases, the BER performance decreases and until for some number of hops L, the BER curves show no significant change or showing very small variations.

Figure 37 depicts the simulation results of both strategies without considering the direct link. It can be seen that starting at L $\geqslant$ 2, the multihop

Figure 37: SISO multihop performance without direct link (16 QAM 1/2, Rayleigh channel, 10 channel realisations). The performance of both strategies degrades as the number of hops L increases. The DF strategy outperforms the AF strategy owing to the coding gain

system cannot outperform the single-hop system. This is due to the great deal of noise amplification introduces by the hops/relays that the relay gain can no longer compensate. In this context, the equivalent system with the DF strategy shows better results than that of the AF strategy, on account of the decoding process presented in each hop. It can also be observed in Figure 63 and Figure 64 that for $L > 6$, the DF strategy brings on a better performance of up to 7 dB compared to that of the AF strategy, which can be clearly seen from the BER curves of $L = 10$. Even though every hop contributes to a propagation error caused by the incorrect decoding process especially at low SNR range, the proposed multihop system with the DF strategy still yields better BER performance at higher SNR than the single-hop system even for $L = 10$, owing to the coding benefit.

Taking the direct link into consideration is proven to exhibit better performance for both strategies on account of the diversity gain. This is as shown in Figure 65 for the AF strategy and Figure 66 for the DF strategy, respectively; and in Figure 38 for the comparison. With diversity, the multihop system with the AF strategy outperforms the single-hop system which can be evidently observed from the BER curves of $L \leqslant 7$. Although similar to the previous case, the performances of the DF strategy still exceed those of the AF strategy. However, compared to the system without diversity, the performance gains induced by the AF strategy with diversity are more significant. For example at $L > 5$, the AF strategy with diversity gives ~ 4
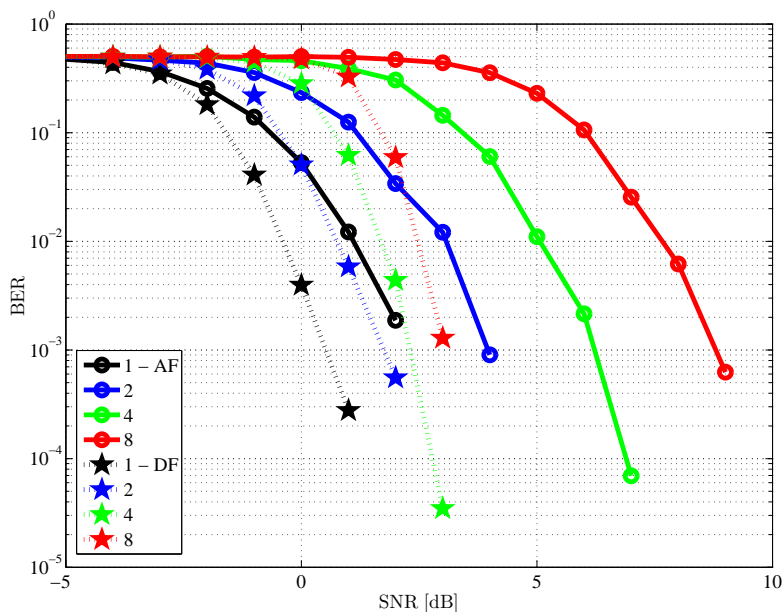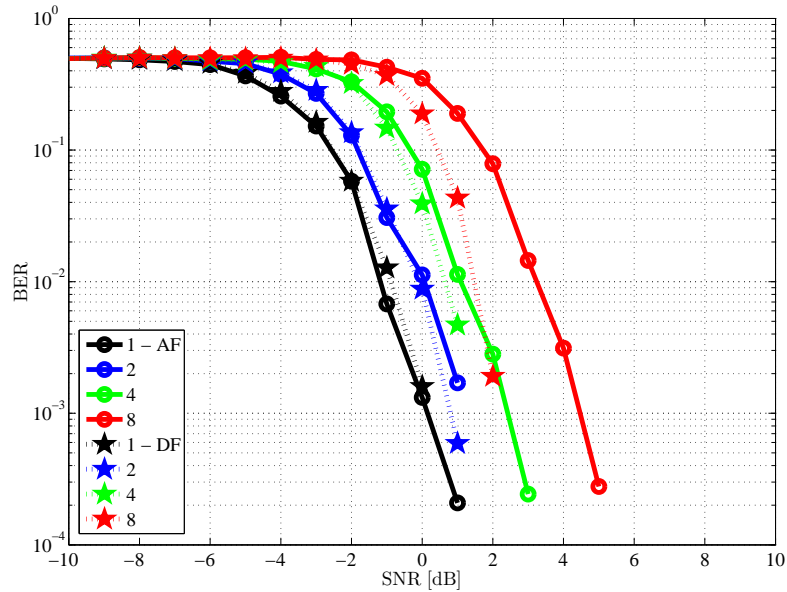
Figure 38: SISO multihop performance with direct link (16 QAM 1/2, Rayleigh channel, 10 channel realisations). For both strategies, the direct link could offer a diversity gain hence it improves the performance

dB improvement, meanwhile the equivalent system with the DF strategy gives only less than 1 dB gain. This supports the statement reported in [81] where the AF relaying with diversity experiences greater performance improvement rate than the equivalent DF relaying. It is also reported therein that under circumstances when the relay positions are optimally chosen, the AF strategy with diversity could even outperform the DF strategy. Since, the former strategy does not imply propagation error as in the latter strategy which limits its performance, especially at low SNR. Furthermore, in accordance to the results reported in [72] which is stating that both strategies have comparable average performance, in that the DF strategy is only slightly better than the AF strategy. Further reported therein, that both strategies perform equally bad at low SNR. This is because they are equivalent to repetition coding, which relatively inefficient at low SNR [73].

From the simulation results, it can be concluded that adding more hops between the source node and the destination node is not advised when the hops have no better link qualities than that of the two-hop system. In this case, adding more hops will only raise the error propagation or else the noise propagation which foreshortens the performance of the system.

In adjacent, another investigation is also performed for the case when the relay nodes are located equidistantly one kilometer away, one after another (step distance). Hence, the source node and the destination node are $(L + 1)$ kilometers apart. In this investigation, the direct link is assumed to be severely faded and can be ignored. Similar with the results from the former

scenario, the latter results demonstrate that for both strategies provided the aforesaid preconditions exhibit no performance enhancement as the number of hops (L) increases. The simulation results of this scenario are presented in Figure 67 and Figure 68 for the AF strategy and the DF strategy, respectively. The results for L = {6..9} are purposely omitted to present a simpler BER curves view. It can be seen clearly that the performance of the AF strategy degrades almost substantially per node addition. It is evidenced that under the aforementioned condition, the relay system with the AF strategy suffers severely from the noise propagation induces by each hop/relay node. However, even though the DF strategy shows less performance gain, its BER performance is not much degraded even when the number of hops/distance is added. It indicates that the coding gain offered by the DF strategy in each hop could keep up with the impact of the large distance. Furthermore, in conformity with the statement in [84], for both strategies as the distance stretches or as the number of hops L increases, the BER curves becomes tight implying the diminishing of the performance gain.

4.2 SINGLE-ANTENNA RELAY ON MIMO SYSTEM

It has been proven in many researches that a MIMO technology can offer better performance than a SISO technology, because it can offer higher spectral efficiency and improve the diversity gain considerably [88] [89]. Furthermore, it is reported in [48] [56] that exploiting relay node could enhance substantially the spatial diversity of the MIMO network, hence improving the performance of the system. However, the performance gain must also be compensated with the hardware complexity. Since increasing the number of antennas implies on the increasing of radio front end complexity and price [76] [77]. Therefore, it is often occurred such condition where having a multi-antenna relay in the system is simply unfavourable. One alternative to still benefit the merit of the relay node in the MIMO network without employing a multi-antenna relay is by assigning a single-antenna relay on the system. Or even more by using multiple single-antenna relays to establish a virtual MIMO system.

Employing a single-antenna relay on the MIMO system will induce the channel to be similar to a MIMO keyhole channel; or accordingly a MIMO multi-keyhole channel when more than one relay is used. Keyhole channel is the channel condition where its gain matrix has a unit rank (single degree of freedom), hence degrading the capacity despite the channel is uncorrelated. This phenomenon may arise when scattering effect near the transmitter and the receiver results in reduced signal correlation. Meanwhile, the diffraction and wave guiding effects cause the rank of the gain matrix decreased [90]. Keyhole effect can be found under several circumstances, i.e., due to metal obstacles with small holes (spatial keyhole); due to diffraction at rooftop edges (diffraction-induced keyhole); or because the signal propagates through street canyons, hallway, subway tunnel, corridors,

single-mode waveguides (modal keyhole) [91]. Nevertheless, based on the measurement reported in [90] [92], ideal keyhole channels are rarely found in real-world environment and difficult to observe. This is because the single non-zero eigenmode assumption is only an approximation of real propagation scenarios.

A study regarding the diversity order of a keyhole channel is reported in [93] which stated that for a number of keyholes/scatterers n_s, the diversity order is upper bounded by $n_t n_s n_r / \max\{n_t, n_s, n_r\}$. It is further deduced and finally yields an upper bound of $n_t n_r$. It indicates that a keyhole channel cannot outmatch the MIMO channel with the same number of transmit antennas n_t and receive antennas n_r. Meanwhile, an investigation regarding the maximum diversity order of a MIMO channel with n_k single-antenna relay(s) is reported in [68], which describes the diversity order as

$$
d = \begin{cases} \min\{n_t, n_r\} n_k, & \text{if } n_t \neq n_r, \\ n_t n_k (1 - \frac{\log(\log(P))}{M \log(P)}), & \text{if } n_t = n_r, \end{cases} \tag{4.6}
$$

where P is the total transmit power used in the whole system; and M is the maximum multiplexing gain which is determined by $\min\{n_t, n_r, n_k\}$. Further investigation is covered in [94] where the lower bound of the DMT of such a system is defined as a function of $\min\{n_t, n_r\}$. Therefore, it can be resolved that employing single-relay nodes is more advisable than increasing the number of relay antennas, simply because it is cheaper in the implementation and hardware costs. It is also therein reported that for such a system, increasing the number of transmit antennas n_t and the number of receive antennas n_r will not improve the performance gain. Moreover, if the relays have different unitary matrices, the diversity could approach $n_t n_r$ when $n_k > \max\{n_t, n_r\}$.

Similar investigation on the single-antenna relay on a MIMO system is reported in [95] where it is shown that the performance of such a system can exceed the performance of the comparable SISO system. Also in [57] and [96] where the performance of the beamforming in a two-hop AF relay network is analysed. It is therein stated that the diversity order of such a system is equal to the minimum number of antennas at the source node and at the destination node. Furthermore, it is demonstrated in [97] that a single antenna relay can be used to provide diversity when the destination node suffers from a keyhole effect.

In the following sections, we will discuss a brief overview regarding a keyhole and a multi-keyhole channel with its equivalent single-antenna relay and multi single-antenna relays, respectively. The performance of a single-antenna relay as well as multi single-antenna relays systems for the AF and DF relaying strategies in the MIMO system will be investigated through simulations. The results are then compared to the equivalent MIMO system. It is to observe whether the use of single-antenna relay(s) can help

mitigate and improve the performance of the MIMO WiMAX system despite the relay channel matrix rank reduction. The system is investigated under the condition when the link between the source node and the destination node is degraded.

4.2.1 *Keyhole Case*

It is stated in [60] [98], that a keyhole channel is considered as a worst scenario of a MIMO propagation channel, that even a multiplexing gain technique become no longer beneficial [99]. Even so, a spatial diversity scheme, such as Alamouti coding [34] can still help reduce the error rate.

Keyhole channel can be considered as a special case of a double-scattering MIMO channel [100]. It is modeled as a pair of two Rayleigh fading channels separated by a keyhole whose dimension is much smaller than the wavelength. Therefore, it has double Rayleigh fading characteristics (i.e. fades twice often as normal i.i.d Rayleigh channel) as a result of a product of two independent Rayleigh distributions [60] [92] [98] [101] [102] [103].
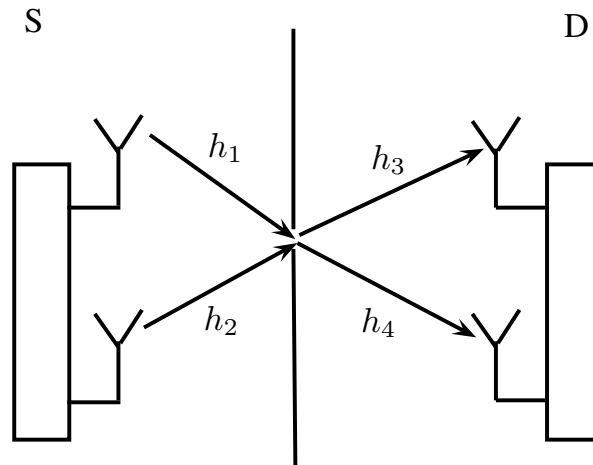
Figure 39: MIMO 2×2 keyhole channel

For a better explanation of a MIMO keyhole channel, let us consider a MIMO channel with the number of transmit antennas $n_t = 2$ and the number of receive antennas $n_r = 2$, as illustrated in Figure 39. Let $\mathbf{H}_{n,m}$ be an element of channel gain matrix $\mathbf{H}$ from the m-th transmit antenna to the n-th receive antenna, where $n = \{1 \dots n_r\}$ and $m = \{1 \dots n_t\}$. $\mathbf{H}$ is given as follows [60]

$$\mathbf{H} = \mathbf{h}_r \, \mathbf{h}_t^H = \begin{pmatrix} h_1 \\ h_4 \end{pmatrix} \begin{pmatrix} h_1 & h_2 \end{pmatrix} = \begin{pmatrix} h_1 h_3 & h_2 h_3 \\ h_1 h_4 & h_2 h_4 \end{pmatrix}, \qquad (4.7)$$

where $\mathbf{h}_t[n_t \times 1]$ and $\mathbf{h}_r[n_r \times 1]$ represent vector gain from source to keyhole and from keyhole to destination, respectively. $()^H$ denotes the Hermitian

transpose. For the correlated capacity, $\mathbf{H}$ is expressed in a Kronecker model as follows

$$\mathbf{H} = \mathbf{R}_R^{1/2} \; \mathbf{G} \; \mathbf{R}_T^{T/2}, \tag{4.8}$$

where $\mathbf{R}_R = \mathbf{R}_R^{1/2} \; \mathbf{R}_R^{H/2}$ and $\mathbf{R}_T = \mathbf{R}_T^{1/2} \; \mathbf{R}_T^{H/2}$ describe the signal correlation at the receiver and at the transmitter, respectively. $\mathbf{G}$ is an independent and identically distributed (i.i.d) complex Gaussian channel matrix between the transmitter and the receiver. However, this model cannot predict the keyhole channel since the correlation used is the mean (conventional) correlation which will overestimate the capacity for the MIMO keyhole channels. Thereby, the generalization is introduced in [92] [104] as

$$\mathbf{H} = \mathbf{R}_R^{1/2} \; \mathbf{G}_R \; \mathbf{T}^{1/2} \; \mathbf{G}_T \; \mathbf{R}_T^{T/2}, \tag{4.9}$$

where $\mathbf{G}_R$ and $\mathbf{G}_T$ are both i.i.d. complex Gaussian matrices distributed with zero mean and unit variance. $\mathbf{T}^{1/2}$ describes the transfer matrix between the transmitter and receiver environments (i.e., scattering and waveguide), which of rank one in a perfect keyhole channel. Thereby, the rank of the channel matrix $\mathbf{H}$ will also be one, disregarding the rank of $\mathbf{R}_R$, $\mathbf{R}_T$, $\mathbf{G}_R$ and $\mathbf{G}_T$. Hence, the MIMO channel model becomes

$$\mathbf{H} = \mathbf{R}_R^{1/2} \; g_R \; g_T^* \; \mathbf{R}_T^{T/2}, \tag{4.10}$$

where $\mathbf{g}_R$ and $\mathbf{g}_T$ are both uncorrelated distribution column vectors.

It is stated in [100] that the use of multiple antennas in the keyhole channels cannot provide the spatial multiplexing gain but only offers the diversity gain. The keyhole channel can be thought of as a cascade of a MISO (with diversity order equal to the number of receive antennas) and a SIMO (with a diversity order equal to the number of transmit antennas). Hence, the multiplexing order can be specified as the minimum number between the transmit and receive antennas ($\min\{n_t, n_r\}$) [104].

The instantaneous capacity of the keyhole channel when the CSI is available only at the receiver is given by [105]

$$C = \ln\left(1 + \frac{\gamma_0}{n_t n_r}\alpha\right), \tag{4.11}$$

where $\alpha = \|\mathbf{h}_t\|^2 \|\mathbf{h}_r\|^2$ is the power gain of the channel, and γ_0 is the total average SNR at the receiver. Further performance analyses of a keyhole channel have been investigated in several papers. The performance investigations in terms of the achievable outage capacity are reported in [100] [106] [107] [108] [109] [110]. The performance investigations of STBC codes under a keyhole effect can be found in [102] [103] [111] [112]. The performance analyses of antenna selection in keyhole channels are covered in [108] [113]. Some papers propose a method to improve the performance under the keyhole effects as in [114] by using the DPC method when the number of transmit antennas is less than the number of receive antennas.
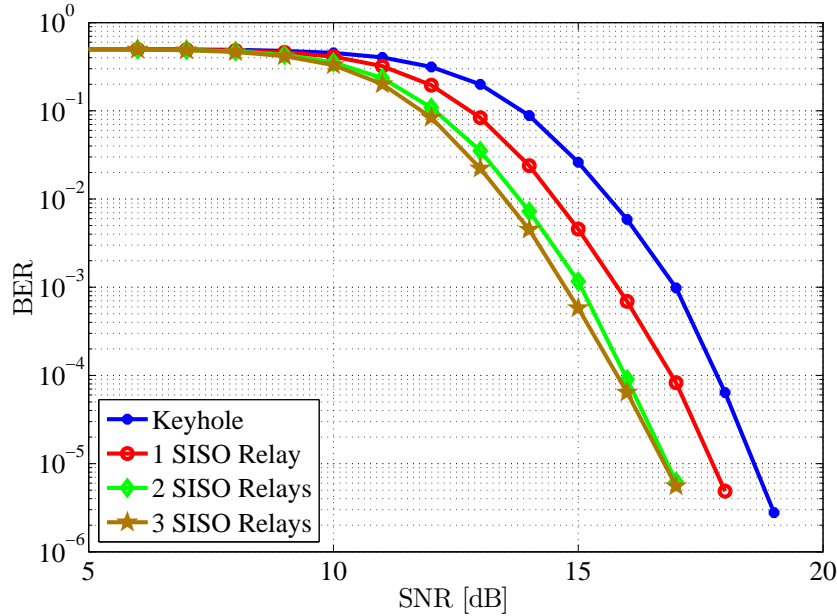
Figure 40: Single-antenna relay(s) on MIMO keyhole channel under deterministic channel [3]

Also the authors in [98] suggest a horizontal array utilization for diffraction-induced keyholes cases. Furthermore, a cooperative diversity scheme is also proposed as a method to mitigate keyhole effects in [91]. In addition to that, in [3] where the performance of single-antenna relays in the MIMO keyhole system is investigated under a deterministic channel (the channel is generated from the system described in Section 2.3.3). It is shown that even when the SR link and the RD link are poor, adding relay node(s) to a MIMO keyhole system could still exhibit performance improvement because of the gain induces by the relay node(s) (see Figure 40 [3]).

4.2.1.1 *System Model*

For this system, we consider a $2 \times 1 \times 2$ system or rather a MIMO system with a SISO relay which is equivalent to the 2×2 MIMO keyhole system. As illustrated in Figure 41, the system comprises of two-antenna source and destination pair and a single-antenna relay. It is assumed that the channel gain between the source node and the destination node is very poor, hence the signals cannot reach the destination node. Therefore, for this case as previously mentioned, the system is also similar to that of a cascade of a MISO and a SIMO system.

Let $\mathbf{x}_m$ be the vector symbol to be transmitted from the m-th antenna of the source node to the relay node and assumed to satisfy the sum power
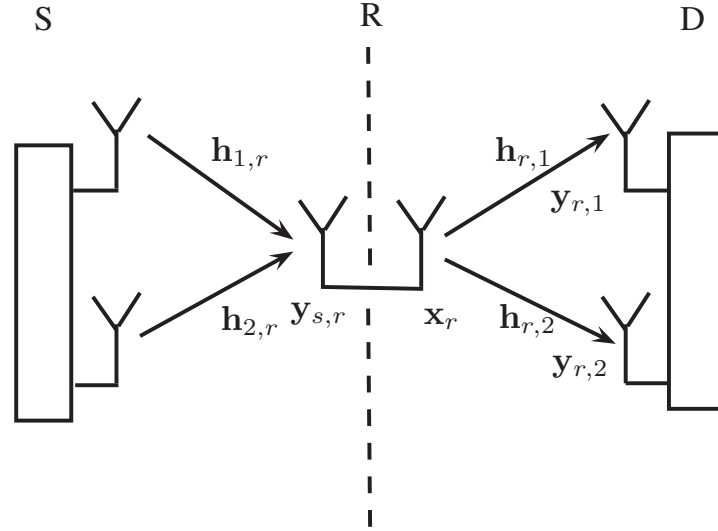
Figure 41: $2 \times 1 \times 2$ MIMO system

constraint of less or equal than 1. Thus, the signal received at the relay node is given by

$$\mathbf{y}_{s,r} = \sum_{m=1}^{N_t=2} \mathbf{h}_{m,r} \sqrt{P_s} \mathbf{x}_m + \mathbf{w}_r, \tag{4.12}$$

where P_s is the total transmit power, $\mathbf{h}_{m,r} \sim \mathcal{CN}(0, \sigma_h^2)$ is the channel coefficients between the m-th transmit antenna of the source node and the relay node. $\mathbf{w}_r$ is the AWGN with zero mean and variance σ_n^2 at the relay node.

The signal received by the n-th antenna in the destination node from the relay node can be written as

$$\mathbf{y}_{r,n} = \mathbf{h}_{r,n} \sqrt{P_r} \mathbf{x}_r + \mathbf{w}_n, \tag{4.13}$$

where P_r is the relay transmit power, $\mathbf{h}_{r,n}$ is the channel coefficients from the relay node to the n-th received antenna, and $\mathbf{w}_n \sim \mathcal{CN}(0, \sigma_n^2)$ is the AWGN at the n-th antenna. $\mathbf{x}_r$ is the signal forwarded from the relay node which can be either the amplified version or the re-encoded version of $\mathbf{y}_{s,r}$, if applying the AF strategy and the DF strategy, respectively. For the case where the direct link is considered, the received signals from the source node and the relay node are then combined at the destination node using the MRC method before the decoding process.

4.2.1.2 *Simulation Results*

For simulation purposes, it is assumed that the distance between the source node and the destination node is two kilometers away, with the relay node is positioned in-between. Furthermore as mentioned in the previous section, the destination node can only receive signals from the relay node since the

signal from the source node is assumed to be severely faded. The system performance in terms of BER is investigated for several cases as provided in Table 10, and then compared to that of the corresponding MIMO and SISO system without relay. The '+X' sign denotes that the SNR of the SR/RD link is X dB higher than that of the SD link. The first case is to investigate the effect of having the relay node near to the source node, likewise having a better SR link than the RD link. Whereas, the third case is on the contrary. The second case represents a condition where both links (the SR and RD links) have equal link qualities whereof in this context the relay node is located midway between the source node and the destination node. For each case, the performances of the AF and DF strategies are studied through simulations under the SUI type 3 channel model.

Condition	Case 1	Case 2	Case 3
S-D Distance [km]	2	2	2
S-R Distance [km]	0.5	1	1.5
SNR S-R [dB]	+10	+5	+5
SNR R-D [dB]	+5	+5	+10

Table 10: Simulated MIMO single-antenna relay (keyhole) cases

The simulation results after 100 channel realisations are plotted in Figure 42. It is shown that the performance of a single-antenna relay on the MIMO system still surpasses the performance of the SISO system by more than 2 dB, which conforms with the result reported in [95]. Moreover, a single-antenna relay can also improve the performance of the 2×2 MIMO system. Although in the second case where the SR and RD link qualities are both equal, i.e., with 5 dB more SNR, it yields no significant performance improvement than the equivalent single hop 2×2 MIMO system. The performance improvements are clearly pointed out in the result of case 1 and 3, where there is at least one good connection between the SR link and the RD link. Furthermore, as also proven in Section 3.3.3, the DF strategy almost always outperforms the AF strategy in all three cases. Moreover, when the SNR of the SR link quality is high or when the relay node is near to the source node as represented in case 1, both relaying strategies show more performance improvement of up to 3 dB and 4 dB for the AF strategy and the DF strategy, respectively.

In addition to that, for comparison purposes with the SISO relay system, the results for the first case are also plotted in Figure 43. It can be observed that a single-antenna relay on the MIMO system outperforms the performance of the SISO relay system by ~ 4 dB. It means that a single antenna relay for the MIMO system is still meritable for the performance improvement of the system. Even though the performance of the MIMO system with a single-antenna relay cannot exceed the equivalent system
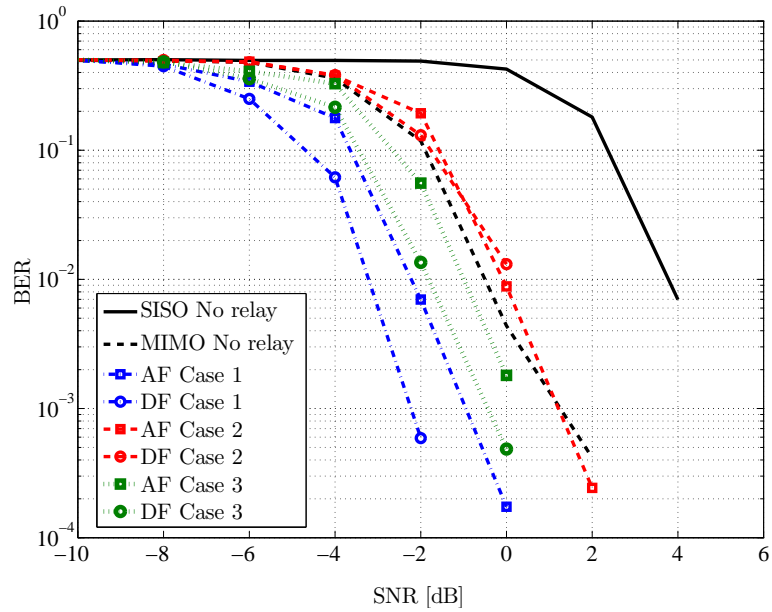
Figure 42: MIMO two-hop single-antenna relay (keyhole) system performance (16 QAM 1/2, SUI3 channel, 100 channel realisations). The performances of Case 1 (good SR link) and Case 3 (good RD link) could outperform that of the MIMO system without relay. Nevertheless, employing single-antenna relay on MIMO system becomes useless when both links (SR and RD) are poor
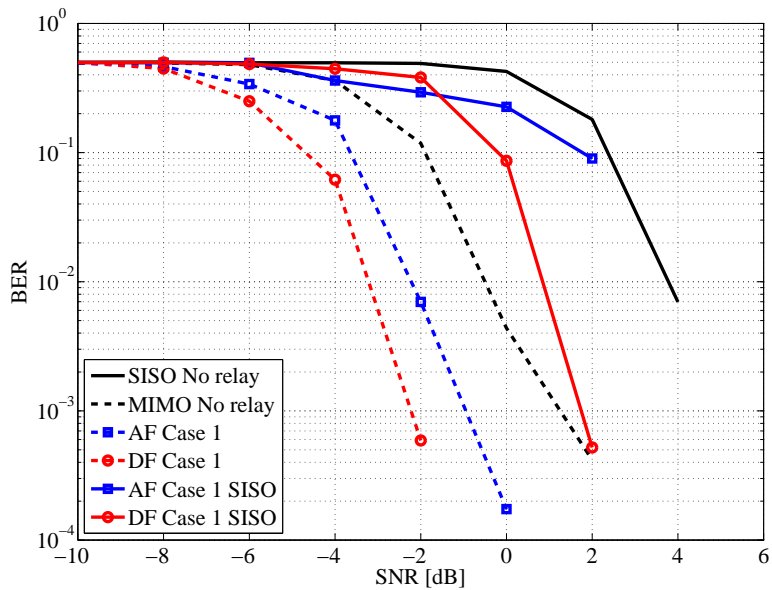

Figure 43: MIMO two-hop single-antenna relay (keyhole) system: Performance comparison of MIMO and SISO relay case 1 (16 QAM 1/2, SUI3 channel, 100 channel realisations). Employing single-antenna relay on MIMO system still offers better performance than the single-antenna relay on SISO system

with the multi-antenna relay (which will be discussed in Chapter 5), it still offers performance amelioration in terms of BER as well as coverage. The performance of the proposed system exceeds that of the direct link MIMO system, which points that the system could also outperform the MIMO keyhole system. This also indicates that adding a relay node could still help extenuating keyhole effects occurred in the channel, regardless whether the direct link is regarded [91] or disregarded. This system would be benefit for the case where employing a multi-antenna relay is unfavourable (i.e. due to cost or complexity); yet better performance is still expected, especially when the link quality between the source node and the destination node is poor.

4.2.2 *Multi-keyhole Case*

Employing single-antenna relays on the MIMO system will induce the channel characteristic of the system to be equivalent to that of the multi-keyhole channel. It is the case when there are more than one keyhole effect occurred in the channel. Multi-keyhole channel is originally introduced in [61] [115] to extend and to generalize the single-keyhole channel model, considering that the channel with more than one keyhole is more often encountered than the single-keyhole. Multi-keyhole channel, as shown in Figure 44, is therein described as an extension of the single-keyhole channel (Equation 4.7),

$$\mathbf{H} \ = \ \sum_{k=1}^{K} a_k \, \mathbf{h}_{r,k} \, \mathbf{h}_{t,k}^{H} \ = \ \mathbf{H}_r \, \mathbf{A} \, \mathbf{H}_t^{H}, \tag{4.14}$$

where K is the number of independent keyholes. a_k is the complex gain of the k-th keyhole, or alternatively for our system model, it is the relay gain. $\mathbf{h}_{t,k}$ and $\mathbf{h}_{r,k}$ are the random vectors representing complex gains from the transmit antennas to the k-th keyhole and from the kth keyhole to the receive antennas, respectively. It is assumed that $E\left\{\mathbf{h}_{t,k}\mathbf{h}_{t,l}^{H}\right\} = E\left\{\mathbf{h}_{r,k}\mathbf{h}_{r,l}^{H}\right\} = 0$ for $k \neq l$, implying that each keyhole is independent to each other. $\mathbf{H}_t \ = \ [\mathbf{h}_{t,1}..\mathbf{h}_{t,K}]$, $\mathbf{H}_r \ = \ [\mathbf{h}_{r,1}..\mathbf{h}_{r,K}]$ denote the $[n_t \times K]$ and the $[n_r \times K]$ matrices, respectively. $\mathbf{A}$ is a diagonal matrix of $diag(a_1, ..., a_K)$. Thus, the instantaneous capacity of a flat quasi-static multi-keyhole channel with the CSI available only at the receiver is expressed as [106]

$$C = \ln \det(\mathbf{I} + \gamma_0 \mathbf{B}_r \mathbf{A} \mathbf{B}_t \mathbf{A}^{H}), \tag{4.15}$$

where $\mathbf{B}_t = \mathbf{H}_t^{H}\mathbf{H}_t/n_t$ and $\mathbf{B}_r = \mathbf{H}_r^{H}\mathbf{H}_r/n_r$. Furthermore, the outage capacity of the multi-keyhole channel is upper bounded by that of the equivalent Rayleigh fading channel given the same outage probability and the number of receive antennas n_r [99]. Also stated in [106], that the mean capacity increases as K increases, however the outage capacity decreases.

Multi-keyhole channel is often related to the double-scattering channel model in [101] since mathematically both are closely related. Nevertheless,
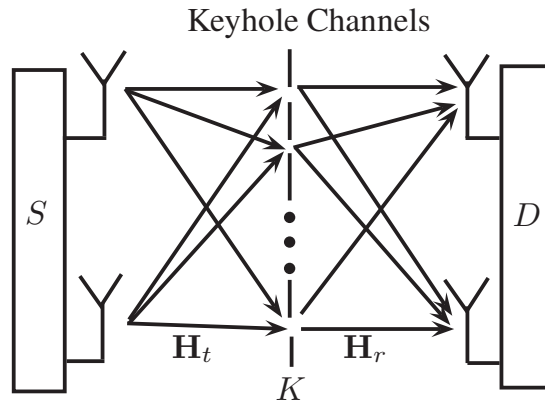
Figure 44: MIMO 2×2 multi-keyhole channel

both are different in the scattering denseness. Double-scattering channel corresponds to the dense scattering environment, since the subchannels are assumed close to each other and correlated. Meanwhile, a multi-keyhole channel represents the sparse scattering environment, where the subchannels (keyholes) are quite distant, therefore independent and uncorrelated.

In [61] [115], multi-keyhole channels are distinguished by their rank into two types,

- Full-rank multi-keyhole MIMO channels (FRMK), when $K \geqslant \min \{n_t, n_r\}$. The multiplexing gain is limited by $\min\{n_t, n_r\}$. As K goes to infinite which causes a richer scattering, the channel distribution becomes asymptotically Rayleigh fading regardless the subchannels channel distribution and correlation.

- Rank-deficient multi-keyhole MIMO channels (RDMK), when $K < \min\{n_t, n_r\}$. The multiplexing gain is determined by K.

Thus, even though the number of relay K increases, the system could not increase its degree of freedom. Hence, it results on an unimproved transmission rate since there is no benefit from the multiplexing gain. However, the spatial diversity gain can still be exploited to improve the reliability of the system by reducing the error probability as the SNR increases. Thus, in return it can contribute to improve the system performance.

Another investigation regarding a multi-keyhole channel can be found in the work of Karawasa and Tsuruta in [116], which demonstrates that to have an average BER comparable to the equivalent MIMO system, the number of antenna K in a multi-keyhole environment must be equal to or greater than the degrees of freedom of the equivalent MIMO environment. Another studies of a multi-keyhole channel are also found in [117] about the ergodic capacity analysis; in [118] regarding the ergodic mutual information; in [99] on the effect of correlation and power imbalance; and also in [119] where a similar multi-keyhole model for MIMO relay system is proposed.

4.2.2.1   *System Model*

As depicted in Figure 45, we consider a two-antenna MIMO system ($n_t = n_r = 2$) with K single-antenna relays to establish a virtual MIMO system. This system can also be regarded as a multi-keyhole channel. We assume that the direct link between the source node and the destination node is severely degraded and therefore can be disregarded. All relays are located at the same distance between the source and the destination. They are positioned with a distance that ensures the received signals having statistically independent fading paths. Furthermore for simplicity purposes, we assume that the source node and the relay nodes are transmitting over an orthogonal channel (time/frequency/space). Hence, causing no interference to other nodes. It is also assumed that all relays are perfectly synchronized, which means that the forwarded signals from the relays arrive concurrently or perfectly separated in time at the destination node. It is expected that the system will benefit from the diversity offered by the relays.
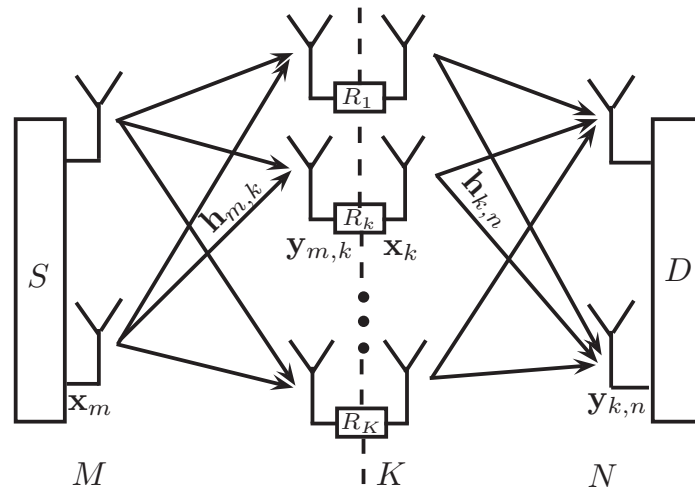
Figure 45: $2 \times K \times 2$ MIMO multi-relay system

Let $\mathbf{x}_m$ be the symbol vector transmitted from m-th antenna of the source node to the k-th relay node and $\mathbf{x}_k$ is the signal forwarded by the k-th relay node to the destination node. The signal arrived at the k-th relay node from the m-th antenna of the source node ($\mathbf{y}_{m,k}$) and the signal received by n-th antenna of the destination node from the k-th relay node ($\mathbf{y}_{k,n}$) are given by

$$\mathbf{y}_{m,k} = \mathbf{h}_{m,k} \sqrt{P_s} \, \mathbf{x}_m + \mathbf{w}_k, \tag{4.16}$$

$$\mathbf{y}_{k,n} = \mathbf{h}_{k,n} \sqrt{P_k} \, \mathbf{x}_k + \mathbf{w}_{k,n}, \tag{4.17}$$

respectively, where P_s and P_k are the source total transmit power and the k-th relay transmit power, respectively. $\mathbf{h}_{m,k}$ is the channel coefficients

between the m-th transmit antenna of the source node and the k-th relay node. $\mathbf{h}_{k,n}$ is the channel coefficients between the k-th relay node and the n-th antenna of the destination node. $\mathbf{w}_k \sim \mathcal{CN}(0, \sigma_k^2)$ and $\mathbf{w}_{k,n} \sim \mathcal{CN}(0, \sigma_{k,n}^2)$ are the AWGN noise at the k-th relay and at the destination node, respectively. $\mathbf{x}_k$ is the forwarded signal from the relay node to the destination node, which is either the scaled version (AF) or the re-encoded version (DF) of $\mathbf{y}_{m,k}$.

4.2.2.2 *Simulation Results*

Our aim is to study the BER performance of the proposed virtual MIMO relay system in a WiMAX network for both relaying strategies, i.e., AF and DF. The impact of increasing the number of relay nodes to the system performance is to be investigated. Similar to the previous section, for the simulation purposes, three scenarios are defined as described in Table 10. We assume that the source node and the destination node are located in a distance of two kilometers between each other. The SNR values of the SR links and the RD links differ for each scenario according to the relay position. The simulations are performed with 16 QAM(1/2) modulation scheme under the SUI type 3 channel [32] for 10 channel realisations and for the number of single-antenna relays, $K = \{1, 2, ..10\}$.

The simulation results for all three cases and all K numbers are shown in Figure 69 - Figure 71 in Appendix A.2. It is demonstrated that adding more single-antenna relays to the WiMAX MIMO system does offer a BER performance enhancement, since the diversity order is also increased. This is also in a good accordance with the results reported in [3], wherein the AF strategy is considered. Nevertheless, the improvement is no longer substantial at $K > 5$ which yields only less than 1 dB gain per relay node addition. Furthermore, it can also be observed in Figure 46- Figure 48, that for $K = 1$ in all three cases, the DF strategy yields better performance than the former strategy. However, at $K \geqslant 2$, the AF strategy shows a better BER performance than the DF strategy, which can be well noticed at a bigger K number. This is due to the fact that there is a propagation error on the relay node caused by the imperfect decoding process in the DF strategy, which subsequently causes the destination node to combine and to decode the already erroneous data.

As depicted in Figure 46, the results of the first case, where the SR link is better than the RD link or when the relay node is near to the source node, mainly show better performance than the other two cases for both strategies. In addition to that, for case 2 and case 3 particularly at higher number of relay K, the DF relaying shows almost similar less performances as shown in Figure 47 (b) and Figure 48 (b), respectively. It conveys that because of its imperfect decoding structure, the DF strategy performances are impaired by the poor link quality of the first hop regardless the link qualities of the next hop. Whereas the AF strategy brings out a better performance as the RD link quality ameliorates. This indicates that the amplified relaying

Figure 46: MIMO multi single-antenna relays performance, Case 1 where the SR link quality is better than the RD link quality. For K = 1, the DF strategy shows better performance than the AF strategy. For K ⩾ 2, the AF strategy outperforms the DF strategy. This is because the latter strategy induces a propagation error on the relay node caused by the imperfect decoding process in the DF strategy.

has better resistance against severe link qualities compared to the decoded relaying. These results show an agreement with the results reported in [72] which demonstrate that the first hop link quality is more significant than the subsequent hops. It can be explained that if the first hop has a good link quality, it can subdue the propagation error or alternatively the noise propagation induces by the decoding structure or the amplifying nature of the relay, respectively.

4.3 CHAPTER SUMMARY

In this chapter, we presented the performance investigations of employing single-antenna relay(s) on both the SISO and the MIMO WiMAX systems using the AF and DF relaying strategies. For SISO systems, we have shown that the performance of each strategy may improve when applying a cooperative scheme or by increasing the number of relay nodes, since it subsequently increases the spatial diversity gain. However, there is a limit where it no longer shows substantial improvement even though the number of relay nodes is increased. Furthermore, adding more hops to the SISO system does not necessarily offer performance gain. Since as the number of hops increases, the error propagation induced by the DF strategy, or likewise the
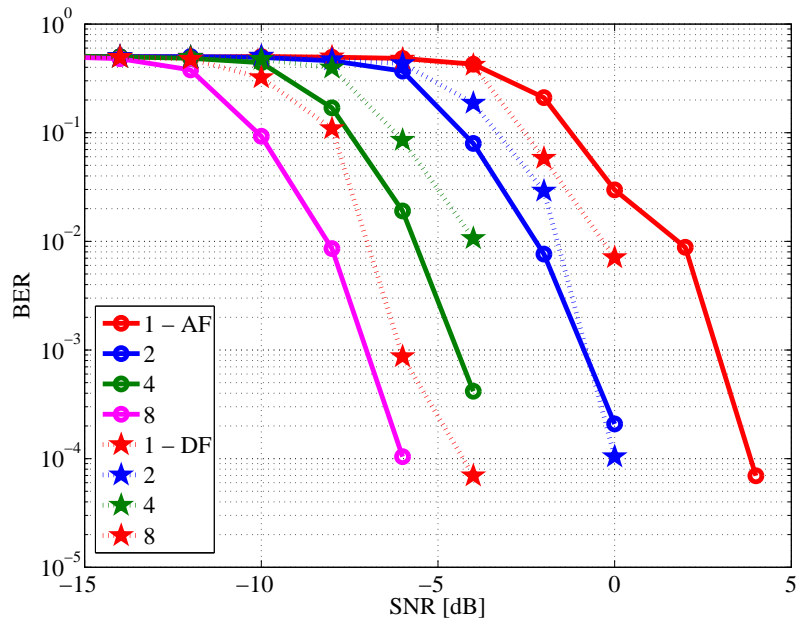
Figure 47: MIMO multi single-antenna relays performance, Case 2 where the SR link and RD link qualities are equally low. For K = 1, the DF strategy shows better performance than the AF strategy. For K $\geqslant$ 2, the AF strategy outperforms the DF strategy. This is because the latter strategy induces a propagation error on the relay node caused by the imperfect decoding process in the DF strategy.

noise propagation by the AF strategy degrades the system performance. Nevertheless, it is shown that the DF strategy outperforms the AF strategy provided that each hop has the same link quality. In addition to that, careful consideration has to be given to the cost of employing more relays in the system, of whether the offered performance gain could compensate the complexity. Moreover, we have presented the study of using a single-antenna relay on the MIMO system and have shown that the performance of the system can be improved in favour. This also infers that relaying could help mitigate the keyhole effect or the degraded channel in the direct link. Moreover, it has been demonstrated that even though the multiplexing gain cannot be obtained through employing more single-antenna relays, the system could still benefit the spatial diversity gain to improve its BER performance. This result is shown valid for both the AF and DF relaying strategies.
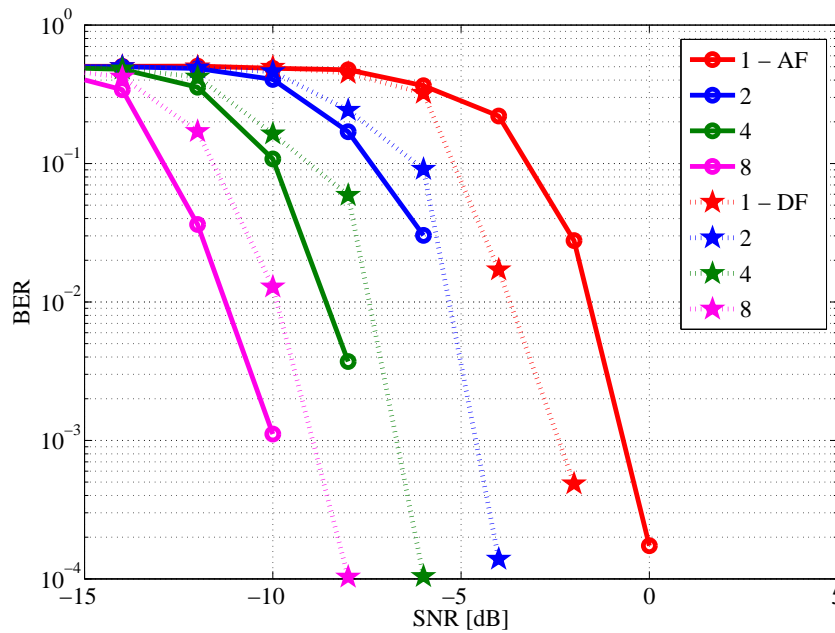
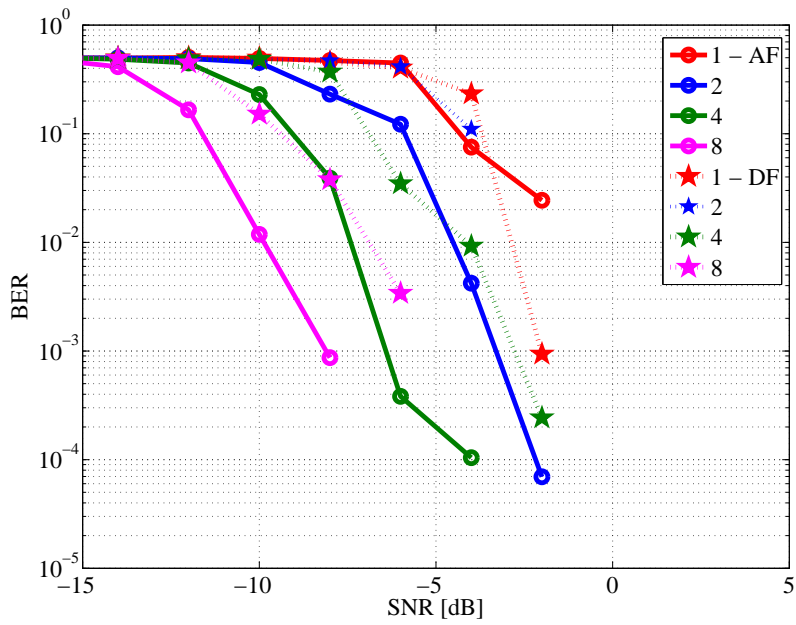Figure 48: MIMO multi single-antenna relays performance, Case 3 where the RDlink quality is better than the SR link quality. For K = 1, the DF strategy shows better performance than the AF strategy. For K ⩾ 2, the AF strategy outperforms the DF strategy. This is because the latter strategy induces a propagation error on the relay node caused by the imperfect decoding process in the DF strategy.

MULTI-ANTENNA RELAY IN WIMAX SYSTEM

Relays are originally focused on improving the transmission reliability and broadening the coverage with low expenditures (i.e., transmit power and cost). Due to the ever-growing demand of higher data rate, relay technology is also prompted to increase the data rate. In the previous chapter, we presented the performance investigation of single-antenna relay(s) when applied to the WiMAX SISO and MIMO systems. It has been shown that by exploiting single-antenna relay, the performance of the SISO and MIMO systems can be increased. Inspired by the potential of relay communications and also the MIMO technology, in this chapter we will focus on the performance investigation of employing multi-antenna relay(s) in the WiMAX MIMO system.

It has been proven in many researches that a MIMO system can offer better performance than a SISO system, because it can offer higher spectral efficiency and improve the diversity gain considerably [88] [89]. Because of its promising features, MIMO technology is considered as one of the key solutions to fulfill the 4G requirements. In fact, MIMO technologies application is the key differentiation between 3G and 4G [120]. Therefore also, in order to achieve its goal in providing a reliable and a high throughput transmission, WiMAX has considered the MIMO solutions in its standard. A single-user MIMO technique is adopted in 802.16e−2005 [7] or likewise in 802.16 − 2009 [1] aiming to improve the link reliability of a point-to-point MIMO transmission. Meanwhile, a multi-user MIMO technique is considered in 802.16m−2011 [5] to allow the BS to transmit multiple data streams to multiple users in the same frequency and time slot [12]. In [48] [105], it is reported that exploiting multi-antenna relay node(s) in the MIMO system could exhibit a significant enhancement on the spatial diversity leading to a capacity improvement, which is of interest in this chapter.

Some investigations on a MIMO relay capacity have been performed by some researchers. For example, researches on the capacity of a MIMO relay where the upper bounds and the lower bounds of the relay system are derived can be found in [56] for regenerative (DF) relay, and in [121] for non-regenerative (AF) relay. Further researches are reported in [122] and [123] where design and configurations of a MIMO wireless relay are proposed. In [124], capacity performance analysis of a relay system with the transmit antenna selection and an MRC is investigated. Furthermore, the performance analysis of a cooperative MIMO relay channel with OSTBC has also been reported in [58]. In this chapter, the performance gain in terms of BER induced by exploiting multi-antenna relay(s) in the MIMO system will

be once again testified through simulations.

The reminder of this chapter is organized as follows. Section 5.1 discusses the DMT analysis of a MIMO relay system. In Section 5.2, the impact of using multi-antenna relay(s) on a single-user MIMO system to the system performance is investigated. Afterwards, the implementation of the multi-antenna relay(s) for a multi-user SISO system is studied in 5.3. Finally, Section 5.4 sums up the results from this chapter.

5.1 DIVERSITY-MULTIPLEXING TRADEOFF

Another alternative to examine a MIMO relay system is by analysing the DMT measure which can provide a fundamental measure of its performance. The DMT analysis is useful in qualifying the fundamental tradeoff between the DoF or the throughput of the system, and the reliability or the robustness of the system against the channel fading effect in the high SNR regime. The DoF is measured from the improvement of the data rate ($Rate$) as the SNR increases, which describes the multiplexing gain (r) of the system. The robustness of the system is evaluated from the error probability descent with the increasing SNR, which identifies the diversity gain (d) of the system. The DMT analysis for a MIMO relay system is the generalization of the DMT analysis for a MIMO channel introduced in [125]. It is shown therein that a MIMO system reaches a multiplexing gain of r and a diversity gain of d, if the data rate and the average error probability satisfy

$$\lim_{SNR \to \infty} \frac{Rate(SNR)}{\log(SNR)} = r, \tag{5.1}$$

$$\lim_{SNR \to \infty} \frac{\log(P_e(SNR))}{\log(SNR)} = -d, \tag{5.2}$$

for which it can also be written as $P_e(SNR) = SNR^{-d}$. Following [125], for a MIMO channel with n_t transmit and n_r receive antennas, the multiplexing gain r is upper bounded by the DoF of the channel which is $\min\{n_r, n_r\}$; and the diversity gain is upper bounded by $n_t n_r$. It is also demonstrated that the optimal diversity gain $d(r)$ given the multiplexing gain $r = \{0, ..., \min\{n_t, n_r\}\}$ for such a MIMO system can be given by the piecewise-linear function joining the (r, d) pairs as follows

$$d_{MIMO}(r) = (n_t - r)(n_r - r), \tag{5.3}$$

for the case when the code length l fulfilled $l \geqslant n_t + n_r - 1$. In other words, for an integer value of r, as many as r transmit and receive antennas provide multiplexing gain and the rests contribute to the diversity gain. Thereof, for a MIMO relay channel with n_t transmit antennas, n_k relay antennas, and n_r receive antennas, the maximal diversity gain is known to be $n_k \min\{n_t, n_r\}$. Meanwhile, the maximal multiplexing gain is determined

as $\min\{n_t, n_k, n_r\}$. Further investigation of the DMT for a full-duplex and a half-duplex relay system are inferred in [126], which are defined as

$$d_{FD}(r) = \min\{d_{n_t,n_k}(r), d_{n_k,n_r}(r)\}, \tag{5.4}$$

$$d_{HD}(r) = \min\left\{d_{n_t,n_k}(\frac{r}{a}), d_{n_k,n_r}(\frac{r}{1-a})\right\}, (0 < a < 1), \tag{5.5}$$

respectively, where a and $(1 - a)$ are the duration of the transmission of the first phase and the second phase of the half-duplex relay system, respectively.

5.2 MULTI-ANTENNA RELAY ON SINGLE-USER MIMO SYSTEM

In this section, we consider the open-loop solution (without feedback) for a single-user MIMO transmission. Principally, it can be implemented using spatial multiplexing techniques or diversity techniques. Spatial multiplexing techniques, which exploit spatial dimension of the channel by transmitting parallel independent data streams, are aimed to increase the data rate of the system with no additional cost of power or bandwidth [127]. Meanwhile, diversity techniques exploit multi-version of the signals at the receiver side, where each of the signals is received from independent fading path (time/frequency/space), to improve the link reliability. One example of the diversity technique is the classic Alamouti STBC [34], which is used in this thesis.

In the following section, the employment of multi-antenna relay(s) in a single-user MIMO system will be investigated for a two-hop system and a multihop system.

5.2.1 *MIMO Two-hop Relay*

For the MIMO two-hop relay system in the following section, the performance investigations will be performed for two scenarios, i.e., the single relay and the multi-relay scenarios.

5.2.1.1 *System Model*

We consider a half-duplex relay system with a two-antenna source-and-destination pair and K two-antenna relays, as shown in Figure 49. It is assumed that the direct link can be ignored due to the large distance and the severe fading effect of the SD channel. The signals received at the k-th relay node in the first stage and at the destination node from the k-th relay node in the second stage are given by

$$\mathbf{y}_{s,k} = \mathbf{H}_{s,k} \sqrt{P_s} \mathbf{x}_s + \mathbf{w}_{s,k}, \tag{5.6}$$

$$\mathbf{y}_{k,d} = \mathbf{H}_{k,d} \sqrt{P_k} \, \mathbf{x}_k \; + \; \mathbf{w}_{k,d}, \qquad\qquad (5.7)$$

respectively, where $\mathbf{H}_{s,k}$ is the channel matrix between the source node and the k-th relay node. $\mathbf{H}_{k,d}$ is the channel matrix between the k-th relay node and the destination node. P_s and P_k are the source total transmit power and the k-th relay total transmit power, respectively. $\mathbf{x}_s$ is the transmitted signal from the source node. $\mathbf{w}_{s,k} \sim \mathcal{CN}(0, \sigma_{s,k}^2)$ and $\mathbf{w}_{k,d} \sim \mathcal{CN}(0, \sigma_{k,d}^2)$ are the noise at the k-th relay node and at the destination node, respectively. $\mathbf{x}_k$ is the transmitted signal from the k-th relay node. If AF relaying strategy is applied, $\mathbf{x}_k$ is given by

$$\mathbf{x}_k = \frac{\mathbf{y}_{s,k}}{\sqrt{P_s |\mathbf{H}_{s,k}|^2 \; + \; \sigma_{s,k}^2}}. \qquad\qquad (5.8)$$

Meanwhile, if the DF relaying strategy is applied, $\mathbf{x}_k$ is the re-encoded version of $\mathbf{x}_s$. The signals from the relay nodes are then combined using the MRC method at the destination node.
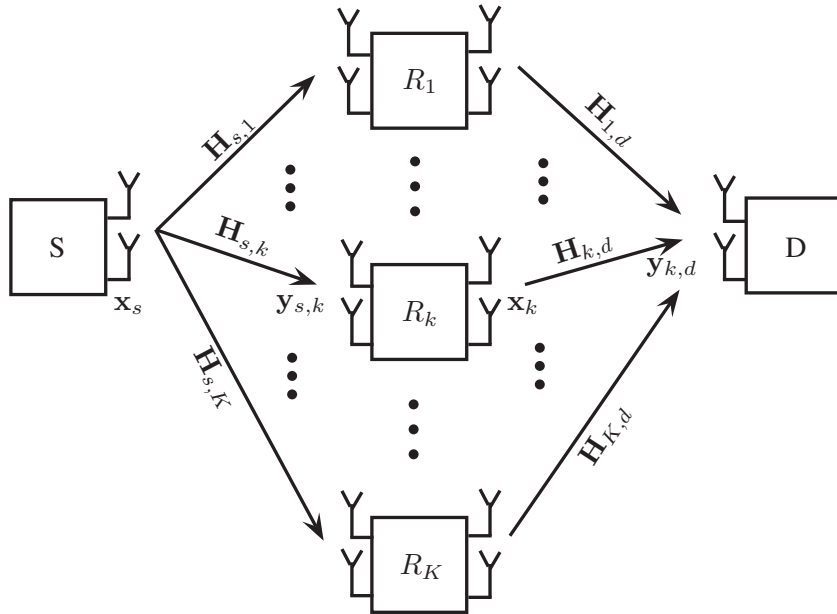
Figure 49: $2 \times K \times 2$ MIMO system

In our model, it is assumed that the channels are orthogonal, therefore the relays do not cause interference to one another. Furthermore, the relays are assumed to be equidistant and they are assigned with equal power allocation.

5.2.1.2 *Simulation Results*

The BER performances of the proposed model are investigated through simulations for a number of relays $K = \{1, 2, 3, 4, 5, 10, 15\}$. First, the inves-

tigation is performed for K = 1 under three cases as defined in Table 11. The first case is to investigate the effect of having the relay node near to the source node, likewise having a better SR link than the RD link. Whereas, the third case is on the contrary. The second case represents a condition where both links (the SR and RD links) have equal link qualities, whereof in this context the relay node is located midway between the source node and the destination node. For each case, the performances of the AF and DF strategies are studied through simulations under the SUI type 3 channel model after a hundred channel realisations. Next, the performance investigation for a two-hop multi-relay system for number of relays K = {2,3,4,5,10,15} is performed. Our objective is to analyse the BER performance gain achieved by inserting more relay nodes to the system.

Condition	Case 1	Case 2	Case 3
S-D Distance [km]	2	2	2
S-R Distance [km]	0.5	1	1.5
SNR S-R [dB]	+10	+5	+5
SNR R-D [dB]	+5	+5	+10

Table 11: Simulated MIMO relay cases

The simulation result for the proposed MIMO two-hop relay system with one relay node is shown in Figure 50. It can be observed that almost all the proposed relay systems yield a better BER performance than the system without relay. The performance improvement is as a result of the power and diversity gains offered by the relay node. For the relay system with the DF strategy, the one with the relay node located near to the destination node (case 3) gives a better performance of ∼ 5 dB betterment compared to the system without relay. It is followed closely by the system with the relay node located near to the source node (case 1). The system with the relay node situated in the middle represented by case 2 shows least performance of ∼ 4 dB improvement. However, it is still eminent compared to the AF strategy in almost all cases. These improved performances are on account of the coding gain offered by the DF strategy. For the proposed system, the DF strategy is more beneficial when the relay node located near to the destination node, or when the RD link quality is good. As for the AF strategy, the system with the relay node located near to the source node (case 1) exhibits better performance by ∼ 4 dB. However, it still cannot surpass the performances of the DF strategy. The performance improvement for the AF strategy is followed subsequently by the case 3 and then the case 2. Unlike the former strategy, the latter exhibits more gain when the relay node is located nearer to the source node. The reason is because when the quality of the SR link is good, the noise propagation caused by the relay node when forwarding the signal to the destination node is lessened. The simulation results also demonstrate that if the quality of both the SR and

RD links are poor, the relay gain cannot compensate the noise propagation effect. Hence, in this case, the relay system with the AF strategy offers no improvement compared to the system without relay.
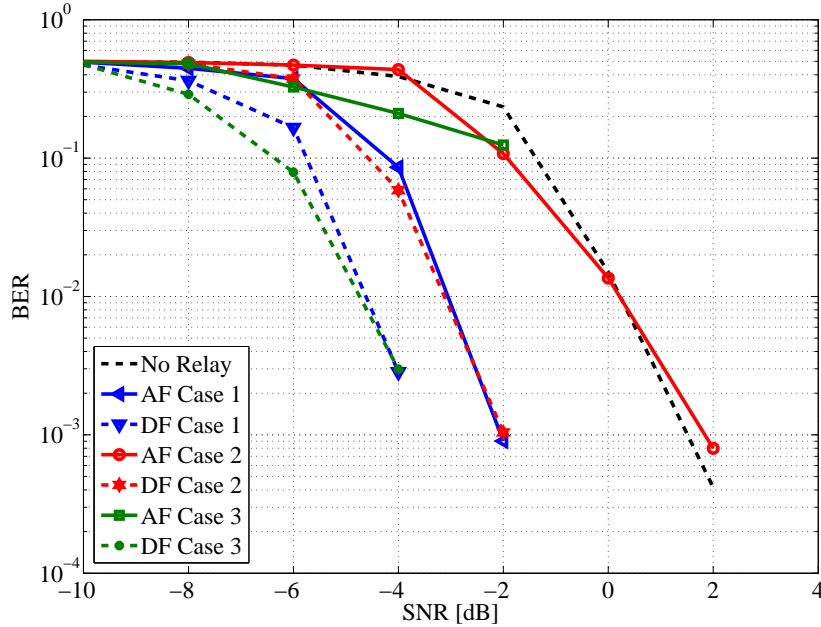
Figure 50: MIMO two-hop relay performance without direct link (16 QAM 1/2, SUI3 channel, 100 channel realisations). The DF strategy outperforms the AF strategy. The case where at least exist one good link (Case 1 and Case 3) yields better performance

Analysing also the results from the previous chapter, it can be resolved that if a transmit diversity is provided in a two-hop system, the DF strategy demonstrates a significant performance improvement when the relay node is located near to the destination node. On the contrary, the AF strategy yields a better performance when the relay node is located near to the source node. However, if there is no transmit diversity, both strategies exhibit better performances only when at least exists one link with a good quality between the SR and the RD links.

The next investigation is performed for a multi-relay two-hop system of $K = \{2, 3, 4, 5, 10, 15\}$. It is to observe the performance improvement offered by more relay nodes. For this purpose, the simulations are done taking up the conditions of case 2. That is where the relay nodes are located in the middle between the source node and the destination node, and the SNR of the relay links is 5 dB better than the SD link. The simulation results are plotted in Figure 51 and Figure 52. It is demonstrated in Figure 53 that adding more relay nodes to the system subsequently enhances the BER performance of up to 1 dB and 2 dB per one relay node addition for the AF and DF strategy, respectively. The improvement is owing to the

higher spatial diversity induces by the relay nodes. Interestingly, the former strategy shows more improvement gain. In fact, it is able to even out with the performance of the DF strategy at higher number of relays nodes K. It is indicating that combining the forwarded noisy signals induces less error than combining the re-encoded signals especially at lower SNR. However, the improvement gain alleviates as K increases. Furthermore, in practice, adding more relay nodes introduces some overheads to the system. This is because alongside the higher hardware cost, the coordination and the synchronization of the relay nodes which are significant to the performance of the system become more complex. Therefore, employing more relay nodes to the system is not always preferential when the performance gain offered is not significant enough to pay off the complexity costs.

Our simulation results indicate that the DF strategy outperforms the AF strategy in both scenarios (single relay and multi-relay) for all given cases. However, for the multi-relay scenario, the given conditions where all relays experience similar link qualities might not represent the real condition sufficiently. In reality, each relay might have different channel condition. Therefore, the relay nodes introduce more diversity to the system which subsequently exhibits a better system performance. Meanwhile, the conditions applied to our model represent either the worst case where all relay nodes having poor link qualities (the curves at low SNR); or the best case where all relay nodes experiencing good link qualities (the curves at high SNR). Nevertheless, it still provides a good insight of how the system may behave given the predefined conditions under the AF and DF relaying strategies.

5.2.2 *MIMO Multihop Relay (L>2)*

In this part, a MIMO relay system model with more than two hops is proposed and investigated. Our objective is to study the impact of adding more hops to the system. It is expected to extend the coverage distance, also at the same time, leastwise, able to retain the BER performance of the system.

5.2.2.1 *System Model*

The considered MIMO $(L+1)$-hop system is illustrated in Figure 54, where the transmission of a pair of two-antenna transmitter and receiver is assisted by $L+1$ intermediate relays. Each relay node is equipped with two receive and transmit antennas and could only receive a signal from the last former node. Thus, the received signal at the relay node l can be expressed as

$$\mathbf{y}_l = \mathbf{H}_{l-1,l} \sqrt{\frac{P_{l-1}}{2}} \, \mathbf{x}_{l-1} \; + \; \mathbf{w}_l, \; l \in \{0, \dots L\}, \tag{5.9}$$

where $\mathbf{H}_{l-1,l}$ is the channel matrix between the relay node $l-1$ and the relay node l. P_{l-1} is the transmit power of the relay node $l-1$. $\mathbf{w}_l \sim \mathcal{CN}(0, \sigma_l^2)$ is

Figure 51: MIMO multi-relay performance with AF strategy (16 QAM 1/2, SUI3 channel, 100 channel realisations). The performance improves as the number of relays K increases owing to the spatial diversity gain. At higher K, the AF strategy shows more improvement compared to the DF strategy although it still cannot outperform the DF strategy
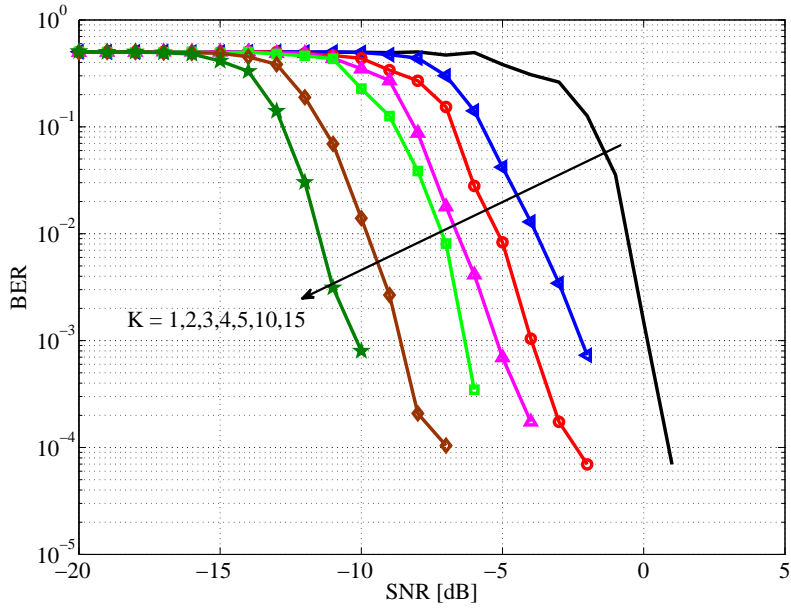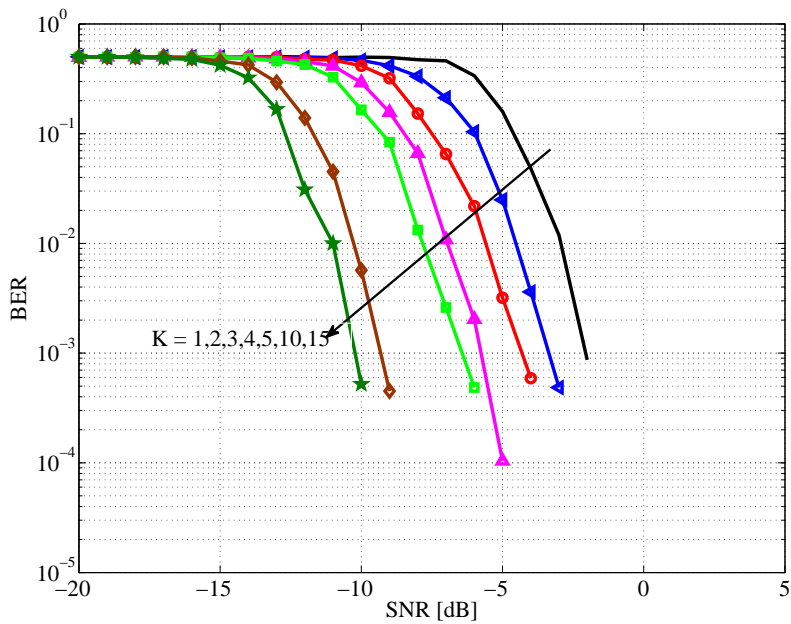

Figure 52: MIMO multi-relay performance with DF strategy (16 QAM 1/2, SUI3 channel, 100 channel realisations). The performance improves as the number of relays K increases owing to the spatial diversity gain. At higher K, the improvement rate declines. Nevertheless, the DF strategy still outperforms the AF strategy
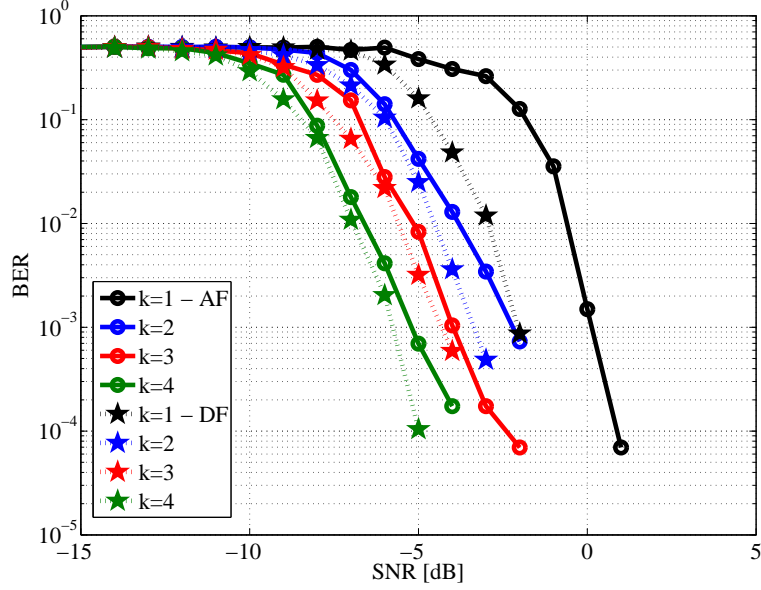
Figure 53: MIMO multi-relay performance comparison (16 QAM 1/2, SUI3 channel, 100 channel realisations). At higher K, the AF strategy shows more improvement compared to the DF strategy although it still cannot outperform the DF strategy
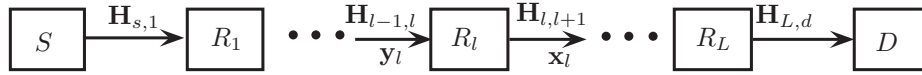
Figure 54: MIMO $(L + 1)$-hop system

the AWGN noise at the relay node l. $\mathbf{x}_{l-1}$ is the forwarded signal from the relay node $l-1$. Furthermore, the node l is the source node if $l == 0$; and is the destination node if $l == L + 1$. If the AF strategy is applied, $\mathbf{x}_{l-1}$ is given by

$$\mathbf{x}_{l-1} = \mathbf{B}\mathbf{y}_{l-1}, \tag{5.10}$$

where $\mathbf{B}$ is the diagonal scaling matrices with the normalization factors

$$\mathbf{B}_{j,j} = \frac{1}{\sqrt{\frac{P_{l-2}}{2}|(\sum_{k=1}^{2}\mathbf{H}_{l-2,l-1}(j,k)|^2) + \sigma_l^2}}, j \in \{1, 2\}. \tag{5.11}$$

If the DF strategy is applied, $\mathbf{x}_{l-1}$ will be the re-encoded version of $\mathbf{x}_{l-2}$ which might not be error-free. Since the error correction code is not implemented in our model, a propagation error can occur. In addition to that, it is assumed for our system that the channels are orthogonal, therefore there are no interferences induce by each node. Furthermore, the relays are assumed to be equidistant and they are assigned with equal power allocation.

5.2.2.2 *Simulation Results*

For the proposed MIMO multihop relay scenario, the BER performance of the system is investigated for the case when the relay nodes are located equidistantly a kilometer away one after another (step distance). Hence, the source node and the destination node are $(L + 1)$ kilometers apart. Furthermore, each hop is assumed to have the same link quality. In this investigation, the direct link is assumed to be severely faded and therefore can be ignored. The proposed system is simulated for the AF and the DF relaying methods and for the number of hops L = $\{1, 2, 3, 4, 5, 10\}$ after one hundred channel realisations under the SUI 3 type A channel model.

   The BER curves for the proposed system using the AF strategy are plotted in Figure 55. It is demonstrated that adding more hops to the proposed system will only degrade the system performance by ~ 2 dB per addition of a hop. It shows that the gain offered by the multi-antenna relay nodes could not help to suppress the noise propagation effect caused by the amplification in each hop, even at higher SNR. However, as shown in Figure 56, when the relay node in each hop applying the decoding relaying technique, the performance of the system can almost be upheld, even for a higher number of hops L. In other words, the coverage of the system can be enlarged without suffering a loss in the BER performance of the whole system. This is owing to the coding gain offered by the relaying strategy, as well as, by the multiple antenna processing. Hence, it can be inferred that in spite of the higher implementation complexity compared to the AF strategy, the DF strategy is opted for the proposed system model.

5.3 MULTI-ANTENNA RELAY ON MULTI-USER MIMO SYSTEM

The multi-user MIMO topic has recently garnered much interest. A system where a single transmitter with multiple antennas is able to serve multiple users simultaneously, becomes more and more anticipated. Such a system could offer not only a higher capacity owing to the multiple antennas technique, but also the gain of multiple access and spectrum efficiency. Therefore, LTE and WiMAX have also considered the MU-MIMO technique as one of their key features to meet the IMT-Advanced requirements. However, those advantages offered by the MU-MIMO system are at the cost of more complexities (i.e. hardware, price, implementation). Furthermore, the nature of the multiple users system presents co-channel interferences between the users. Therefore, the performance of such a system depends mainly on the interference cancellation technique and the multi-user scheduling strategies [128].

   In a multi-user network, the capacity of the system is often investigated through its DoF, also known as the maximal multiplexing gain or the pre-log factor. It describes the scaling behaviour of the network sum capacity

Figure 55: MIMO multihop AF performance with step distance (16 QAM 1/2, SUI3 A channel, 100 channel realisations). The performance degrades substantially as the number of hops L increases due to the noise propagation
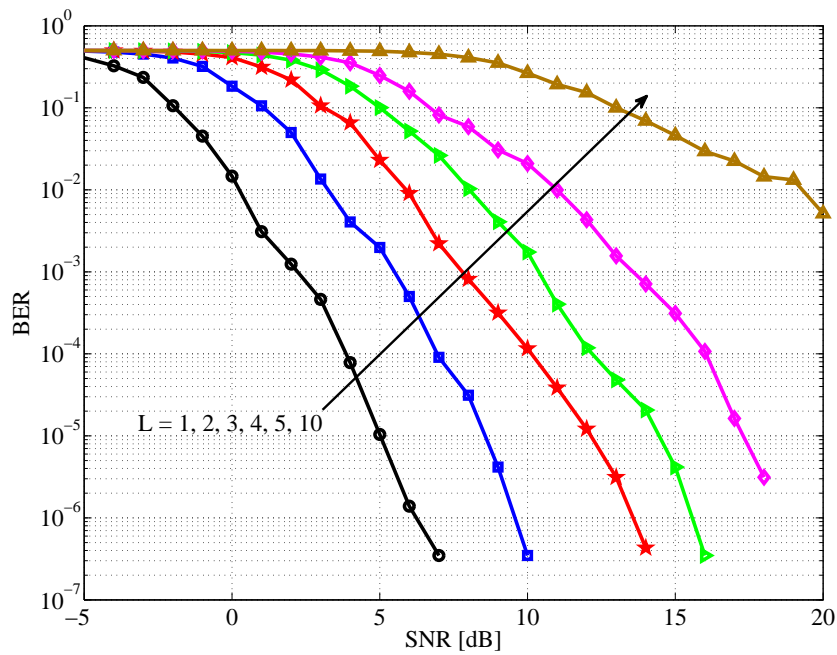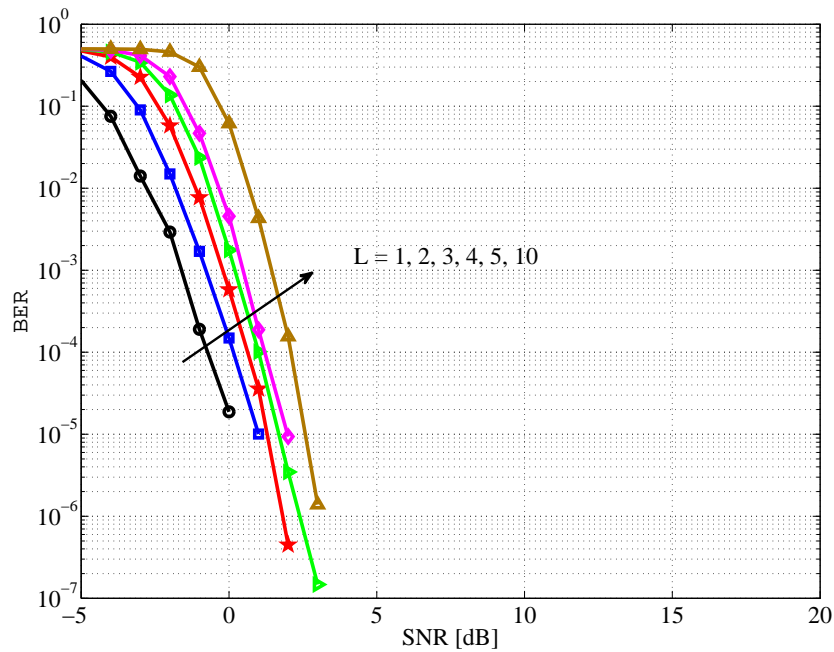

Figure 56: MIMO multihop DF performance with step distance (16 QAM 1/2, SUI3 A channel, 100 channel realisations). Owing to the coding gain, the DF strategy is proven to be beneficial since it can maintain the BER performance even though the number of hops L increases

C_Σ at high SNR. This corresponds to a number of parallel independent channels that can be exploited, which is defined as

$$DoF \equiv \lim_{SNR \to \infty} \frac{C_\Sigma(SNR)}{\log(SNR)}. \tag{5.12}$$

It is reported in [129], that without the knowledge of the CSI, the spatial DoF of a MIMO multi-user will be lost. Also reported therein, that a DoF of a MU-MIMO system with a total transmitter antennas of N_t and a total receiver antennas of N_r, given the CSI knowledge, for a BC channel and a MAC channel are equal to that of the SU-MIMO point-to-point (P2P) channel, which is defined as

$$DoF(BC) = DoF(MAC) = DoF(P2P) = \min\{N_t, N_r\}. \tag{5.13}$$

Some investigations regarding the DoF of a multi user channel have also been reported in [130] for the K users interference channel in time varying channel. It is reported that if the interference cancellation technique is applied, the maximum DoF is given by $KN/2$, where $N = N_t = N_r$ is the number of antennas at each node. Also reported therein that the DoF of K users interference channel with M_i transmitter antennas and N_i receiver antennas for $i \in \{1, \dots K\}$ is upper bounded by $\frac{1}{2} \sum_{i=1}^{K} \min\{M_i, N_i\}$. Similar investigation also reported in [129], where the upper bound of the DoF for $K = 2$ users is given by $\min\{M_1 + M_2, N_1 + N_2\}$. In [131], an investigation for X channel with K_t number of transmitters and K_r number of receivers, each equipped with A antennas, results in the upper bound and the lower bound of the DoF which are defined as $\frac{AK_tK_r}{K_t+K_r-\frac{1}{A}} \leqslant DoF \leqslant \frac{AK_tK_r}{K_t+K_r-1}$. In addition to that, further investigation concerning a multi user relay system can be found in [131], where the DoF of K single-antenna parallel networks (half-duplex two-hop relay) with L relay nodes is defined as $\frac{KL}{2(K+L+1)}$. Also in [132], an investigation of single-antenna relays system with L number of relays, and K number of transmitter and receiver yields the DoF of $\min\left\{K, \frac{K}{2} + \frac{L}{2(K-1)})\right\}$.

Compared to the conventional SU-MIMO, the MU-MIMO system has better resistant against propagation problems, such as spatial correlation and channel rank degradation. It has been investigated in [133] [134] [135] (and the references therein) that spatial correlation which degrades the performance of the SU-MIMO system is found to be beneficial in the MU-MIMO system especially when the multi-user scheduling is employed. Since it can reduce the channel hardening effect [1]. This can be explain because the scheduler will choose the user with the high channel gain, therefore the channel fluctuations (i.e., induces by the spatial correlation) are necessary to guarantee a fair treatment of all users. Furthermore, in the MU-MIMO system, the full rank of the channel matrix can be maintained owing to the

---

1 Channel hardening is a condition where as the number of transmit antennas increases, the channel state fluctuations measured by its variance decreases rapidly (hardens) while its mean improves [136].

adequate users separation.

In this thesis, we will focus only on the interference cancellation for a downlink MU-MIMO system. To suppress the interferences from other users, the knowledge of local CSI of all users is required in the transmitter for tailoring the precoding matrices for each user. This becomes the challenge in such a system. With full knowledge of CSI in the transmitter side, it is shown in [137] that the capacity of the interference channel can be equal to that of a channel when there were no interference. Because of the computational complexity of the precoding matrices, this technique is more efficient when the calculation is performed on the transmitter side. There are two types of precoding techniques, linear precoding (ZF, MMSE) and non-linear precoding (vector perturbation, Dirty-Paper-Coding, Tomlinson-Harashima). In this work, we limit our discussion to linear precoding technique. Considering that despite its sub-optimal performance compared to the non-linear precoding, the former technique has lower overhead [138].

5.3.1 *Linear Precoding*

The idea of linear precoding technique is similar to that of SDMA, where the transmitter separates the users spatially by assigning different precoding matrix to each user. One example of linear precoding technique is block diagonalization (BD) method which is the topic of interest in this section. This method is a generalization of ZF beamforming which allows the transmitter to transmit the signal only to the desired user by nullifying the directions to undesired users. The BD method for interference cancellation in the MU-MIMO is first investigated in [139], where it is shown that, despite its suboptimal sum capacity compared to the DPC method [140], this method could asymptotically approach the capacity at high SNR.

To understand how the BD method works, let us consider a MIMO downlink system, as shown in Figure 57. The system consists of a source node with N_t antennas and K destinations each with N_r antennas. The number of transmit antenna N_t should be $N_t \geqslant K N_r$. Furthermore, only a single independent transmit and receive streams are considered in the system. Let $\mathbf{x}_k$ be the $[N_r \times 1]$ transmitted symbol vector for user k, and $\mathbf{H}_k = [\mathbf{H}_{1,k}^H \ \mathbf{H}_{2,k}^H \ ... \ \mathbf{H}_{k,k}^H \ ... \ \mathbf{H}_{K,k}^H]^H$ denotes the $[N_r \times N_t]$ channel matrix between the source node and the k-th user. Thus, the received signal at the k-th user is given as

$$\mathbf{y}_k \ = \mathbf{H}_k \sum_{l=1}^{K} \mathbf{W}_l \mathbf{x}_l + \mathbf{n}_k$$

$$= \mathbf{H}_k \mathbf{W}_k \mathbf{x}_k + \mathbf{H}_k \sum_{l=1,l \neq k}^{K} \mathbf{W}_l \mathbf{x}_l + \mathbf{n}_k,$$

(5.14)

where $\mathbf{W}_k$ is the $[N_t \times N_r]$ precoding matrix for the k-th user, and $\mathbf{n}_k \sim \mathcal{CN}(0, \sigma_k^2)$ is the additive white Gaussian noise vector at the k-th user.. $\{\mathbf{H}_k \mathbf{W}_l\}$ for $k, l = \{1 ... K\}$ is the effective channel matrix of the l-th user from the k-th user. The first term represents the desired signal for the k-th
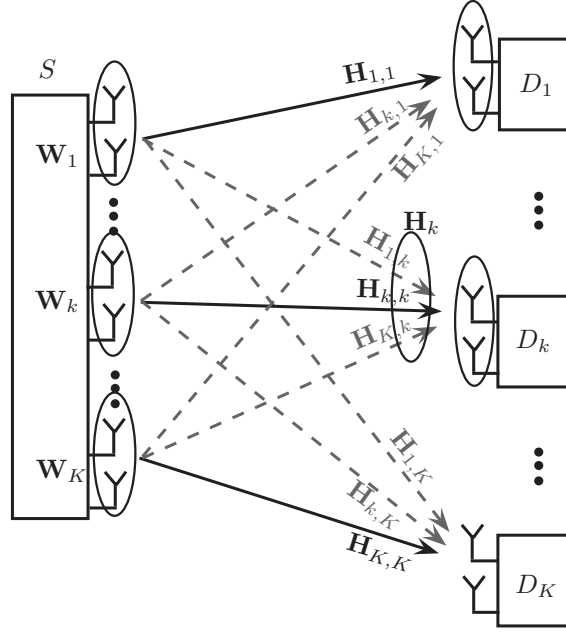
Figure 57: MIMO multi-user downlink system ($N_t = 2K$, $N_r = 2$)

user and the second term corresponds to the interference signal to the k-th user from other users that need to be cancelled out. To ensure the received signal $\mathbf{y}_k$ is interference free at the k-th user, the effective channel matrix $\{\mathbf{H}_k\mathbf{W}_l\}_{l \neq k}$ [N_rxN_r] should follow,

$$\mathbf{H}_k\mathbf{W}_l = \mathbf{0}_{N_r \times N_r}, \forall l \neq k. \tag{5.15}$$

Hence, the received signals $\mathbf{y}$ can be written as follows,

$$
\begin{bmatrix} \mathbf{y}_1 \\ \mathbf{y}_2 \\ ... \\ \mathbf{y}_K \end{bmatrix} = \begin{bmatrix} \mathbf{H}_1\mathbf{W}_1 & \mathbf{H}_1\mathbf{W}_2 & ... & \mathbf{H}_1\mathbf{W}_K \\ \mathbf{H}_2\mathbf{W}_1 & \mathbf{H}_2\mathbf{W}_2 & ... & \mathbf{H}_2\mathbf{W}_K \\ ... & ... & ... & ... \\ \mathbf{H}_K\mathbf{W}_1 & \mathbf{H}_K\mathbf{W}_2 & ... & \mathbf{H}_K\mathbf{W}_K \end{bmatrix} \begin{bmatrix} \mathbf{x}_1 \\ \mathbf{x}_2 \\ ... \\ \mathbf{x}_K \end{bmatrix} + \begin{bmatrix} \mathbf{n}_1 \\ \mathbf{n}_2 \\ ... \\ \mathbf{n}_K \end{bmatrix}
$$
$$
= \begin{bmatrix} \mathbf{H}_1\mathbf{W}_1 & 0 & ... & 0 \\ 0 & \mathbf{H}_2\mathbf{W}_2 & ... & 0 \\ ... & ... & ... & ... \\ 0 & 0 & ... & \mathbf{H}_K\mathbf{W}_K \end{bmatrix} \begin{bmatrix} \mathbf{x}_1 \\ \mathbf{x}_2 \\ ... \\ \mathbf{x}_K \end{bmatrix} + \begin{bmatrix} \mathbf{n}_1 \\ \mathbf{n}_2 \\ ... \\ \mathbf{n}_K \end{bmatrix}. \tag{5.16}
$$

In order to fulfill the condition in Equation 5.15, the precoding matrix $\mathbf{W}_k$ should be designed so that it lies on the nullspace of $\tilde{\mathbf{H}}_k$ [$(KN_r - N_r) \times N_t$]. $\tilde{\mathbf{H}}_k = [\mathbf{H}_1^H \, ...\mathbf{H}_{k-1}^H \, \mathbf{H}_{k+1}^H \, ... \, \mathbf{H}_K^H]^H$ is the channel gain matrix of all users other than user k. First, let $\tilde{\mathbf{H}}_k$ be SVD-decomposed into

$$\tilde{\mathbf{H}}_k = \tilde{\mathbf{U}}_k\tilde{\mathbf{\Sigma}}_k[\tilde{\mathbf{V}}_k^{(1)}\tilde{\mathbf{V}}_k^{(0)}]^H, \tag{5.17}$$

where $\tilde{\mathbf{U}}_k$ [$N_r \times N_r$] and $\tilde{\mathbf{\Sigma}}_k$ [N_rxN_t] are the left singular matrix and the matrix of singular values in a decreasing order, respectively. $\tilde{\mathbf{V}}_k^{(1)}$ [$(KN_r -$

N_r) x N_t] and $\tilde{\mathbf{V}}_k^{(0)}$ [N_rxN_t] are the right singular matrices that correspond to the non-zero singular values of $\tilde{\mathbf{H}}_k$ and to the zero singular values of $\tilde{\mathbf{H}}_k$, respectively. $\tilde{\mathbf{V}}_k^{(0)}$ lies in the nullspace of $\tilde{\mathbf{H}}_k$, since $\tilde{\mathbf{H}}_k\tilde{\mathbf{V}}_k^{(0)H} = \mathbf{0}_{(KN_r-N_r) \times N_r}$. Hence, $\tilde{\mathbf{V}}_k^{(0)}$ can be exploited as the precoding matrix $\mathbf{W}_k$ of the k-th user. Such that, assigning $\mathbf{W}_k$ with any linear combination of the columns of $\tilde{\mathbf{V}}_k^{(0)}$ will satisfy the null-constraint. The transmitted signal $\mathbf{x}$ and the received signal $\mathbf{y}_k$ at the k-th user can be expressed as

$$\mathbf{x} = \sum_{l=1}^{K} \mathbf{W}_l\mathbf{x}_l, \tag{5.18}$$

$$\begin{aligned}
\mathbf{y}_k &= \mathbf{H}_k\,\mathbf{x} + \mathbf{n}_k \\
&= \mathbf{H}_k\,(\sum_{l=1}^{K} \mathbf{W}_l\mathbf{x}_l) + \mathbf{n}_k \\
&= \mathbf{H}_k\tilde{\mathbf{V}}_k^{(0)H}\mathbf{x}_k + \mathbf{H}_k\underbrace{\sum_{l=1,l\neq k}^{K} \tilde{\mathbf{V}}_l^{(0)H}\mathbf{x}_l}_{=0} + \mathbf{n}_k \\
&= \mathbf{H}_k\tilde{\mathbf{V}}_k^{(0)H}\mathbf{x}_k + \mathbf{n}_k.
\end{aligned} \tag{5.19}$$

In the receiver side, the ZF method is applied to the received signal $\mathbf{y}_k$ to estimate the desired signal. Hence, the estimated signal $\tilde{\mathbf{x}}_k$ is given by

$$\tilde{\mathbf{x}}_k = (\mathbf{H}_{eff,k}^H\mathbf{H}_{eff,k})^{-1}\mathbf{H}_{eff,k}\,\mathbf{y}_k, \tag{5.20}$$

where $\mathbf{H}_{eff,k} = \mathbf{H}_k\mathbf{W}_k$ is the effective channel matrix for the k-th user.

However, for this conventional BD method to work, it requires that the total number of all receive antennas from all users should be less or equal to the number of the transmit antennas ($N_t \geqslant K\,N_r$). This becomes the limitation of this method. Furthermore, the BD method does not consider the interference from other transmitters (MAI). In addition to that, due to the nature of the ZF method which depends on the SNR, this method has less performance on low SNR regime. For the latter problem, the MMSE approach can be exploited to improve the performance on the low SNR [141]. Meanwhile, the first two problems can be solved by applying a post-processing filter in the receiver side [128] to overcome the MAI.

The MAI can be represented by a MIMO multi-user system with K users as illustrated in Figure 58, where the interference between users is present. Let $\mathbf{V}_k$ be the receive linear post-processing matrix of the k-th user and $\mathbf{H}_k = [\mathbf{H}_{1,k}^H\,\mathbf{H}_{2,k}^H\,...\,\mathbf{H}_{K,k}^H]^H$ denote the channel matrix at the k-th user. Thus, the received signal at the k-th user can be expressed as

$$\mathbf{y}_k = \mathbf{V}_k^H\mathbf{H}_{k,k}\mathbf{W}_k\mathbf{x}_k + \mathbf{V}_k^H\sum_{l=1,l\neq k}^{K} \mathbf{H}_{l,k}\mathbf{W}_l\mathbf{x}_l + \mathbf{V}_k^H\mathbf{n}_k, \tag{5.21}$$

where $\mathbf{V}_k$ must meet the following condition

$$\mathbf{V}_k^H\sum_{l=1,l\neq k}^{K} \mathbf{H}_{l,k}\mathbf{W}_l = 0, \forall k \in \{1, ... K\}. \tag{5.22}$$
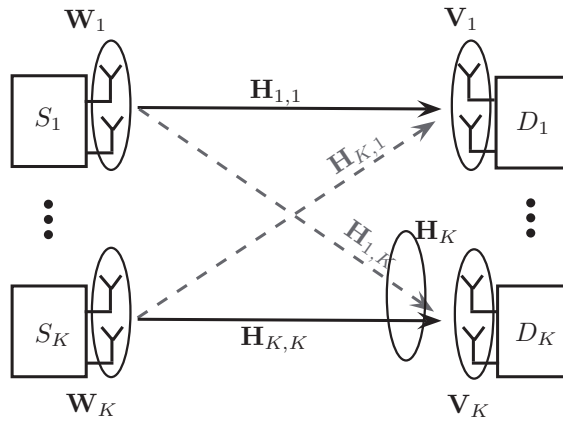
Figure 58: MIMO multi-user system with MAI ($N_t = 2$, $N_r = 2$)

Consequently, $\{\mathbf{W}_k, \mathbf{V}_k\}_{k=1}^K$ must be calculated jointly to find the optimal solution which requires an iterative computation. Since it does the interference suppression, in this thesis we refer this method as "interference alignment" (IA). The interferences are regarded to have a comparable strength as the desired signal. Therefore, the interferences are cancelled by orthogonalizing the channel, such that the interferences are projected to a different subspace than the desired signal.

The idea of the iterative IA approach is to calculate a new effective channel matrix for each transmitter k based on the receive post-processing matrix $\mathbf{V}_k$. Initially, $\mathbf{V}_k$ is randomly drawn with the standard normal distribution. Afterwards, from the new effective channel matrix, the transmit precoding matrix $\mathbf{W}_k$ is recalculated to reach a zero interference condition. The receive post-processing matrix $\mathbf{V}_k$ is also recalculated in the same way by exploiting the idea of reciprocity of the wireless channel [2]. The iterations are performed until a convergence condition is fulfilled (i.e., maximal number of iteration or the minimum power of leakage interference at the receiver is reached). The total interference leakage at the k-th receiver caused by other transmitters ($l \neq k$) is given by [142] [143]

$$\mathbf{I}_k = \text{trace}[\mathbf{V}_k^H \mathbf{Q}_k \mathbf{V}_k] \leqslant \epsilon, \tag{5.23}$$

where ϵ is the constant value of the minimum interference leakage power set as threshold. $\mathbf{Q}_k$ is the interference covariance matrix at the k-th receiver,

$$\mathbf{Q}_k = \sum_{l=1, l \neq k}^K P_k \mathbf{H}_{k,l} \mathbf{W}_l \mathbf{W}_l^H \mathbf{H}_{k,l}^H, \tag{5.24}$$

where P_k is the transmit power at the k-th transmitter. Furthermore in the reciprocal network, to recalculate the post-processing matrix, the total

---

2 Reciprocity in the sense that the signaling dimensions where the receiver experiences the least interference from other users are also the same signaling dimensions where it causes interference to other user when it becomes transmitter in the reciprocal network [142]

interference leakage at the receiver l caused by other transmitters ($k \neq l$) is given by

$$\overleftarrow{I_l} = \mathrm{trace}[\overleftarrow{V}_l^H \overleftarrow{Q}_l \overleftarrow{V}_l] \leqslant \epsilon, \tag{5.25}$$

where $\overleftarrow{Q}_l$ is the interference covariance matrix at the l-th receiver,

$$\overleftarrow{Q}_l = \sum_{k=1, k \neq l}^{K} \overleftarrow{P}_l \overleftarrow{H}_{l,k} \overleftarrow{W}_k \overleftarrow{W}_k^H \overleftarrow{H}_{l,k}^H . \tag{5.26}$$

P_k and P_l are the transmit power at the k-th transmitter and the l-th transmitter, respectively. ϵ is the constant value of the minimum interference leakage power. $\mathbf{H}_{k,l}$ and $\mathbf{H}_{l,k}$ are the channel matrix from the k-th transmitter to the l-th receiver and vice versa. The iterative approach [142] can be summarized as follows,

- initialize arbitrarily the precoding matrices $\mathbf{W}_1, \dots \mathbf{W}_K$,

- optimize the interference suppression matrices (post-processing filters) $\mathbf{V}_1, \dots \mathbf{V}_K$ based on the fixed precoding matrices. This is done by calculating the smallest eigenvalue of the interference covariance matrix $\mathbf{Q}_k$, since it represents the subspace with the least interference. Thus, if $\lambda_{\mathbf{Q}_k}$ is the eigenvectors of covariance matrix $\mathbf{Q}_k$, the $\mathbf{V}_k$ of a single independent stream is given by,

$$\mathbf{V}_k = \min(\lambda_{\mathbf{Q}_k}). \tag{5.27}$$

  Therefrom, $\mathbf{I}_k$ is computed according to Equation 5.23.

- optimize the precoding matrices $\mathbf{W}_1, \dots \mathbf{W}_K$ for a fixed post-processing matrices. Similar as in the previous step, this is done by calculating the smallest eigenvalue of the interference covariance matrix $\overleftarrow{Q}_l$. Thus, if $\lambda_{\overleftarrow{Q}_l}$ is the eigenvectors of covariance matrix $\overleftarrow{Q}_l$, the $\overleftarrow{V}_l$ or the $\mathbf{W}_l$ of a single independent streams is given by,

$$\overleftarrow{V}_l = \min(\lambda_{\overleftarrow{Q}_k}). \tag{5.28}$$

  Therefrom, $\overleftarrow{I}_l$ is computed according to Equation 5.26.

- repeat the processes from step 2 until the convergence criterion is satisfied. That is when the minimum interference leakage power is less than a predefined ϵ, or the iteration number reaches a predefined maximum number of iterations.

5.3.2 *System Model*

In this section, the BD method and the IA approach are applied to a half-duplex relay MU-MIMO system for the scenario as shown in Figure 59. In this network, the relay is situated in between two adjacent cells to
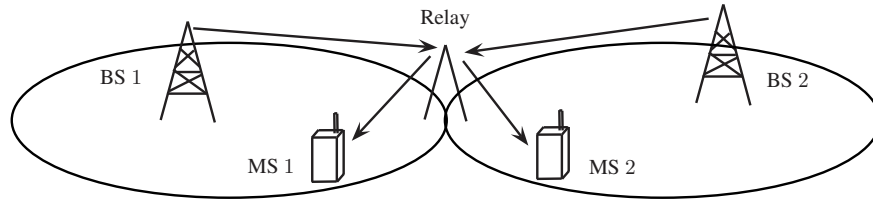
Figure 59: MIMO multi-user relay network. A relay is employed to assist the transmission of two adjacent cells

assist the transmission from both BSs to the corresponding users or mobile stations in the cell edge of each cell. The proposed system is modelled as a two (K = 2) source-and-destination pairs assisted with a relay node. The communications between the source nodes and the destination nodes can only take place through the relay node since the signal from BS cannot reach the mobile station in the cell edge. In other words, there is no direct link between the source nodes and the destination nodes. In this context, the relay node behaves as the multi-user transmitter. The source nodes and the destination nodes are each equipped with two antennas ($N_t = N_r = 2$), meanwhile the relay node is equipped with each four transmit antennas and four receive antennas. We assume that the first two transmit and receive antennas on the relay node are intended for the first source-destination pair. Also, the third and fourth transmit and receive antennas on the relay node are intended for the second pair as shown in Figure 60. We assume that the antennas on each node are spatially uncorrelated.

Figure 60: MIMO multi-user relay system (K = 2)

For the SR links or the links between the source nodes and the relay node, the first source node is paired with the first two antennas on the relay node. Meanwhile, the second source node is paired with the last two antennas on

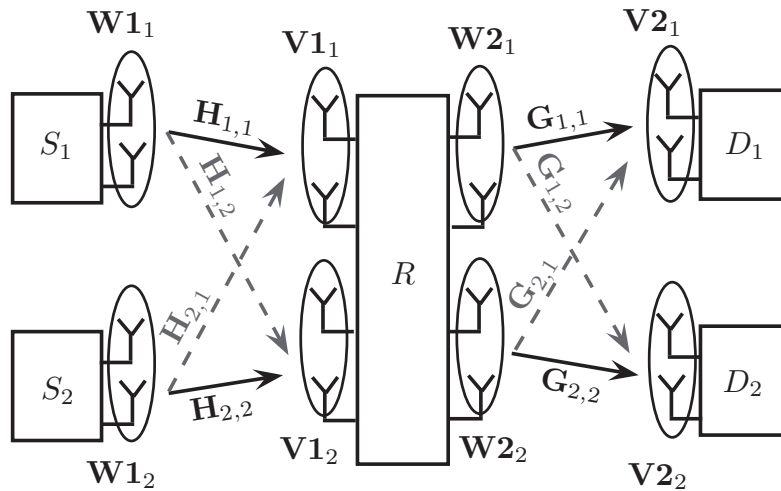the relay node. As for the RD links or the links between the relay node and the destination nodes, there are two scenarios considered. The first scenario is by pairing the first two of the relay antennas with the first destination node and the last two of the relay antennas with the second destination node. In other words, the channel is no longer seen as a BC channel but an interference channel, hence the IA approach is implemented. The second scenario is to implement the BD method, where for each destination node, two relay transmit antennas with highest channel gain are selected for transmitting the signal. The performance of both scenarios will be investigated through simulations for the AF and the DF relaying strategies.

For the links between the source nodes and the relay node, a pair of the precoding $\mathbf{W1}$ and the post-processing matrices $\mathbf{V1}$ are calculated based on the channel matrix $\mathbf{H}$. Similarly, for the links between the relay node and the destination nodes, the precoding matrix $\mathbf{W2}$ and the post-processing matrix $\mathbf{V2}$ are designed based on the channel matrix $\mathbf{G}$. Thus, on the first stage, the k-th destination node filters the signal with the predefined precoding matrix $\mathbf{W1}_k$ and afterwards sends it to the relay node. The relay node filters the received signals from the first two antennas with the post-processing matrix $\mathbf{V1}_1$, and from the last two antennas with $\mathbf{V1}_2$. On the second stage, before forwarding the signals to the desired destination node, the relay node filters the signal for the k-th destination node with the precoding matrix $\mathbf{W2}_k$. Finally, at the destination node k, the forwarded signal is filtered with the post-processing filter $\mathbf{V2}_k$ for the first scenario; or equalized with the ZF method as in Equation 5.20 for the second scenario.

For the DF strategy, the process is quite straightforward. However, for the AF strategy, the relay node does not decode the signal, rather simply multiplies the received signal with a linear precoding matrix $\mathbf{F}$, which is defined as follows,

$$\mathbf{F}_k = \mathbf{V1}_k \mathbf{W2}_k. \tag{5.29}$$

In this case, the linear precoding matrix for the relay node with the AF strategy is achieved from two separate linear precoding calculations of both channel matrix $\mathbf{H}$ and $\mathbf{G}$. Consequently, the source nodes, the relay node, and the destination nodes must have knowledge about the CSI. This is actually not the optimal solution since it burdens the relay node with the calculation of the precoding matrix to guarantee forwarding the right signal to the desired destination node. Another alternative is to calculate the interference suppression matrix for both links jointly, as reported in [144]. In that paper, an iterative and a non-iterative method based on the BD approach are proposed to calculate the linear precoding matrix on the relay which maximizes the sumrate. Therein, only the relay node and the destination nodes need to have full knowledge of CSI. It is demonstrated that the proposed methods outperform the conventional BD, but the proposed schemes need more complex calculations and rigorous optimisation

problems. Another investigation is found in [145], where the IA approach is exploited in a multi-user two way relay networks.

5.3.3 *Simulation Results*

Our aim is to investigate the BER performances of the proposed system model for both scenarios as summarized in Table 12. For chasteness, we called the first and the second scenario as the IA-IA and the IA-BD, respectively. For this purpose, it is assumed that the SD link and the RD link experience the same channel condition. The simulations are performed for the AF and the DF relaying strategies under a flat fading Rayleigh channel. The simulation results are plotted in Figure 62 after 50 channel realisations.

	SR link	RD link
1	IA	IA
2	IA	BD

Table 12: Simulated MIMO multi-user relay

Firstly, we compare the sum-rate performance of both linear precoding methods which corresponds to the sum-rate performance of the RD link. As depicted in Figure 5, the BD method shows a better average sum-rate compared to the IA approach, especially at higher SNR. This is because the BD method is able to fully eliminate (orthogonalize) the interference from other user. Meanwhile, the IA approach suppresses the interference by aligning it to different subspace (may not be exactly orthogonal) than the subspace of the desired signal. Furthermore, IA approach does not aligns the desired signal to its best subspace (i.e., subspace with the highest gain) but to the subspace which has less interference from and to other user. In addition to that, for both methods, the receiver side benefits the CSI to perform ZF method, which explains the sum-rate improvement at higher SNR.

Similarly, as shown in Figure 6, the IA-BD scenario yields a better BER performance than the IA-IA scenario for both relaying strategies. However, the difference of both scenarios is modest for the DF strategy. This can be explained since the IA approach considers the interference from other user as noise. Consequently, when the relay node applies the AF relaying technique, the target user will suffer more noise. This gives the reason for the better BER performance shown by the IA-BD scenario compared to the IA-IA scenario which is ~ 4 dB. Meanwhile, if the relay node performs the DF relaying technique, the noise can be addressed through the decoding process. Therefore, the IA-IA scenario can level the performance of the IA-BD scenario which is less than 1 dB at BER level of 10^{-3}. It is found that the DF strategy could offer a coding gain to the performance of the
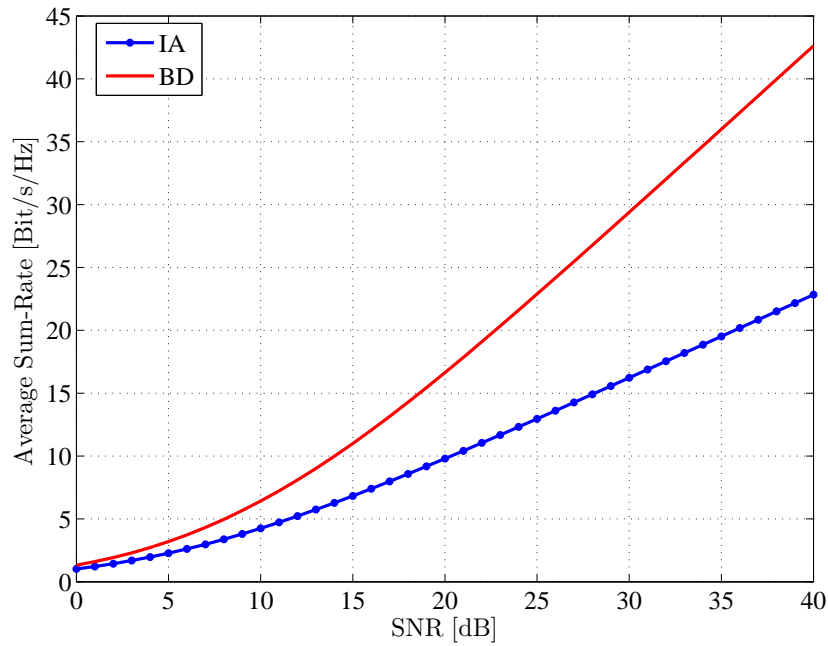
Figure 61: Average sum-rate for BD method and IA approach vs SNR for the case K = 2, Nt = Nr = 2). The block diagonalization (BD) method yields better sum-rate performance, because the BD method is able to fully eliminate (orthogonalize) the interference from other user. Meanwhile, the interference alignment (IA) approach suppresses the interference by aligning it to different subspace (may not be exactly orthogonal) than the subspace of the desired signal. Furthermore, IA approach does not aligns the desired signal to its best subspace

proposed system model with the IA-IA scenario of about 3 dB.
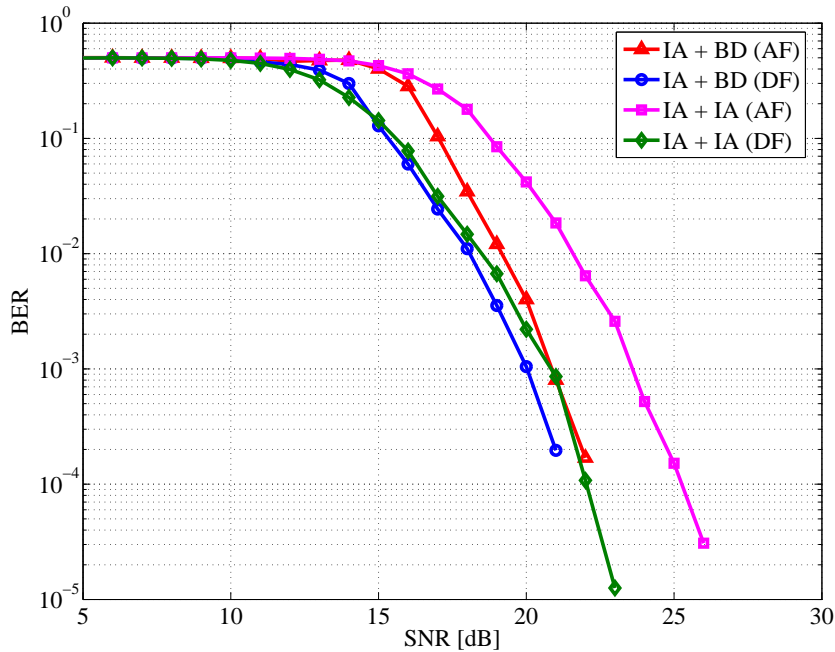
Figure 62: MIMO multi-user relay performance (16 QAM 1/2, Rayleigh channel, 50 channel realisations). The IA+BD method yields better performance for each relaying strategy due to the intra-antenna channel gain. Employing the DF strategy in the IA+IA method reduces the noise effect, hence improving the performance

It can also be observed that due to the limitation of the ZF-based method, which works only in the low noise and in the high power environment, the proposed linear precoding methods provide a good performance only at higher SNR. Meanwhile, at lower SNR, the methods still cannot overcome the noise effect. For the future work, this issue will be solved by implementing an MMSE-based linear precoding which is able to reduce the noise effect, since it considers also the noise variance in the calculation to maximize the SINR.

5.4 CHAPTER SUMMARY

In this chapter we have presented several investigations on the MIMO relay system for the AF and DF relaying strategies under a multi-user and a single user system, respectively. For a SU-MIMO system, it has been demonstrated that employing the multi-antenna relay(s) on the two-hop SU-MIMO relay system, under the system constraints given in this section, will be beneficial. Particularly, if there is at least one good link between the SR and the RD links, regardless of the relaying technique used. Moreover, employing more

relay nodes is proven to subsequently increase the spatial diversity gain. This, in return, enhances the system performance as the number of relays K increases, of course with more implementation overhead, such as, synchronization and scheduling. It is also demonstrated that the DF strategy outperforms the AF strategy in all cases by the cost of implementation complexity. It is also shown that the DF strategy exhibits a better performance when the relay node is located near to the destination node. Since the relay could effectively harvest the coding gain offered by the technique. Meanwhile, the AF strategy yields a better result when the relay node is placed near to the source node where the noise propagation effect can be best reduced. As for the SU-MIMO $(L + 1)$-hop system, it is shown that for a given case, the DF strategy could still preserve the BER performance of the whole system even for a large number of hops L. Meanwhile, the AF strategy suffers a significant performance degradation as the number of hops L increases.

For the MU-MIMO relay system, we have presented a multi-user system, where a relay node assists the transmission of K = 2 users pairs. The interference suppression on the SR link is performed by using IA approach. Meanwhile for the RD link, the BD method and IA approach are each implemented and investigated. The BD method yields better sum-rate performance than the IA approach since the latter does not align the signal to its best subspace and may not fully orthogonalize the interference. Furthermore, it is also demonstrated that the system with the BD method gives better BER performance compared to the system with only IA approach. This is because the IA approach considers the interference as noise, therefore it induces more noise effect to the target user. However, it is shown that by applying the DF relaying strategy on the relay node, the noise effect caused by the IA approach can be reduced. This is owing to the coding gain offered by the strategy.

CONCLUSIONS

6

In this final chapter, the contributions of the dissertation will be summarized and the future research possibilities will be suggested.

6.1 CONTRIBUTIONS

In this dissertation, we have presented the measurement procedure and the propagation analyses of a WiMAX system in the suburban area. Furthermore, to improve the performance of a WiMAX system, we have presented various relay systems covering the SISO and the MIMO models. Furthermore, for the MIMO relay system, both single-user and multi-user cases have also been discussed. The corresponding performance analyses of the proposed systems have also been provided.

In Chapter 2, we presented a measurement campaign of the WiMAX system in a suburban area of Hetzwege, Germany. The propagation analyses, covering the small scale and large scale fading characteristics of the measured system are reported. Based on the large scale fading analysis, it indicates that the area has a path loss model which is closer to the COST-231 Hata model. Meanwhile, the small scale fading analysis shows that the channel characteristics of the measured suburban area can be classified as the SUI type B terrain model. The area has, for most of the part, the Ricean fading characteristic. Furthermore, it is resolved that the measured area does not experience a frequency selective fading since the MED value corresponding to the derived RMS delay of the area is far below the specified guard interval duration of a WiMAX signal.

In Chapter 3, we presented a cooperative system consists of a source node, a relay node, and a destination node. It is proven that the cooperative scheme could improve the performance of the system owing to the diversity gain, regardless of the relaying technique applied. It is also shown that the performance of a relay system depends on the relay location or, in other words, on the SR and RD link qualities. Under the given system constraints, it is demonstrated that the DF strategy outperforms the AF strategy. Although, both strategies do not offer performance improvement at low SNR. This is due to the noise propagation caused by the AF strategy, or the decoding error propagation introduced by the DF strategy. Lastly, an algorithm to find the optimal position of the relay based on the RSSI distributions of the area is proposed. It has been shown that the proposed algorithm could improve the throughput of the system which is represented by the improvement of the MCS used; and also the coverage performance

of the system which is represented by the reduction of the blank spots.

In Chapter 4, we presented a single-antenna relay system for a SISO and a MIMO WiMAX systems. For a SISO system, we have demonstrated that the performance of the relay system, notwithstanding the relaying strategy applied in the relay node, can be enhanced when the diversity is introduced through cooperation between the source node and the relay node. The diversity gain can also be increased by employing more relay nodes to the system. However, it is found that at a certain number of relay nodes, the improvement is no longer significant. Furthermore, it is demonstrated that adding more hops to the SISO system does not necessarily offer a performance gain. This is because, as the number of hops increases, the error propagation induced by the DF strategy, or likewise the noise propagation by the AF strategy scales up and degrades the whole system performance. Despite the performance improvement induces by adding more relay nodes to the system, a careful consideration has to be given to the cost issues (i.e., implementation and hardware), of whether the offered performance gain could compensate the complexity. Moreover, we presented the study of using a single-antenna relay on the MIMO system and have shown that the performance of the system can be improved in favour. This also infers that relaying could help to improve the system performance when the direct link suffers from a keyhole-effect. Moreover, it is demonstrated that eventhough the multiplexing gain cannot be obtained through employing more single-antenna relays, the system could still benefit the spatial diversity gain to improve its BER performance.

In Chapter 5, we have presented a MIMO relay system for both single user and multi-user scenario. For a SU-MIMO system, it is demonstrated that having a relay node on the system is only beneficial when there exists at least a good link between the SR and the RD links. Furthermore, it is shown that employing more relay nodes on the two-hop relay system is proven to subsequently increase the spatial diversity gain. This, in return, enhances the system performance as the number of relays K increases. We also provided the performance comparison of the AF and DF relaying strategy, where it is shown that the DF strategy outperforms the AF strategy in all given cases. It is also proven that the DF strategy yields better performance when the relay node is located near to the destination node. That is where the relay could effectively benefit the diversity gain and the coding gain offered by the technique. Meanwhile, the AF strategy exhibits better result when the relay node is near to the source node, where the noise propagation effect can be best repressed. Furthermore, we evidenced that for an $(L + 1)$-hop system, the DF strategy is proven to be more robust in maintaining the performance of the system as the number of hops L increases compared to the AF strategy. As for the MU-MIMO relay system, we presented a multiuser system with a relay node to assist the transmission of $K = 2$ users pairs. It is shown that the BD method yields less sum-rate performance than the IA approach since the latter does not align the signal to its best subspace

and may not fully orthogonalize the interference. Furthermore, it is also found that employing the BD method for the interference cancellation on the proposed MU-MIMO relay system yields a better BER performance than when the IA approach is applied. This is because the latter approach considers the interference as noise, therefore it induces more noise effect to the target user. It is further shown that the coding gain offered by the DF strategy on the relay node is able to reduce the noise enhancement caused by the IA approach.

6.2 FUTURE RESEARCHES

Several interesting issues still remain open from this dissertation and are encouraged for further investigation. Some recommended topics for future research are as followings,

- A MU-MIMO interference relay channel: an optimal interference alignment technique needs to be investigated for a MU-MIMO system which consists of K ternary (source-relay-destination) communications.

- An MMSE-based linear precoding technique for a MU-MIMO relay system: as the results shown in Chapter 5, a multi-user system with the ZF-based linear precoding suffers from the noise effect, especially at low SNR. On the contrary, an MMSE-based linear precoding deals better with the noise effect. Since it considers the noise variance in the calculation to maximize the SINR at the receiver. Therefore, despite its higher complexity, an MMSE-based linear precoding is opted as an alternative to improve the system performance, especially at a high noise environment.

- Relay technology in CRN: a relay or a cooperative network is also encouraged for CRN. One example is for the spectrum sensing process where more than one sensing nodes cooperate in collecting the information about the spectrum occupation. This results in more robust detection and therefore reducing the probability of missed detection. Another example is to exploit the CRN user as a relay node to assist the transmission of the primary users. As a favour, the primary users give a time or a spectrum incentive to the CRN user.

SIMULATION RESULTS

A.1 SINGLE-ANTENNA RELAY ON SISO MULTIHOP SYSTEM

In the following are the BER performance curves of the $(L+1)$-hop system for $L = \{1, 2, ..., 10\}$ for the case with and without direct link. It is assumed that the source node and the destination node are five kilometers distant and the relay nodes are located equidistantly in-between with 5 dB more SNR than that of the SD link.

Figure 63 and Figure 64 show the simulation results for the case without direct link of the AF strategy and the DF strategy, respectively. Figure 65 and Figure 66 depict the simulation results for the case when the direct link is considered for the AF strategy and the DF strategy, respectively.

Figure 63: SISO multihop AF performance without direct link (16 QAM 1/2, Rayleigh channel, 10 channel realisations). The performance degrades as the number of hops L increases. Starting at $L \geqslant 2$, it cannot outperform the single-hop system due to the great deal of noise amplification

Figure 67 and Figure 68 present the BER performance curves for the case when the relay nodes are located equidistantly one kilometer away, one
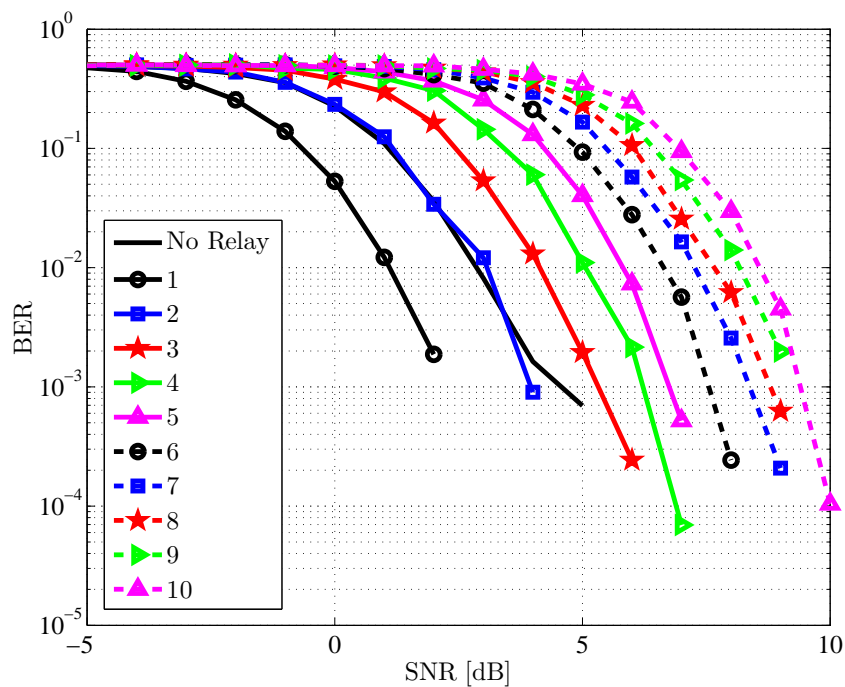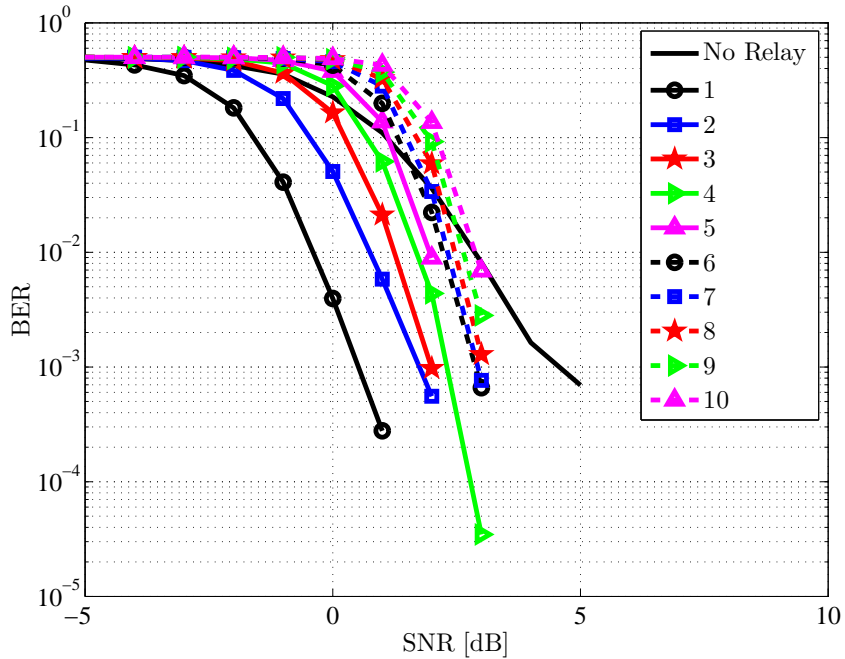
Figure 64: SISO multihop DF performance without direct link (16 QAM 1/2, Rayleigh channel, 10 channel realisations). The performance degrades as the number of hops L increases. Nevertheless, at higher SNR, the DF strategy outperforms the AF strategy owing to the coding gain

after another (step distance). Hence, the source node and the destination node are $(L+1)$ kilometers apart. In this investigation, the direct link is assumed to be severely faded and can be ignored.

A.2 SINGLE-ANTENNA RELAYS ON SISO TWO-HOP SYSTEM

In the following are the BER performance curves of the single antenna relays on a SISO two-hop system for the three cases with number of single-antenna relays of $K = \{1, 2, 3, 4, 5, 10, 15, 20, 25, 30\}$. Figure 69 shows the results for the case where the relay node is located near to the source node, and the SR link and the RD link are 10 dB and 5 dB higher than the SD link, respectively. Figure 70 depicts the results for the case where the relay node is located at the same distance between the source node and the destination node, and with the SR and RD links of 5 dB SNR higher than the SD link. Figure 71 presents the results for the case where the relay node is located near to the destination node, and the SR and RD links are 5 dB and 10 dB better than the SD link, respectively.

Figure 65: SISO multihop AF performance with direct link (16 QAM 1/2, Rayleigh channel, 10 channel realisations). The direct link could offer a diversity gain hence it improves the performance
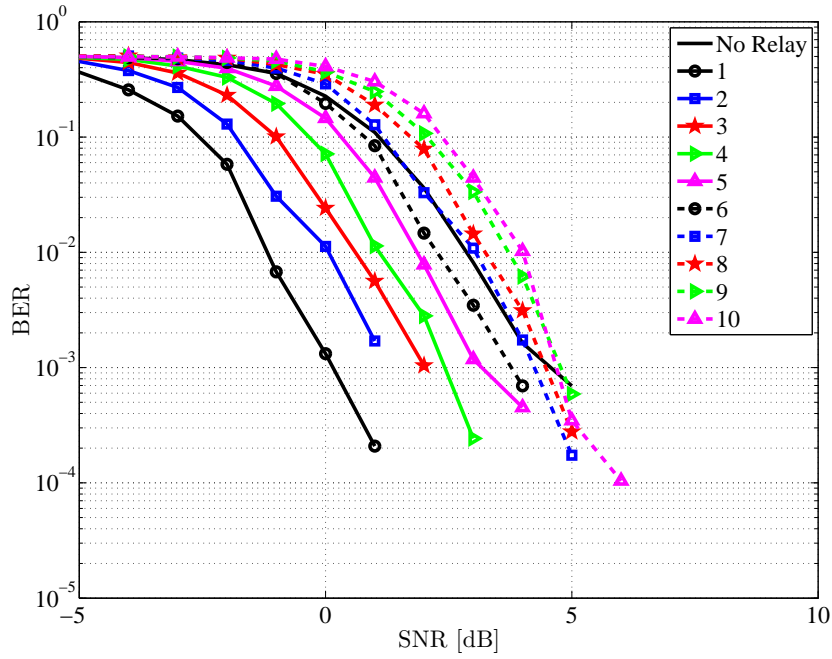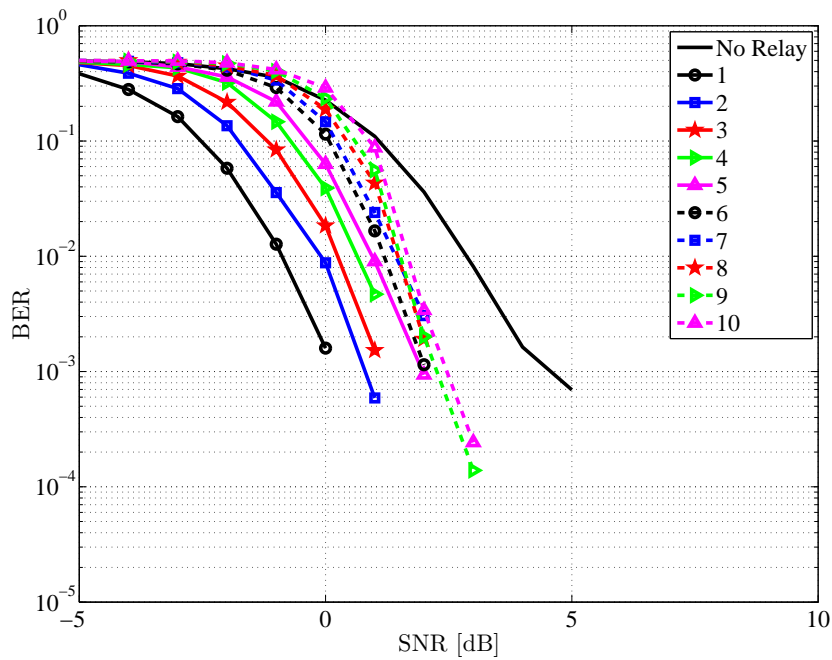

Figure 66: SISO multihop DF performance with direct link (16 QAM 1/2, Rayleigh channel, 10 channel realisations). The direct link could offer a diversity gain hence it improves the performance
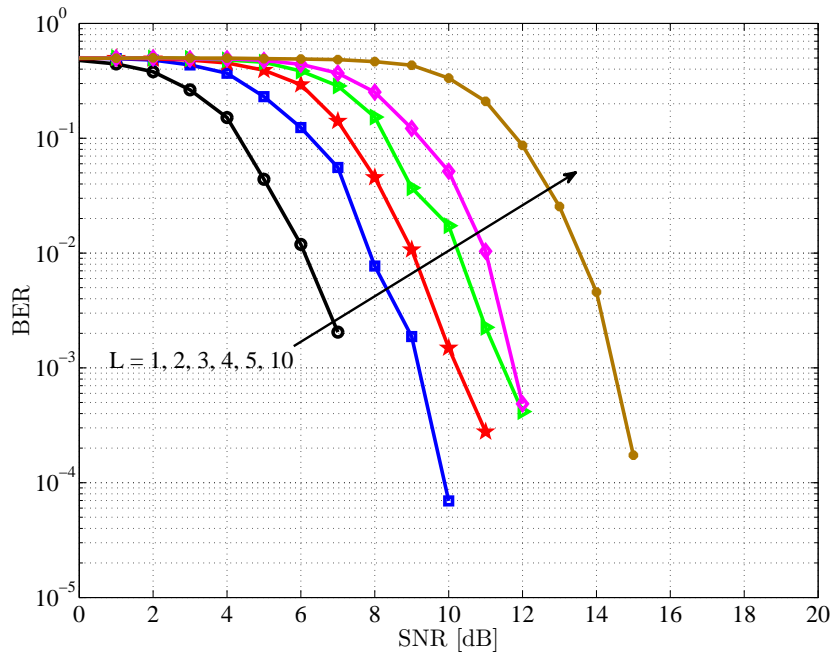
Figure 67: SISO multihop AF with step distance (16 QAM 1/2, Rayleigh channel, 10 channel realisations). The performance degrades significantly as the number of hops L increases due to the noise propagation
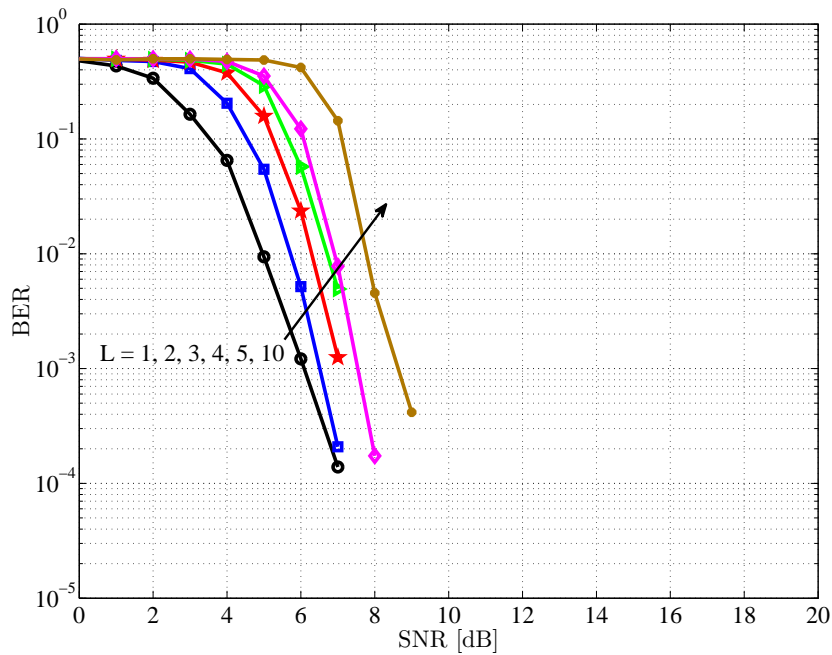
Figure 68: SISO multihop DF with step distance (16 QAM 1/2, Rayleigh channel, 10 channel realisations). The DF strategy could almost maintain the performance as the number of hops L increases on account of the coding gain
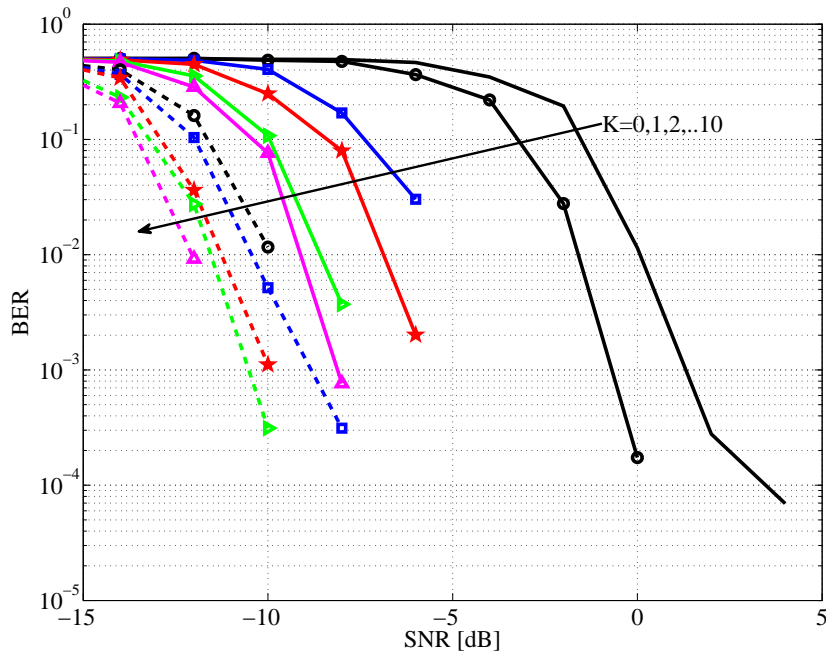
(a) AF: SR +10 dB, RD +5 dB
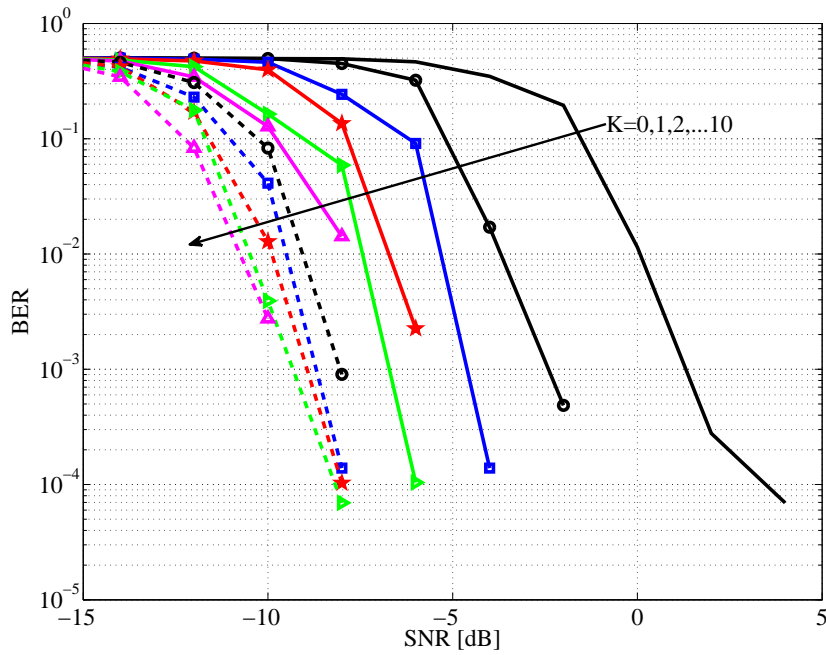
(b) DF: SR +10 dB, RD +5 dB

Figure 69: MIMO multi single-antenna relays performance, Case 1 (16 QAM 1/2, SUI3 channel, 10 channel realisations). The performance improves as the number of relays K increases. The AF strategy shows more significant improvement at higher K compared to the DF strategy
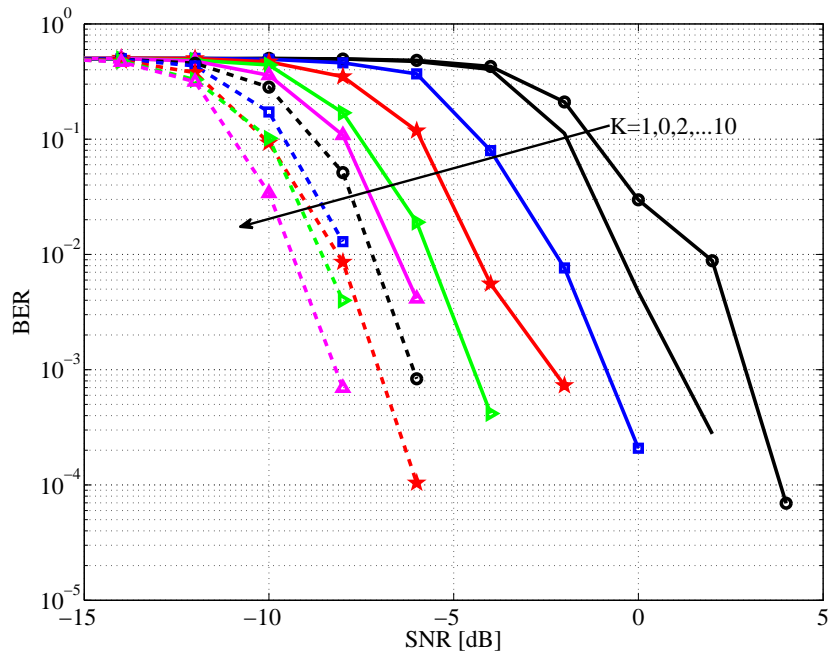
(a) AF: SR +5 dB, RD +5 dB
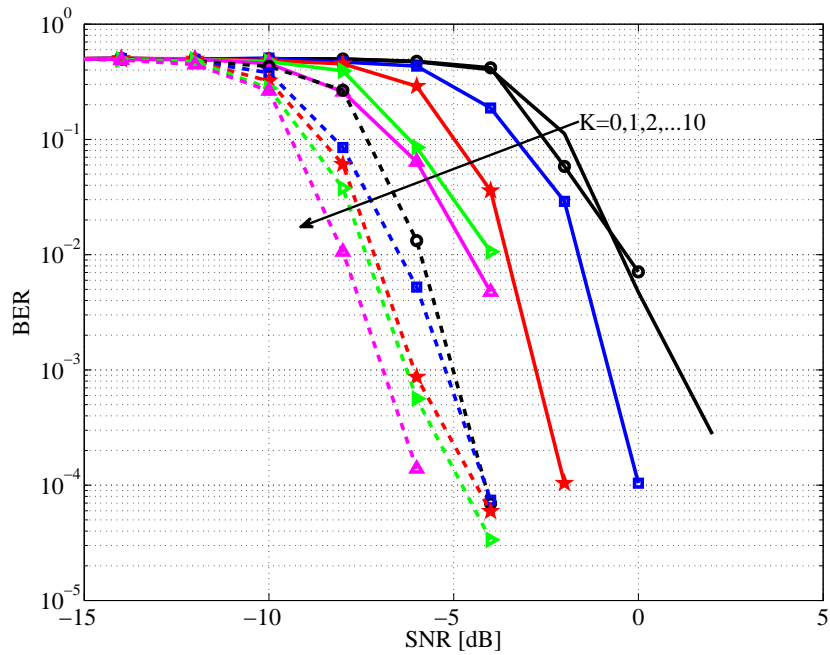
(b) DF: SR +5 dB, RD +5 dB

Figure 70: MIMO multi single-antenna relays performance, Case 2 (16 QAM 1/2, SUI3 channel, 10 channel realisations). The performance improves as the number of relays K increases. The AF strategy shows more significant improvement at higher K compared to the DF strategy

(a) AF: SR +5 dB, RD +10 dB

(b) DF: SR +5 dB, RD +10 dB

Figure 71: MIMO multi single-antenna relays performance, Case 3 (16 QAM 1/2, SUI3 channel, 10 channel realisations). The performance improves as the number of relays K increases. The AF strategy shows more significant improvement at higher K compared to the DF strategy
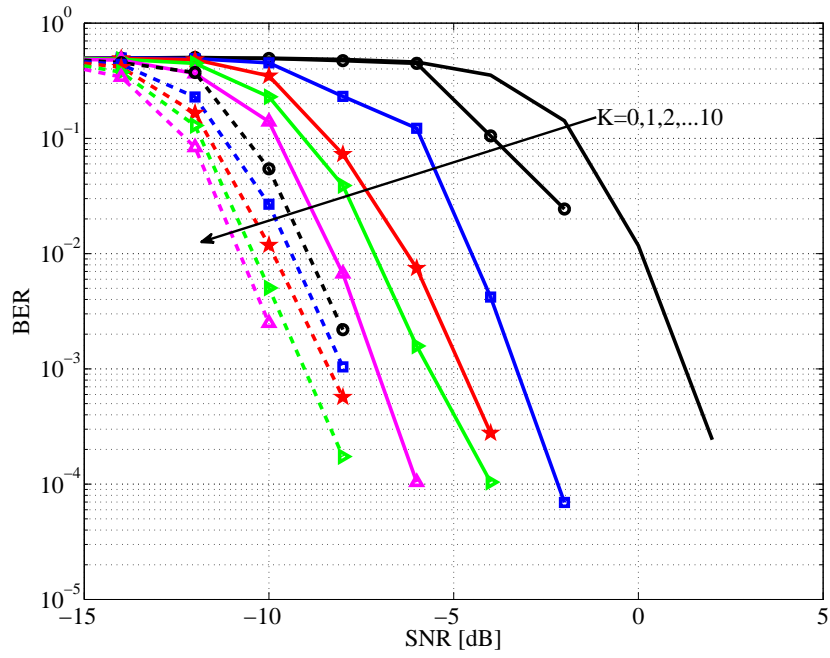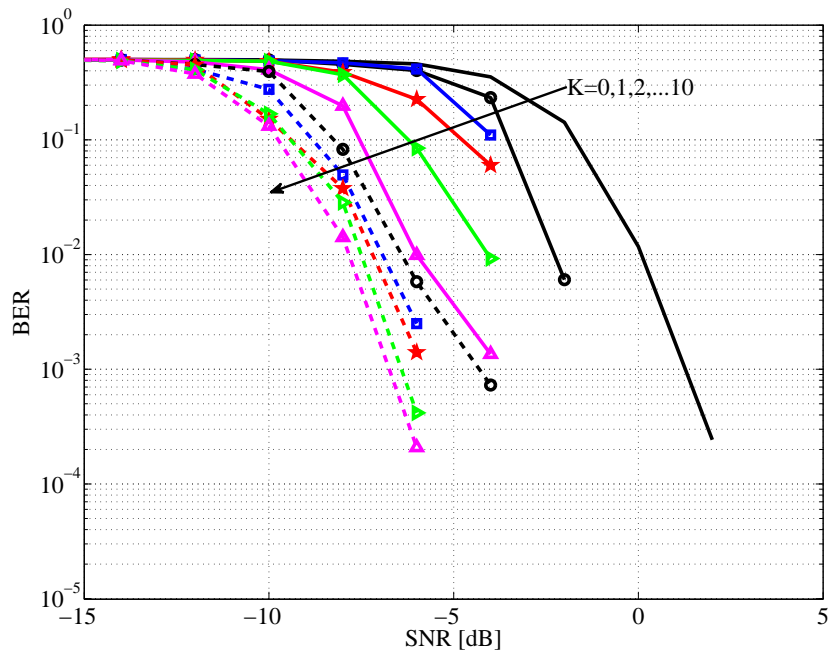
[1] IEEE, "Std 802.16-2009 part 16: Air interface for broadband wireless access systems," tech. rep., IEEE, May 2009.

[2] C. Thein, A. Anggraini, T. Kaiser, and K. L. Chee, "Throughput coverage simulations based on signal level measurements at 825 MHz and 3535 MHz," in *4th International Conference on Signal Processing and Communication Systems (ICSPCS)*, 2010.

[3] H. B. Dang, "MIMO keyhole under deterministic channel in WiMAX relay system," Master's thesis, Institut für Kommunikationstechnik, Leibniz Universität Hannover, April 2011.

[4] I. P802.16j-2009, "IEEE standard for local and metropolitan area networks part 16: Air interface for broadband wireless access systems amendment 1: Multiple relay specification," tech. rep., IEEE, June 2009.

[5] IEEE, "Std 802.16m-2011 part 16: Air interface for broadband wireless access systems. amendment 3: Advanced air interface," tech. rep., IEEE, May 2011.

[6] IEEE, "Std 802.16-2004 part 16: Air interface for fixed broadband wireless access systems," tech. rep., IEEE, October 2004.

[7] IEEE, "Std 802.16e-2005 part 16: Air interface for fixed and mobile broadband wireless access systems," tech. rep., IEEE, February 2005.

[8] Z. Abate, *WiMAX RF Systems Engineering*. USA: Artech House, 2009.

[9] J. G. Andrews, A. Ghosh, and R. Muhamed, *Fundamentals of WiMAX: Understanding Broadband Wireless Networking*. England: Pearson Education, Inc., 2007.

[10] K.-C. Chen and J. R. B. d. Marca, *Mobile WiMAX*. England: John Wiley and Sons, 2008.

[11] K. Fazel and S. Kaiser, *Orthogonal Frequency Division Multiplexing for Wireless Communications*. England: John Wiley and Sons Ltd, 2003.

[12] M. Katz and F. H. P. Fitzek, *WiMAX evolution: emerging technologies and applications*. UK: John Wiley and Sons Ltd, 2009.

[13] Y. G. Li and G. L. Stueber, *Orthogonal Frequency Division Multiplexing for Wireless Communications*. USA: Springer, 2006.

[14] H. Yaghoobi, "Scalable OFDMA physical layer in IEEE 802.16 WirelessMAN," *Intel Technology Journal Issue 3*, vol. 8, pp. 201–212, August 2004.

[15] E. Pelet, J. Salt, and G. Wells, "Effect of wind on foliage obstructed line-of-sight channel at 2.5 GHz," *IEEE Transactions on Broadcasting*, vol. 50, pp. 224–232, September 2004.

[16] M. Cheffena and T. Ekman, "Modeling the dynamic effects of vegetation on radiowave propagation," in *IEEE International Conference on Communications, 2008. ICC '08*, pp. 4466–4471, May 2008.

[17] K. L. Chee, A. Anggraini, T. Kürner, and T. Kaiser, "Effects of carrier frequency, antenna height and season on broadband wireless access in rural areas," *IEEE Transaction on Antennas and Propagation*, vol. 60, pp. 3432–3443, July 2012.

[18] K. L. Chee and T. Kurner, "Towards a realistic propagation prediction model - a self-tailored 3D-digital elevation model with clutter information," in *2009 Proceedingsof the ITG Conference on Microwave Remote Sensing and Navigation (WFMN)*, (Chemnitz, Germany), November 2009.

[19] K. L. Chee and T. Kurner, "Effect of terrain irregularities and clutter distribution on wave propagation at 3.5 GHz in suburban area," in *2010 Proceedings of the Fourth European Conference on Antennas and Propagation (EuCAP)*, (Barcelona, Spain), April 2010.

[20] `http://www.remcom.com/wireless-insite`.

[21] Rohde & Schwarz GmbH & Co. KG, *R&S©TSMW Universal Radio Network Analyzer Scanner for drive tests and I/Q streaming*, 05.00 ed., January 2010.

[22] Rohde & Schwarz GmbH & Co. KG, *R&S©ROMES4 Drive Test Software Mobile coverage and QoS measurements in wireless communications*, 04.00 ed., September 2010.

[23] P. Grønsund, O. Grøndalen, T. Breivik, and E. Engelstad, "Fixed WiMAX field trial measurements and the derivation of a path loss model," in *Mosharaka International Conference on Communication Systems and Circuits, M-CSC 2007*, 2007.

[24] C. A. 231, "Digital mobile radio towards future generation systems, final report," Tech. Rep. EUR 18957, European Communities, 1999.

[25] V. Erceg, L. J. Greenstein, S. Y. Tjandra, S. R. Parkoff, A. Gupta, B. Kulic, A. A. Julius, and R. Bianchi, "An empirically based path loss model for wireless channels in suburban environments," *IEEE Journal on Selected Areas in Communications*, vol. 17, pp. 1205–1211, July 1999.

[26] V. Erceg, K. Hari, M. Smith, and D. Baum, "Channel models for fixed wireless applications," tech. rep., IEEE 802.16 Broadband Wireless Access Working Group, February 2001.

[27] G. L. Stüber, *Principles of Mobile Communication*. Springer US, 2 ed., 2000.

[28] T. Rappaport, *Wireless Communications - Principles and Practice.* Prentice Hall Communications Engineering and Emerging Technologies, Series, 2002.

[29] F. J. Massey, "The kolmogorov-smirnov test for goodness of fit," *Journal of the American Statistical Association*, vol. 46, no. 253, pp. 68 – 78, 1951.

[30] J. Durbin, "Kolmogorov-Smirnov tests when parameters are estimated with applications to tests of exponentiality and tests on spacings," *Biometrika*, vol. 62, pp. 5–22, 1975.

[31] K.-Y. Lin, R.-T. Juang, H.-P. Lin, W.-J. Shyu, and P. Ting, "Link adaptation of MIMO-OFDM transmission exploiting the rician channel K-factor," in *IEEE Mobile WiMAX Symposium, 2009. MWS '09*, pp. 184–188, July 2009.

[32] V. Erceg, K. Hari, M. Smith, and D. Baum, "Channel models for fixed wireless applications," tech. rep., IEEE 802.16 Broadband Wireless Access Working Group, 2003.

[33] C. Mehlführer, S. Caban, and M. Rupp, "Experimental evaluation of adaptive modulation and coding in MIMO WiMAX with limited feedback," *EURASIP Journal on Advances in Signal Processing, Special Issue on MIMO Systems with Limited Feedback*, vol. 2008, Article ID 837102, p. 12 pages, 2008.

[34] S. Alamouti, "A simple transmit diversity technique for wireless communications," *IEEE Journal on Selected Areas in Communications*, vol. 16, pp. 1451–1458, October 1998.

[35] I.-R. R. M.2134, "Requirements related to technical performance for IMT-Advanced radio interface(s)," tech. rep., International Telecommunication Union, November 2008.

[36] E. van der Meulen, "A survey of multi-way channels in information theory 1961-1976," *IEEE Transactions on Information Theory*, vol. 23, pp. 1–37, January 1977.

[37] T. Cover and A. Gamal, "Capacity theorems for the relay channel," *EEE Transactions on Information Theory*, vol. 25, pp. 572–584, September 1979.

[38] A. Sendonaris, E. Erkip, and B. Aazhang, "User cooperation diversity. part I. system description," *IEEE Transactions on Communication*, vol. 51, pp. 1927–1938, November 2003.

[39] A. Sendonaris, E. Erkip, and B. Aazhang, "User cooperation diversity-part II. implementation aspects and performance analysis," *IEEE Transactions on Communication*, vol. 51, pp. 1939–1948, November 2003.

[40] J. Laneman, D. Tse, and G. Wornell, "Cooperative diversity in wireless networks: Efficient protocols and outage behaviour," *IEEE Transactions on Information Theory*, vol. 50, pp. 3062–3080, December 2004.

[41] LTE-Advanced, "TR 36.913: Requirements for further advancements for evolved universal terrestrial radio access (E-UTRA) LTE-advanced release 9," tech. rep., 3GPP, December 2009.

[42] B. Chun, E.-R. Jeong, J. Joung, Y. Oh, and Y. Lee, "Pre-nulling for self-interference suppression in full-duplex relays," in *APSIPA Annual Summit and Conference*, October 2009.

[43] T. Riihonen, S. Werner, and R. Wichman, "Spatial loop interference suppression in full-duplex MIMO relays," in *2009 Conference Record of the Forty-Third Asilomar Conference on Signals, Systems and Computers*, pp. 1508–1512, November 2009.

[44] P. Larsson and M. Prytz, "MIMO on-frequency repeater with self-interference cancellation and mitigation," in *Vehicular Technology Conference, 2009. VTC Spring 2009. IEEE 69th*, pp. 1–5, April 2009.

[45] P. Lioliou, M. Viberg, M. Coldrey, and F. Athley, "Self-interference suppression in full-duplex MIMO relays," in *2010 Conference Record of the Forty Fourth Asilomar Conference on Signals, Systems and Computers (ASILOMAR)*, pp. 658–662, November 2010.

[46] E. van der Meulen, "Three-terminal communications channels," *Advances in Applied Probability*, vol. 3, pp. 120–154, Spring 1971.

[47] A. Gamal and S. Zahedi, "Capacity of a class of relay channels with orthogonal components," *IEEE Transactions on Information Theory*, vol. 51, pp. 1815–1817, May 2005.

[48] G. Kramer, M. Gastpar, and P. Gupta, "Cooperative strategies and capacity theorems for relay networks," *IEEE Transactions on Information Theory*, vol. 51, pp. 3037–3063, September 2005.

[49] P. Gupta and P. Kumar, "The capacity of wireless networks," *IEEE Transactions on Information Theory*, vol. 46, pp. 388–404, March 2000.

[50] M. Gasper and M. Vetterli, "On the asymptotic capacity of gaussian relay channels," *IEEE symposium on Information Theory*, vol. , p. 195, June 2002.

[51] R. Nabar, H. Bolcskei, and F. Kneubuhler, "Fading relay channels: performance limits and space-time signal design," *IEEE Journal on Selected Areas in Communications*, vol. 22, pp. 1099–1109, August 2004.

[52] G. Farhadi and N. Beaulieu, "Ergodic capacity analysis of wireless relaying systems in Rayleigh fading," in *Proc. of ICC' 08*, pp. 3730–3735, May 2008.

[53] S. Chen, W. Wang, and X. Zhang, "Ergodic and outage capacity analysis in cooperative diversity systems under Rayleigh fading channels," in *Proc. of ICC' 09*, June 2009.

[54] S. Shrestha and K.-H. Chang, "Analysis of outage capacity performance for cooperative DF and AF relaying in dissimilar Rayleigh fading channels," in *Proc. of ISIT'08*, pp. 494–498, July 2008.

[55] M. Yuksel and E. Erkip, "Multiple-antenna cooperative wireless systems: a diversity-multiplexing tradeoff perspective," *IEEE Transactions on Information Theory*, vol. 53, pp. 3371–3393, October 2007.

[56] B. Wang, J. Zhang, and A. Host-Madsen, "On the capacity of MIMO relay channels," *IEEE Transactions on Information Theory*, vol. 51, pp. 29–43, January 2005.

[57] R. Louie, Y. Li, and B. Vucetic, "Performance analysis of beamforming in two hop amplify and forward relay networks," in *ICC '08. IEEE International Conference on Communications*, pp. 4311–4315, May 2008.

[58] B. Chalise and L. Vandendorpe, "Outage probability analysis of MIMO relay channel with orthogonal space-time block codes," *IEEE Commun Letters*, vol. 12, pp. 280–283, April 2008.

[59] S. Chen, W. Wang, and X. Zhang, "Performance analysis of OSTBC transmission in amplify-and-forward cooperative relay networks," *IEEE Transactions on Information Theory*, vol. 59, pp. 105–113, January 2010.

[60] D. Chizhik, G. Foschini, and R. Valenzuela, "Capacities of multi-element transmit and receive antennas: Correlations and keyholes," *Electronics Letters*, vol. 36, pp. 1099–1100, June 2000.

[61] G. Levin and S. Loyka, "Multi-keyholes and measure of correlation in MIMO channels," in *23rd Biennial Symposium on Communications*, pp. 22–25, 2006.

[62] J. Boyer, D. D. Falconer, and H. Yanikomeroglu, "Multihop diversity in wireless relaying channels," *IEEE Transactions on Communication*, vol. 52, pp. 1820–1830, October 2004.

[63] M. Yu, J. Li, and H. Sadjadpour, "Amplify-forward and decode-forward: the impact of location and capacity contour," in *Military Communications Conference, 2005. MILCOM 2005. IEEE*, vol. 3, pp. 1609–1615, October 2005.

[64] H. Li and Q. Zhao, "Distributed modulation for cooperative wireless communications," *IEEE Signal Processing Magazine*, vol. 23, pp. 30–36, September 2006.

[65] Q. Zhao and H. Li, "Performance of differential modulation with wireless relays in Rayleigh fading channels," *IEEE Commun Letters*, vol. 9, pp. 343–345, April 2005.

[66] W. Cho, R. Cao, and L. Yang, "Optimum resource allocation for amplify-and-forward relay networks with differential modulation," *IEEE Transactions on Signal Processing*, vol. 56, pp. 5680–5691, November 2008.

[67] Y. P. Hong, W.-J. Huang, and K. C.-C.Jay, *Cooperative Communications and Networking*. Springer, 2010.

[68] Y. Jing and B. Hassibi, "Cooperative diversity in wireless relay networks with multiple-antenna nodes," in *International Symposium on Information Theory, 2005. ISIT 2005. Proceedings*, pp. 815–819, September 2005.

[69] K. Azarian, H. El Gamal, and P. Schniter, "On the achievable diversity-multiplexing tradeoff in half-duplex cooperative channels," *IEEE Transactions on Information Theory*, vol. 51, pp. 4152–4172, December 2005.

[70] N. Prasad and M. Varanasi, "Diversity and multiplexing tradeoff bounds for cooperative diversity protocols," in *International Symposium on Information Theory, 2004. ISIT 2004. Proceedings*, June 2004.

[71] G. Kramer, M. Gastpar, and P. Gupta, "Capacity theorems for wireless relay channels," in *Proc. 41th Annual Allerton Conf. on Commun., Control, and Computing*, p. 10 pages, October 2003.

[72] M. Yu and J. Li, "Is amplify-and-forward practically better than decode-and-forward or vice versa?," in *Proceedings. (ICASSP'05). IEEE International Conference on Acoustics, Speech, and Signal Processing*, vol. 3, pp. iii/365 – iii/368, March 2005.

[73] A. Nosratinia, T. Hunter, and A. Hedayat, "Cooperative communication in wireless network," *Communications Magazine, IEEE*, vol. 42, pp. 74–80, October 2004.

[74] A. Florea and H. Yanikomeroglu, "On the scalability of relay based wireless networks," in *IEEE Wireless Communications and Networking Conference 2006*, vol. 1, pp. 242–245, 2006.

[75] M. Gastpar and M. Vetterli, "On the capacity of wireless networks: the relay case," in *INFOCOM 2002. Twenty-First Annual Joint Conference of the IEEE Computer and Communications Societies. Proceedings. IEEE*, vol. 3, pp. 1577–1586, 2002.

[76] A. Molisch and M. Win, "MIMO systems with antenna selection," *Microwave Magazine, IEEE*, vol. 5, pp. 46–56, March 2004.

[77] S. Sanayei and A. Nosratinia, "Antenna selection in MIMO systems," *Communications Magazine, IEEE*, vol. 42, pp. 68–73, October 2004.

[78] R. Pabst, B. Walke, D. Schultz, P. Herhold, H. Yanikomeroglu, S. Mukherjee, H. Viswanathan, M. Lott, W. Zirwas, M. Dohler, H. Aghvami, D. Falconer, and G. Fettweis, "Relay-based development concepts for wireless and mobile radio," *IEEE Communication Magazine*, vol. 42, pp. 80–89, September 2004.

[79] H. Yanikomeroglu, "Fixed and mobile relaying technologies for cellular networks," in *Second Workshop on Applications and Services in Wireless Networks (ASWN'02)*, (Paris, France), pp. 75–81, July 2002.

[80] J. Boyer, D. Falconer, and H. Yanikomeroglu, "A theoretical characterization of the multihop wireless communications channel without diversity," in *2001 12th IEEE International Symposium on Personal, Indoor and Mobile Radio Communications*, vol. 2, pp. 116–120, September 2001.

[81] J. Boyer, D. Falconer, and H. Yanikomeroglu, "A theoretical characterization of the multihop wireless communications channel with diversity," in *Global Telecommunications Conference, 2001. GLOBECOM '01. IEEE*, vol. 2, pp. 841–845, 2001.

[82] M. Hasna and M.-S. Alouini, "Outage probability of multihop transmission over nakagami fading channels," *Communications Letters, IEEE*, vol. 7, no. 5, pp. 216–218, 2003.

[83] M. Hasna and M.-S. Alouini, "End-to-end outage probability of multihop transmission over lognormal shadowed channels," in *The Arabian Journal for Science and Engineering*, vol. 28-2C, December 2003.

[84] L. Yang, M. Hasna, and M.-S. Alouini, "Average outage duration of multihop communication systems with regenerative relays," *IEEE Transactions on Wireless Communications*, vol. 4, pp. 1366–1371, July 2005.

[85] G. Karagiannidis, T. Tsiftsis, and R. Mallik, "Bounds for multihop relayed communications in nakagami-m fading," *IEEE Transactions on Communications*, vol. 54, pp. 18–22, January 2006.

[86] J. K. Lee, J. Yang, and D. K. Kim, "An approximation of the outage probability for multi-hop AF fixed gain relay," *CoRR*, vol. abs/0812.0904, p. 3 pages, 2008.

[87] G. Amarasuriya, C. Tellambura, and M. Ardakani, "New performance approximations for multi-hop fixed-gain AF relay networks," in *2011 IEEE International Conference on Communications (ICC)*, pp. 1–5, June 2011.

[88] I. E. Telatar, "Capacity of multi-antenna gaussian channels," *European Transactions on Telecommunications*, vol. 10, pp. 585–595, November 1999.

[89] A. Paulraj, R. Nabar, and Gore, *Introduction to Space-Time Wireless Communications.* Cambridge University Press, 2003.

[90] P. Almers, F. Tufvesson, and A. F. Molisch, "Measurement of keyhole effect in a wireless multiple-input multiple-output (MIMO) channel," *Communications Letters, IEEE*, vol. 7, pp. 373–375, August 2003.

[91] O. Souihli and T. Ohtsuki, "Cooperative diversity can mitigate keyhole effects in wireless MIMO systems," in *Global Telecommunications Conference, 2009. GLOBECOM 2009. IEEE*, pp. 1–6, December 2009.

[92] P. Almers, F. Tufvesson, and A. Molisch, "Keyhole effect in MIMO wireless channels: Measurements and theory," *IEEE Transactions on Wireless Communications*, vol. 5, pp. 3596–3604, December 2006.

[93] S. Yang and J.-C. Belfiore, "Diversity-multiplexing tradeoff of double scattering MIMO channels," *IEEE Transactions on Information Theory*, vol. 57, pp. 2027–2034, April 2011.

[94] C. Rao and B. Hassibi, "Diversity-multiplexing gain trade-off of a mimo system with relays," in *2007 IEEE Information Theory Workshop on Information Theory for Wireless Networks*, pp. 1–5, July 2007.

[95] M. Mühlhaus, O. Braz, and F. Jondral, "The impact of relay stations on MIMO systems," *FREQUENZ*, vol. 62, pp. 278 – 280, November 2008.

[96] R. Louie, Y. Li, H. Suraweera, and B. Vucetic, "Performance analysis of beamforming in two hop amplify and forward relay networks with antenna correlation," *IEEE Transactions on Wireless Communications*, vol. 8, pp. 3132–3141, June 2009.

[97] O. Souihli and T. Ohtsuki, "The MIMO relay channel in the presence of keyhole effects," in *IEEE International Conference on Communications (ICC)*, pp. 1–5, May 2010.

[98] D. Chizhik, G. Foschini, M. Gans, and R. Valenzuela, "Keyholes, correlations, and capacities of multielement transmit and receive antennas," *IEEE Transactions on Wireless Communications*, vol. 1, pp. 361–368, April 2002.

[99] G. Levin and S. Loyka, "From multi-keyholes to measure of correlation and power imbalance in MIMO channels: Outage capacity analysis," *IEEE Transactions on Information Theory*, vol. 57, pp. 3515–3529, June 2011.

[100] H. Shin and J. H. Lee, "Capacity of multiple-antenna fading channels: spatial fading correlation, double scattering, and keyhole," *IEEE Transactions on Information Theory*, vol. 49, pp. 2636–2647, October 2003.

[101] D. Gesbert, H. Bolcskei, D. Gore, and A. Paulraj, "Outdoor MIMO wireless channels: models and performance prediction," *IEEE Transactions on Communications*, vol. 50, pp. 1926–1934, December 2002.

[102] H. Shin and J. H. Lee, "Effect of keyholes on the symbol error rate of space-time block codes," *Communications Letters, IEEE*, vol. 7, pp. 27–29, January 2003.

[103] H. Shin and J. H. Lee, "Performance analysis of space-time block codes over keyhole MIMO channels," in *PIMRC 2003. 14th IEEE Proceedings on Personal, Indoor and Mobile Radio Communications*, vol. 3, pp. 2933–2937, September 2003.

[104] D. Gesbert, H. Bolcskei, D. Gore, and A. Paulraj, "MIMO wireless channels: capacity and performance prediction," in *Global Telecommunications Conference, 2000. GLOBECOM '00. IEEE*, vol. 2, pp. 1083–1088, 2000.

[105] G. J. Foschini and M. J. Gans, "On limits of wireless communications in a fading environment when using multiple antennas," *Wirel. Pers. Commun.*, vol. 6, pp. 311–335, March 1998.

[106] G. Levin and S. Loyka, "On the outage capacity distribution of correlated keyhole MIMO channels," *IEEE Transactions on Information Theory*, vol. 54, pp. 3232–3245, July 2008.

[107] A. Maaref and S. Aissa, "Impact of spatial fading correlation and keyhole on the capacity of MIMO systems with transmitter and receiver csi," *IEEE Transactions on Wireless Communications*, vol. 7, pp. 3218–3229, August 2008.

[108] A. Müller and S. Joachim, "Capacity of multiple-input multiple-output keyhole channels with antenna selection," in *European Wireless Conference, EW2007*, (Paris, France), April 2007.

[109] X. Cui and Z. Feng, "Lower capacity bound for MIMO correlated fading channels with keyhole," *Communications Letters, IEEE*, vol. 8, pp. 500–502, August 2004.

[110] G. Li and G. Zang, "Capacity of keyhole MIMO system over non-double Rayleigh fading channels," in *IET International Conference on Wireless, Mobile and Multimedia Networks*, pp. 1–3, November 2006.

[111] S. Sanayei, A. Hedayat, and A. Nosratinia, "Space time codes in keyhole channels: Analysis and design," *IEEE Transactions on Wireless Communications*, vol. 6, pp. 2006–2011, June 2007.

[112] Y. Gong and K. Letaief, "On the error probability of orthogonal space-time block codes over keyhole MIMO channels," *IEEE Transactions on Wireless Communications*, vol. 6, pp. 3402–3409, September 2007.

[113] S. Sanayei and A. Nosratinia, "Antenna selection in keyhole channels," *IEEE Transactions on Communications*, vol. 55, pp. 404–408, March 2007.

[114] P. T. Kulkarni, M. H. Lee, and R. P. Paudel, "Performance analysis of dirty-paper coding over MIMO keyhole channels," in *2006. ICECE '06.*

International Conference on Electrical and Computer Engineering, pp. 402–407, December 2006.

[115] G. Levin and S. Loyka, "Multi-keyhole MIMO channels: Asymptotic analysis of outage capacity," in *IEEE International Symposium on Information Theory*, pp. 1305–1309, July 2006.

[116] T. M. and Y. Karasawa, "Multi-keyhole model for MIMO repeater system evaluation," *IEICE Transactions on Communication (Japanese edition)*, vol. J89-B, pp. 1746–1754, September 2006.

[117] X. Liu, X. Zhang, H. Zhang, and D. Yang, "Ergodic capacity analsis of MIMO multi-keyhole channel in Rayleigh fading," *IEICE Transactions on Communication*, vol. E93-B, pp. 353–360, February 2010.

[118] C. Zhong, S. Jin, K.-K. Wong, and M. McKay, "Ergodic mutual information analysis for multi-keyhole MIMO channels," *IEEE Transactions on Wireless Communications*, vol. 10, pp. 1754–1763, June 2011.

[119] Y. Karasawa, M. Tsuruta, and T. Taniguchi, "Multi-keyhole model for MIMO radio-relay systems," in *The Second European Conference on Antennas and Propagation. EuCAP 2007*, pp. 1–6, November 2007.

[120] Q. Li, G. Li, W. Lee, M. il Lee, D. Mazzarese, B. Clerckx, and Z. Li, "MIMO techniques in WiMAX and LTE: a feature overview," *Communications Magazine, IEEE*, vol. 48, pp. 86–92, May 2010.

[121] H. Bolcskei, R. Nabar, O. Oyman, and A. Paulraj, "Capacity scaling laws in MIMO relay networks," *IEEE Transactions on Wireless Communications*, vol. 5, pp. 1433–1444, June 2006.

[122] X. Tang and Y. Hua, "Optimal design of non-regenerative MIMO wireless relays," *IEEE Transactions on Wireless Communications*, vol. 6, pp. 1398–1407, April 2007.

[123] Y. Fan and J. Thompson, "MIMO configurations for relay channels: Theory and practice," *IEEE Transactions on Wireless Communications*, vol. 6, pp. 1774–1786, May 2007.

[124] S. Chen, W. Wang, X. Zhang, M. Peng, and D. Zhao, "Capacity performance of amplify-and-forward MIMO relay with transmit antenna selection and maximal-ratio combining," in *Global Telecommunications Conference, 2009. GLOBECOM 2009. IEEE*, pp. 1–6, December 2009.

[125] L. Zheng and D. Tse, "Diversity and multiplexing: a fundamental tradeoff in multiple-antenna channels," *IEEE Transactions on Information Theory*, vol. 49, pp. 1073–1096, May 2003.

[126] D. Gunduz, A. Goldsmith, and H. Poor, "Diversity-multiplexing tradeoffs in MIMO relay channels," in *Global Telecommunications Conference, 2008. IEEE GLOBECOM 2008. IEEE*, pp. 1–6, December 2008.

[127] H. Bolcskei, D. Gesbert, and A. Paulraj, "On the capacity of OFDM-based spatial multiplexing systems," *IEEE Transactions on Communications*, vol. 50, pp. 225–234, February 2002.

[128] D. Gesbert, M. Kountouris, R. Heath, C. Chae, , and T. Sälzer, "From single user to multiuser communications: Shifting the MIMO paradigm," *IEEE Signal Processing Magazine*, vol. 24, pp. 36–46, October 2007.

[129] S. A. Jafar and M. J. Fakhereddin, "Degrees of freedom in multiuser MIMO," *CoRR*, vol. abs/cs/0510055, p. 7, 2005.

[130] V. Cadambe and S. Jafar, "Interference alignment and degrees of freedom of the K -user interference channel," *IEEE Transactions on Information Theory*, vol. 54, pp. 3425–3441, August 2008.

[131] V. R. Cadambe and S. A. Jafar, "Interference alignment and the degrees of freedom of wireless X networks," *IEEE Transaction on Information Theory*, vol. 55, pp. 3893–3908, September 2009.

[132] S.-W. Jeon, S.-Y. Chung, and S. Jafar, "Degrees of freedom of multi-source relay networks," in *47th Annual Allerton Conference on Communication, Control, and Computing, 2009. Allerton 2009*, pp. 388–393, October 2009.

[133] D. Park and S. Y. Park, "Performance analysis of multiuser diversity under transmit antenna correlation," *IEEE Transactions on Communications*, vol. 56, pp. 666–674, April 2008.

[134] H. Wang, P. Wang, L. Ping, and X. Lin, "On the impact of antenna correlation in multi-user MIMO systems with rate constraints," *IEEE Communications Letters*, vol. 13, pp. 935–937, December 2009.

[135] H. Kim, N. Kim, W. Choi, and H. Park, "Performance of multiuser transmit diversity in spatially correlated channels," *IEEE Communications Letters*, vol. 14, pp. 824–826, September 2010.

[136] B. Hochwald, T. Marzetta, and V. Tarokh, "Multiple-antenna channel hardening and its implications for rate feedback and scheduling," *IEEE Transactions on Information Theory*, vol. 50, pp. 1893–1909, September 2004.

[137] M. Costa, "Writing on dirty paper (corresp.)," *IEEE Transactions on Information Theory*, vol. 29, pp. 439–441, May 1983.

[138] Q. Spencer, C. Peel, A. Swindlehurst, and M. Haardt, "An introduction to the multi-user MIMO downlink," *Communications Magazine, IEEE*, vol. 42, pp. 60–67, October 2004.

[139] Q. Spencer, A. Swindlehurst, and M. Haardt, "Zero-forcing methods for downlink spatial multiplexing in multiuser MIMO channels," *IEEE Transactions on Signal Processing*, vol. 52, pp. 461–471, February 2004.

[140] Z. Shen, R. Chen, J. Andrews, R. Heath, and B. Evans, "Sum capacity of multiuser MIMO broadcast channels with block diagonalization," *IEEE Transactions on Wireless Communications*, vol. 6, pp. 2040–2045, June 2007.

[141] D. Schmidt, C. Shi, R. Berry, M. Honig, and W. Utschick, "Minimum mean squared error interference alignment," in *2009 Conference Record of the Forty-Third Asilomar Conference on Signals, Systems and Computers*, pp. 1106–1110, November 2009.

[142] K. Gomadam, V. Cadambe, and S. Jafar, "Approaching the capacity of wireless networks through distributed interference alignment," in *2008. IEEE GLOBECOM 2008. IEEE Global Telecommunications Conference*, pp. 1–6, December 2008.

[143] S. Peters and R. Heath, "Interference alignment via alternating minimization," in *Speech and Signal Processing, 2009. ICASSP 2009. IEEE International Conference on Acoustics*, pp. 2445–2448, April 2009.

[144] J. Hwang, K.-J. Lee, H. Sung, and I. Lee, "Block diagonalization approach for amplify-and-forward relay systems in MIMO multiuser channels," in *2009 IEEE 20th International Symposium on Personal, Indoor and Mobile Radio Communications*, pp. 3149–3153, September 2009.

[145] R. Ganesan, T. Weber, and A. Klein, "Interference alignment in multiuser two way relay networks," in *2011 IEEE 73rd Vehicular Technology Conference (VTC Spring)*, pp. 1–5, May 2011.

- Anggia Anggraini, Jürgen Peissig, and Thomas Kaiser, *"Virtual MIMO in WiMAX Relay System"*, In Proc. of the International Symposium on Signal, Systems and Electronics (ISSSE), Potsdam, Germany, October 2012

- Anggia Anggraini, Thi Chung Le, Jürgen Peissig, and Thomas Kaiser, *"MIMO Multi-User Relay System"*, In Proc of the International Symposium on Signal, Systems and Electronics (ISSSE), Potsdam, Germany, October 2012

- Chung Le, Emil Dimitrov, Anggia Anggraini, Jürgen Peissig, and Hans-Peter Kuchenbecker, *"Effect of Spatial Correlation on MMSE-Based Interference Alignment in a Multiuser MIMO MB-OFDM System"*, In Proc. of the 8th IEEE International Conference on Wireless and Mobile Computing, Networking and Communications (WiMob), Barcelona, Spain, 2012

- Kin Lien Chee, Anggia Anggraini, and Thomas Kürner, *"Effects of carrier frequency, antenna height and season on broadband wireless access in rural areas"*, IEEE Transaction on Antennas and Propagation, Vol. 60, No. 07, 2012

- Kin Lien Chee, Anggia Anggraini, Thomas Kaiser, and Thomas Kürner, *"Outdoor-to-Indoor Propagation Loss Measurements for Broadband Wireless Access in Rural Areas"*, In Proc. of the 5th European Conference on Antennas and Propagation (EUCAP), pp 1376-1380, April 2011

- Christoph Thein, Kin Lien Chee, Anggia Anggraini, and Thomas Kaiser, *"Throughput Coverage Simulations Based on Signal Level Measurements at 825 MHz and 3535 MHz"*, In Proc. of the 4th International Conference on Signal Processing and Communication Systems (ICSPCS'2010), Gold Coast, Australia, December 2010

- A. Anggraini, A. Waal, and T. Kaiser, *"Design and Implementation of a Real-Time OFDM-based System for VHF Radio (DRM+)"*, in 12th International OFDM Workshop 2007, Hamburg, Germany, August 2007

Anggia Nurul Kusuma Anggraini
geboren am 24.12.1980 in Lembang, Indonesia

1998 − 2002	Studium der Informationstechnik an der Institut Teknologi Bandung in Bandung, Indonesia
2002	Bachelorarbeit an der Institut Teknologi Bandung in Bandung, Indonesia
18.06.2002	Verleihung des akademischen Grades "Bachelor of Science (B.Sc.)" durch die Institut Teknologi Bandung in Bandung, Indonesia
01.08.2002 − 31.08.2003	Mitarbeiter am CCAR bei Institut Teknologi Bandung in Bandung, Indonesia
2003 − 2006	Studium der Informations- und Elektrotechnik an der Universität Duisburg-Essen
2005 − 2006	Masterarbeit, Schwerpunkt Nachrichtentechnik, an der Universität Duisburg-Essen
20.02.2006	Verleihung des akademischen Grades "Master of Science (M.Sc.)" durch die Universität Duisburg-Essen in Duisburg
01.08.2006 − 30.06.2009	Ingenieur am MimoOn GmbH in Duisburg (Teilzeit)
01.11.2006 − 30.09.2012	Wissenschaftlicher Mitarbeiterin am Institut für Kommunikationstechnik an der Gottfried-Wilhelm-Leibniz-Universität-Hannover in Hannover bei Herrn Prof. Dr.-Ing. T. Kaiser